Biological reduction of soluble uranium by an indigenous bacterial community

By

Maleke Mathews Maleke

July 2013

University of the Free State

Universiteit van die Vrystaat

Yunivesithi ya Freistata

Biological reduction of soluble uranium by an indigenous bacterial community

By

Maleke Mathews Maleke

Submitted in fulfilment of the requirements for the degree

MAGISTER SCIENTIAE

In the
Department of Microbial, Biochemical and Food Biotechnology
Faculty of Natural and Agricultural Sciences
University of the Free State
Bloemfontein
South Africa

July 2013

Supervisor: Prof. E. van Heerden

Co-Supervisors: Dr. P.J. Williams

Dr E. Botes

This dissertation is dedicated to my parents (Mosoetsa and Moselantja Maleke), sister (Matshediso) and Lerato Gaje.

"Trust in the Lord with all your heart and lean not on your own understanding; In all your ways acknowledge Him, and He will make your paths straight"

Proverbs 3:5-6

Acknowledgements

I would like to express my gratitude and deep appreciation towards:

- **God**, for giving me grace and privilege to pursue this study and completing it in spite of many challenges faced.
- Many thanks to my supervisor, **Prof. Esta van Heerden**, for her guidance, encouragement, patience and for always believing in me. I could not have done this project without her.
- My co-supervisor, **Dr Peter Williams**, for his assistance, encouragement, suggestions in this project and willingness to read my dissertation.
- My co-supervisor, **Dr Elsabe Botes** for her suggestions, helpful critical comments and for her assistant with the final preparation of the manuscript.
- **Center for Microscopy** (UFS, Bloemfontein, South Africa) for their help with preparing the matrix samples for SEM-EDX.
- **Dr Frederick Roelofse** (Department of Geology, UFS, Bloemfontein, South Africa) for his help with the SEM-EDX work.
- Thanks to my father, **Tseliso Mosoetsa John Maleke** for the sacrifices he made in order for me to have access to tertiary education. I love you.
- To my three pillars of strength, **Moselantja Maleke**, **Matshediso Maleke** and **Lerato Gaje**, thank you for the love, encouragement and support you showed during the study. I love you all.
- Special thanks to the **National Research Foundation** for funding this research.
- Finally all my **friends** for various contributions and support during the study.

Declaration

I hereby declare that this thesis is submitted by me for the Magister Scientiae degree at the University of the Free State. This work is solely my own and hasn't been previously submitted by me at any other University or Faculty, and the other sources of information used have been acknowledged. I further grant copyright of this thesis in favour of the University of the Free State.

MM Maleke

July 2013

CONTENTS

CHAPTER 3

List of Figures

Chapter 1

Chapter 3

Chapter 4

List of Tables

Chapter 1

Chapter 3

Chapter 4

List of Abbreviations

^{o}C	Degree celcius
16S	Small ribosomal subunit
A	Absorbance
APS	Ammonium persulfate
ATP	Adenosine triphosphate
BLAST	Basic Logical Alignment Search Tool
bp	Base pairs
Br-PADAP	2-(5-bromo-2-pyrdulazo)-5-diethylaminophenol
BSA	Bovine serum albumin
DNA	Deoxyribonucleic acid
dNTPs	Deoxyribonucleoside triphosphate
Eh	Electric activity
EHDMA	Ethylhexadecyldimethylammonium bromide
EDTA	Ethylenediaminetetraacetate
g	Acceleration due to gravity
g/cm	gram per centimetre
gDNA	Genomic DNA
km	kilometre
l	litre

M	Molar
µg/ml	microgram per millilitre
µl	microlitre
µm	micrometre
µS/cm	microsiemens per centimetre
mS/cm	millisiemens per centimetre
m	metre
mg/kg	milligram per kilogram
mg/l	milligram per litre
ml	millilitre
mV	millivolts
MW	Molecular weight
ng/µl	Nanogram per microlitre
pmol	Picomoles
rDNA	Ribosomal DNA
t	Ton
TAE	Tris, Acetic acid, EDTA
TEA	Triethanolamin
TEMED	N,N,N’,N’-tetramethylethylenediamine
UV	Ultraviolet
v/v	Volume per volume

w/v	Weight per volume
x	Times

Chapter 1

1.1 Introduction

Uranium (U) is the 49th most abundant element in the earth's crust and was first discovered in 1789 by Martin Heinrich Klaproth (Craft *et al*., 2004; Wall and Krumholz, 2006). It is the 92nd element in the periodic table with a relative atomic mass of 238.03. In addition, uranium is a heavy metal with a specific gravity of approximately 19.07 g/cm, boiling and melting temperatures of 3818°C and 1132°C respectively (Bem and Bou-Rabee, 2004). Its abundance in the earth crust varies from 2 to 4 mg/kg U_3O_8 in soil and is comparable to concentrations of arsenic, beryllium, molybdenum and tungsten, but higher than silver, bismuth, cadmium and mercury (Bajwa *et al*., 2003). It occurs in numerous minerals and is also found in lignite, monazite sand and phosphate rocks (Bajwa *et al*., 2003). In the environment it occurs mainly as a uraninite (UO_2), pitchblende ($U_3O_8^{2+}$) or as secondary minerals (Nagy *et al*., 2009). Uranium(IV) as uraninite forms minerals such as coffinite (a complex with silicate), while U(VI) as uranyl may form complexes with oxides, silicates, phosphate and vandates (Elless and Lee, 1998). Some examples of these minerals are outlined in Table 1.1 (Heshmati-Rafsanjani, 2009).

Uranium is one of the most toxic metals and has 16 isotopes, all of which are radioactive (Khani, 2011). Naturally occurring uranium contains by weight three isotopes, namely ^{238}U, ^{235}U and small amounts of ^{234}U, which all emit alpha particles (Table 1.2) (Bem and Bou-Rabee, 2004). The most abundant isotope is ^{238}U (99.2745%) and has the longest half-life. On the contrary, ^{234}U is the least abundant with a short half-life compared to the other two isotopes (Bem and Bou-Rabee, 2004). The decaying chain of these isotopes includes radioactive elements which decay to lead (Figure 1.1) (Bleise *et al*., 2003).

Table 1.1: Uranyl minerals that may form in porous media (Taken from Heshmati-Rafsanjani, 2009).

Mineral	Composition
Oxides and Hydroxides	
Schoepite	$(UO_2)_8O_8(OH)_{12}.12H_2O$
Meta-schoepite	$(UO_2)_8O_8(OH)_{12}.10H_2O$
Dehydrated schoepite	$UO_3.(2\text{-}x)H_2O$
Becquerelite	$Ca(UO_2)_6O_4(OH)_6.8H_2O$
Clarkeite	$Na[(UO_2)O(OH)].H_2O$
Compreignacite	$K_2U_6O_{19}.12H_2O$
Carbonates	
Rutherfordine	UO_2CO_3
Liebigite	$CaUO_2(CO_3)_3.11H_2O$
Silicates	
Siddyrite	$(UO_2)_2SiO_4.2H_2O$
Uranophane	$Ca(H_3O)_2(UO_2SiO_4)_2.3H_2O$
β-uranophhane	$Ca(UO_2)SiO_3(OH)_2.5H_2O$
Weeksite	$K_2(UO_2)_2Si_6O_{15}.14H_2O$
Coffinite	$USiO_4$
Phosphates	
Autunite	$Ca(UO_3)_2(PO_4)_2.10H_2O$
Meta-autunite	$Ca(UO_2)_2(PO_4)_2.(2\text{-}6)H_2O$
Uranyl-orthophosphate	$(UO_2)_3(PO_4)_2.4H_2O$
Sodium meta-autunite	$Na_2(UO_2)_2(PO_4)_2.8H_2O$
Meta-ankkoleite	$K_2(UO_2)_2(PO_4)_2.6H_2O$
Phosphateuranylite	$Ca(UO_2)_3(PO_4)_2(OH)_2.6H_2O$
Saleeite	$Mg(UO_2)_2(PO_4)_2.10H_2O$
Vandates	
Carnonite	$K_2(UO_2)_2(VO_4)_2.3H_2O$
Tyuyamunite	$Ca(UO_2)_2(VO_4)_2.(2\text{-}5\text{-}8)H_2O$

Table 1.2: Characteristics of uranium isotopes in natural uranium (Bleise et al., 2003).

Isotope	Half-life(years)	Relative mass (%)	Specific Activity (Bq/s*)
^{238}U	4.47×10^{9}	99.2745	12 455
^{235}U	7.04×10^{8}	0.720	80 011
^{234}U	2.46×10^{5}	0.0055	231×10^{6}

*Bq/s = Becquerel per second

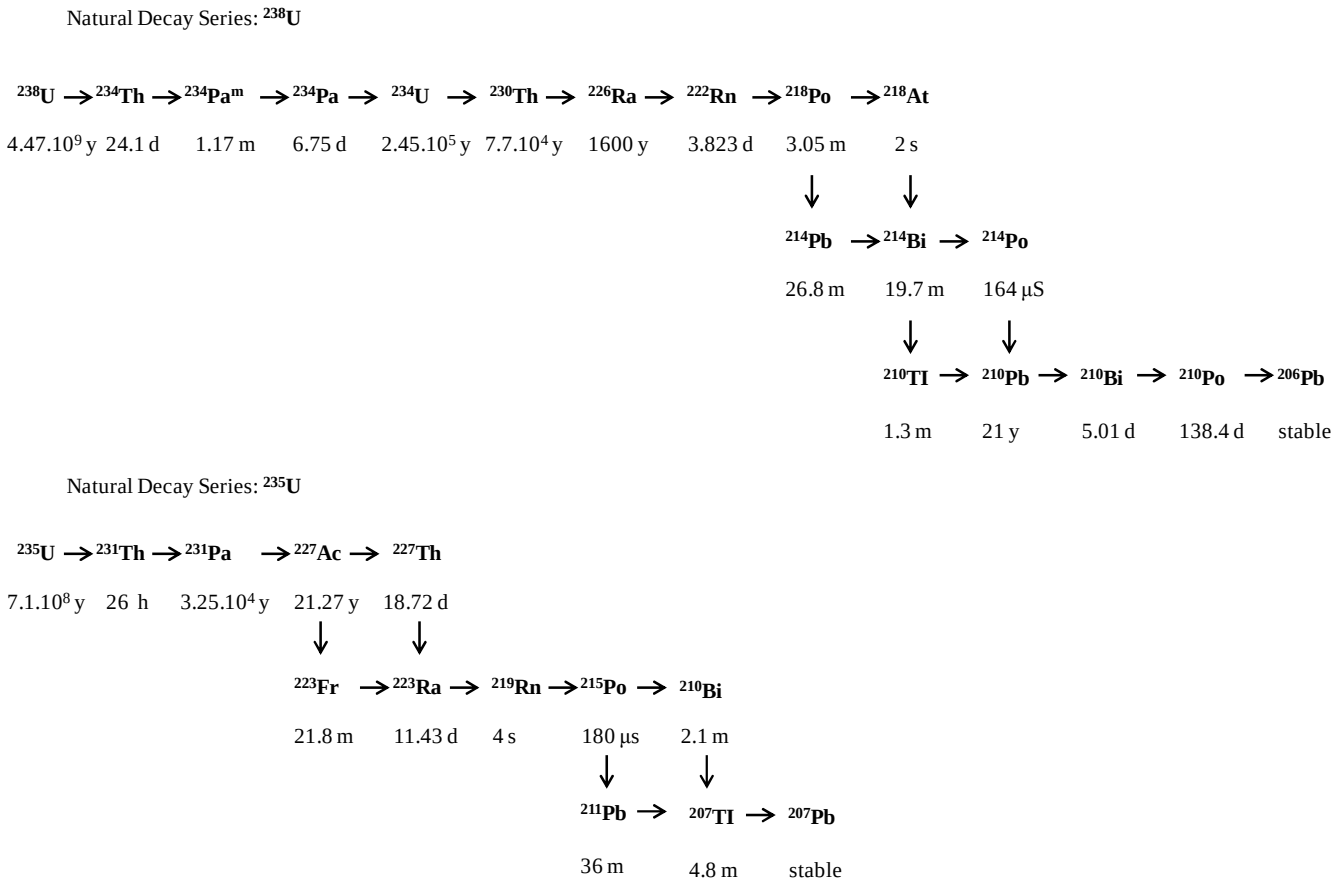

Figure 1.1: The decay chain of U isotopes.

The important use of enriched uranium is for the manufacturing of reactor fuel that is used for the generation of electricity (Koeberg) and previously uranium was also used in weapons (Tripathi *et al*., 2008). Of the three abundant isotopes, the most important is ^{235}U (Bleise *et al*., 2003; Bem and Bou-Rabee, 2004). This isotope is used in the production of energy because it has the ability to release energy in a chain reaction with a neutron, hence it is said to be fissile (Bem and Bou-Rabee, 2004). Figure 1.2 shows the split of a ^{235}U nucleus and the resulting large release of energy during this process. However, in order for this uranium isotope to be used in nuclear energy generation, its relative mass (0.72 %) has to be increased to approximately 5 % (Bleise *et al*., 2003).

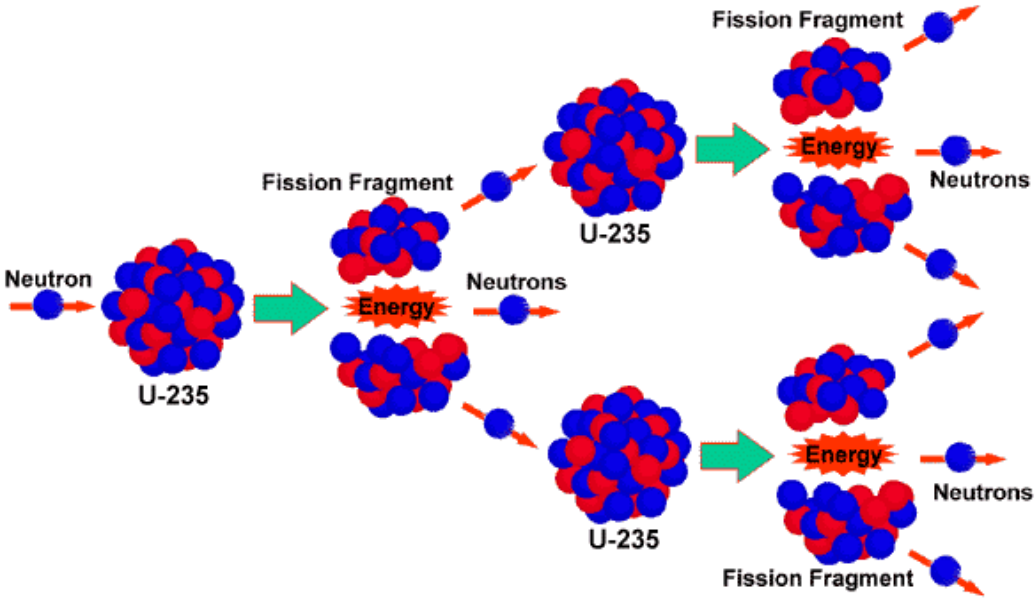

Figure 1.2: Fission of a ^{235}U nucleus (Galperin, 1992).

In gold mining, the gold bearing ore processes during milling emerges as tailings. The tailings are then mixed with sulphuric acid to recover the gold minerals. After removing the gold bearing minerals, the remaining solution is treated with sodium carbonate/bicarbonate solution to change the pH of the solution in order to extract the uranium using ion exchange technology (Bajwa *et al*., 2003). In uranium ore mining, the ore is milled and treated with sodium carbonate/bicarbonate in order to preferentially leach the uranium from other impurities due to the low solubility of other minerals in sodium carbonate/bicarbonate solutions (Bajwa *et al*., 2003; Tripathi *et al*., 2008). During these processes the resulting by-products (sludge, ion exchange materials and solvents) that are stored on site can contaminate

the site with uranium (Bajwa *et al*., 2003). As a result, it is without doubt that human activities such as mineral exploitation, ore transportation, smelting and refining, disposal of the tailings and waste waters around mines are the main source of groundwater and soil contamination with heavy metals such as uranium (Ato *et al*., 2010; Bhagure and Mirgane, 2011).

Uranium is ubiquitous in nature as it is found in soil, rocks, sediments and groundwater (Bleise *et al*., 2003). When exposed to air, this metal is mainly found in an oxidized form due to the fact that it is easily oxidized and becomes coated with a layer of oxide (Bleise *et al*., 2003). There are different forms of uranium in soil and sediments (Lofty *et al*., 2012).

Naturally, uranium exists in four oxidation states, namely U(III) to U(VI), with U(IV) and U(VI) being the most common (Kalin *et al*., 2005; Suzuki and Banfield, 2004). In aqueous systems, uranium speciation that influences solubility is controlled by pH and the oxidation reduction potential/Eh (refer to Figure 1.3) (Martinez *et al*., 2007; Kumar *et al*., 2011). In relation to pH and Eh, trivalent uranium can only be found in very reducing conditions in acidic solutions (pH less than 3), while the pentavalent uranium only occurs in small proportions over a limited redox potential range and disproportionates to tetra- and hexavalent states (Nagy *et al*., 2009). As a result, in oxidizing conditions uranium will occur in the U(VI) oxidation state in the form of uranyl ions (UO_2^{2+}) which is highly mobile and soluble in groundwater at pH less than 5.5 (Figure 1.3) (Finneran *et al*., 2002a). It is, therefore, a major groundwater pollutant (Suzuki and Banfield, 2004; Kilincarslan and Akylin, 2005). In contrast, the U(IV) oxidation state occurs under reducing conditions as uraninite precipitate (UO_2) (Finneran *et al*., 2002a; Suzuki *et al*., 2005) which renders it insoluble and immobile (Suzuki *et al*., 2005).

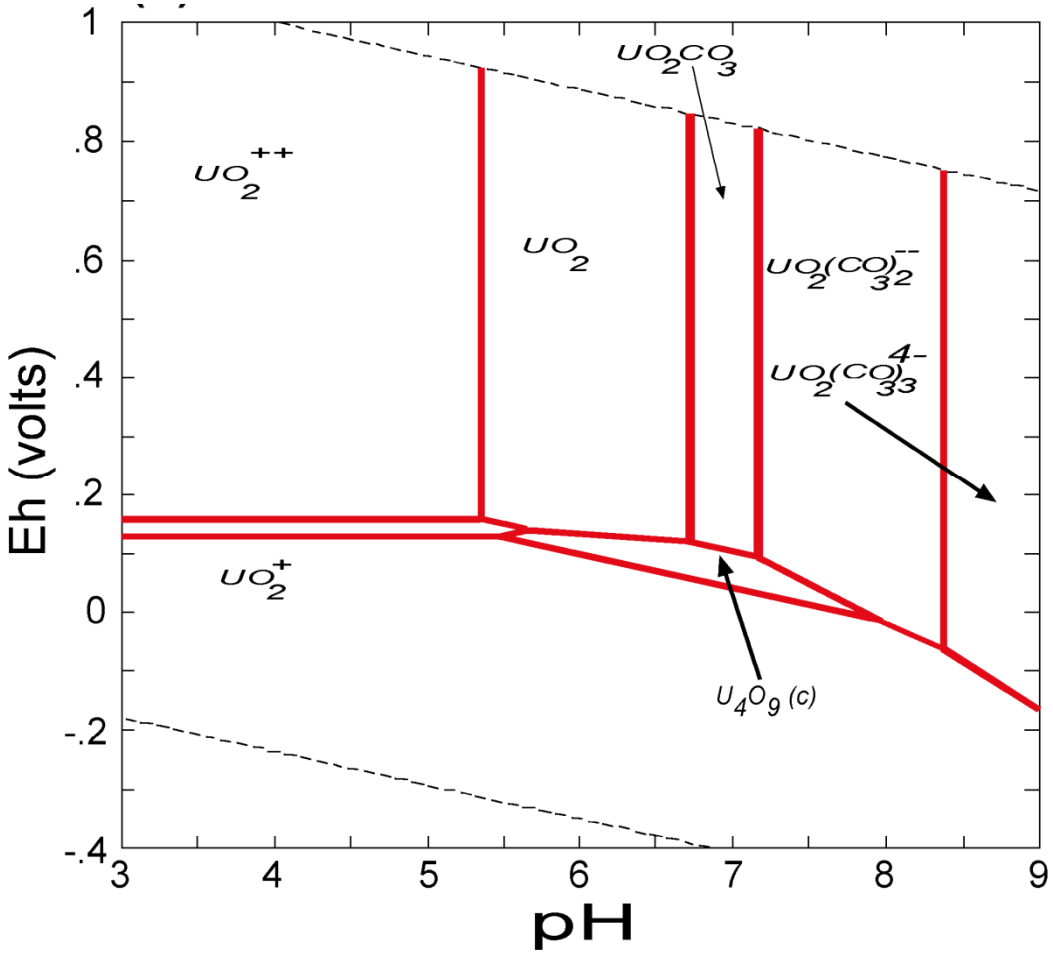

Figure 1.3: Eh-pH diagram for aqueous uranium species under oxidizing environmental conditions (Ander and Smith, 2002)

1.2 Microbial metal interactions

Microbes can interact with metals of various kinds encountered in the environment (Gadd, 2010). Some of these metals have incomplete filled d-orbitals providing heavy metal cations which form complex compounds in the cell (Hu *et al*., 2005). These metals can play a role in the metabolic processes of the microbe, as they are essential and required by the microbe for micro nutrients, known as 'trace elements' (Rathnayake *et al*., 2010). However, some of the metals have detrimental effects on the microbe as they can form free radicals, resulting in DNA damage, lipid peroxidation and depletion of protein sulfhdryls (Udofia *et al*., 2009). Even so, microbes have evolved to allow themselves to thrive in areas contaminated with these heavy metals (Rathnayake *et al*., 2010). One resistance mechanism they possess is their ability to reduce metals from a higher oxidation state to their lower oxidation states, thus in the process rendering the metal less toxic. A few examples of these types of mechanisms include the reduction of Fe(III) to Fe(II), Cr(VI) to Cr(III) and U(VI) to U(IV) (Fredrickson *et al*., 2000; Finneran *et al*., 2002b). Other resistance mechanisms include exclusion by a permeability barrier, intra and extracellular sequestration as well as active transport and efflux pumps (Rathnayake *et al*., 2010).

In addition to the above mentioned processes, there are other interactions between a metal and a microbe, and the type of interaction depends on whether the organism is prokaryotic or eukaryotic (Ehrlich, 1997). Both types of organisms have the ability to form metabolic products, such as acids or ligands, or form anions, such as sulfides or carbonates, that will precipitate the dissolved metal ions (Enrlich, 1997). In addition, either the microbes can bind metal ions in their vicinity at the cell surface or they may transport them into the cell for various intracellular functions (Ehrlich, 1997). On the other hand, only prokaryotes are capable of the oxidation of Mn(II), Fe(II), Co(II), or their reduction and conserve energy from these reactions (Ehrlich, 1997). In contrast, metals such as Hg(II) or Ag(I) can be reduced to Hg(0) and Ag(0) respectively, but microbes do not conserve energy from their reduction (Ehrlich, 1997). Several of these interactions can be used in the bioremediation of contaminated sites with uranium (Goulhen *et al*., 2006) as they immobilize/precipitate the uranyl ions (Martinez *et al*., 2007). To date four mechanisms involved in the immobilization of uranium have been described (Figure 1.4), namely (a) biosorption, (b) bioaccumulation, (c)

biomineralization and (d) microbial reduction of soluble metal species to the insoluble species (Chabalala and Chirwa, 2010a; b).

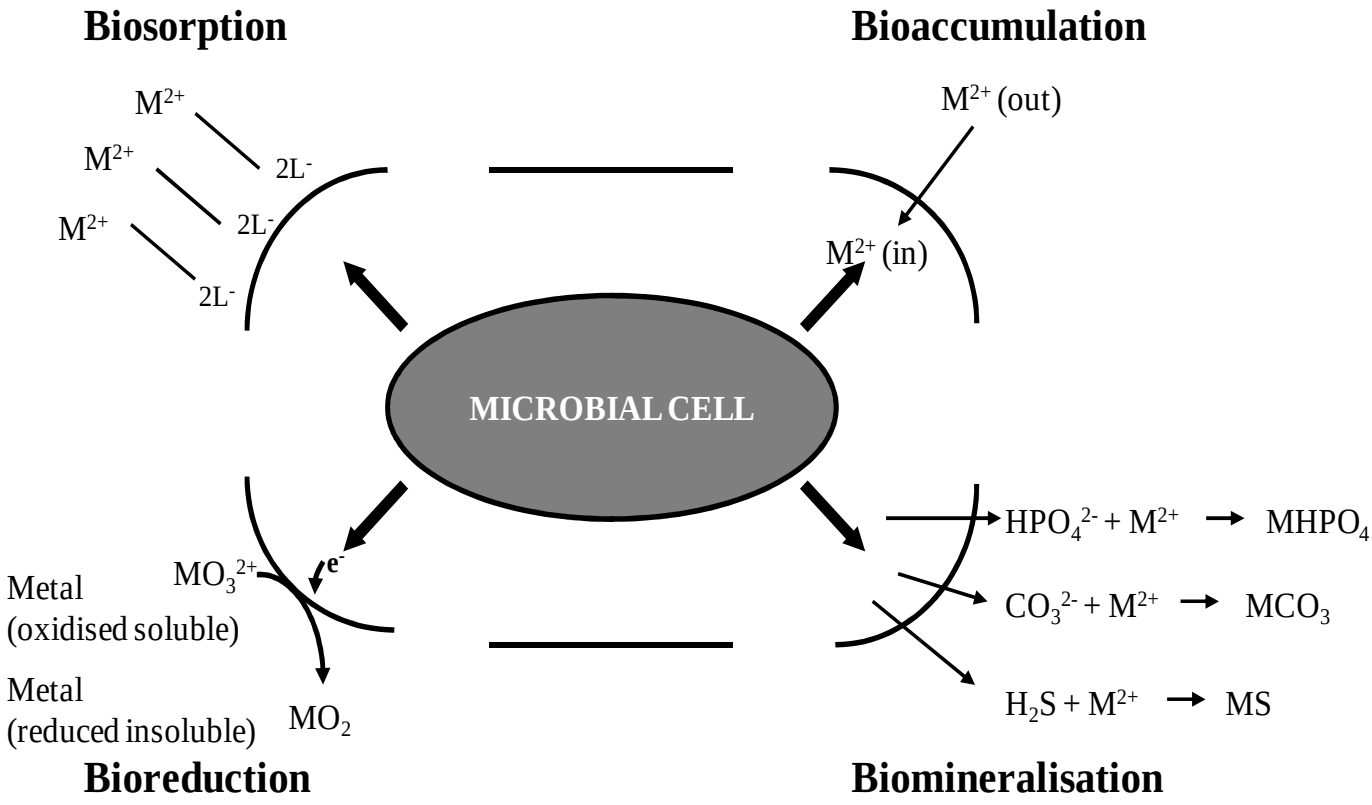

Figure 1.4: Diagram illustrating the diverse types of interactions that can take place between a microbial cell and the immobilization of uranyl ion in solution (Taken from Vaughan and Lloyd, 2011).

1.2.1 Biosorption

Biosorption can be defined as a passive process of metal sequestration and concentration by chemical sites (functional groups such as carboxyl, sulfonate, phosphate, hydroxyl, amino, or imino residues) naturally present on the surface of the microbial cell (Suzuki and Banfield, 2004; Brandl and Faramarzi, 2006). Biosorption is metabolism-independent, thus it can be performed by both living and metabolically inactive microbial biomass (Ehrlich, 1997; Lovley and Coates, 1997; Lloyd and Lovley, 2001; Seyrig, 2010). This interaction is composed of both adsorption, which is the accumulation of metals at the surface, and absorption, which is the active transport according to the nutritional requirements of the cells biomass (Figure 1.5) (Suzuki and Banfield, 2004). In case of uranium, the biosorption interactions involved include three possible mechanisms, however, the uranium remains in the U(VI) oxidation state (Tabak *et al*., 2005). These mechanisms include:

- Sorption on surface sites
- Surface precipitation
- Precipitation with bacterial cell lysate

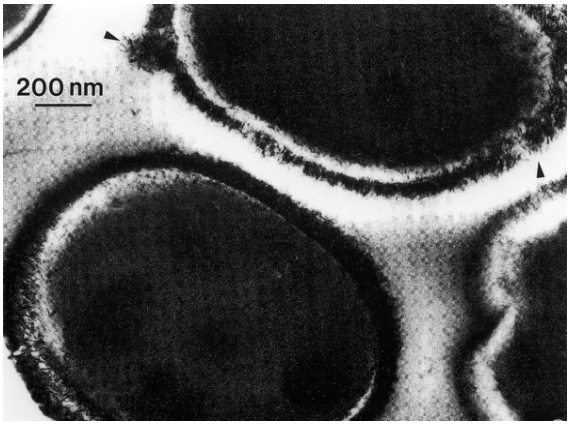

Figure 1.5: Transmission electron microscopy image of uranium biosorption accumulated as crystalline nanofibrils on the outer surface of *S. cerevisiae* from aqueous solution. Illustration of nanofribils of uranium accumulated in a 0.2 µm surface envelope region of *S. cerevisiae* (Taken from Murr, 2006).

Although biosorption is rapid it can be influenced by the organism used and environmental conditions (e.g pH, temperature, agitation, incubation time and metal concentration) (Parameswari *et al*., 2009; El-Hendawy *et al*., 2009). However, according to Ahalya and co-workers (2003) the effects of temperature (in the range of 20 - 35^{o}C) on biosorption is small compared to other influencing factors, as the temperature will not damage the structural components of the cells in contact with the metal. On the other hand, pH is the most important parameter as it affects the chemistry of the metal, the activity of the functional groups in the biomass and the competition of metallic ions (Ahalya *et al*., 2003). Parameswari and co-workers (2009) stated that biosorption is a two phased process, an initial fast phase followed by the phase of slower adsorption. They speculated that the initial fast uptake might be due to the availability of abundant metal species and the empty binding sites of the microbe, while the slower phase might be due to saturation of metal binding sites (Parameswari *et al*., 2009). According to a study done by Volesky and May-Phillips (1995), the best absorbant of uranium were non-living cells. Through their work, dead cells of *Saccharomyces cerevisiae* removed approximately 40% more uranium than their living counterparts (Volesky and May-Phillips, 1995). As stated by Finlay *et al* (1998), this phenomenon is due to the fact that live biomass usually functions under physiologically permissive conditions and may fail due to metal toxicity. However, metabolically inactive cells are prone to saturation at relatively low levels of metals (Finlay *et al*., 1998).

1.2.2 Bioaccumulation

Bioaccumulation of metals is the mechanism in which a metabolically active microbe will immobilize and precipitate the soluble metal by transporting it through the cell membrane and accumulating it within the cells as solid particles (Brandl and Faramarzi, 2006). Combinations of metabolism- and temperature-independent and metabolism-dependent steps are involved in the bioaccumulation of metals by actively growing cells (Wang and Hu, 2008). Bioaccumulation involves two steps, with the first step said to be rapid. Wang and Hu (2008) also states that the first step, which is metabolism- and temperature-independent, involves metal ions binding at the cell's surface. This is then followed by a second step (metabolism-dependent), which is slower, that accumulates large quantities of components within the cell. Many microbial species are capable of bioaccumulation of metals and these include bacteria, fungi, yeast and algae (Wang and Hu, 2008). Furthermore, in the case of uranium bioaccumulation, the capability of microorganisms is as follows: bacteria > yeast > fungi (Murr, 2006).

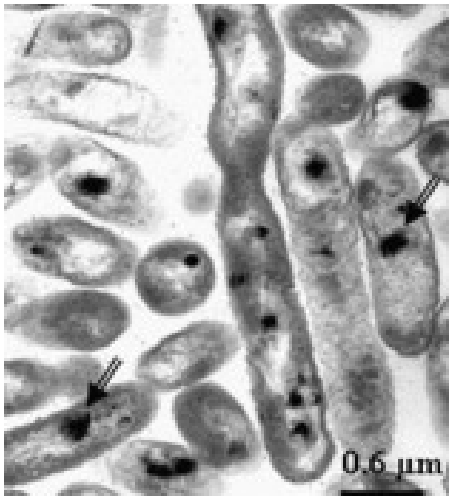

Figure 1.6: Transmission electron microscopy of thin sections of the cells of *Stenotrophomonas maltophilia* JG-2 treated with uranium. The arrows indicate the presence of U in the uranium deposits (Taken from Merroun and Selenska-Pobell, 2008).

1.2.3 Biomineralization

Biomineralization is a process that precipitates metals with enzymatically liberated ligands, such as carbonates, phosphates, oxides, sulfides and hydroxides (Lloyd and Lovley, 2001; Martinez *et al*., 2007; Gadd, 2010). Amongst the ligands, phosphates are obvious candidates for the microbially mediated removal of metals via biomineralization in the form of their biomass-bound polycrystalline metal phosphates $MHPO_4$ (M=metal) (Basnakova and Macaskie, 1997).

A study by Macaskie and co-workers (2000) showed the bioprecipitation of uranyl ions by *Citrobacter* sp. N14 (Figure 1.7). Through this study they found that the *Citrobacter* sp. N14 accumulated UO_2^{2+} via precipitation with phosphate ligand liberated from the phosphatase activity in the form of uranyl phosphate ($HUO_2PO_4.4H_2O$) (Macaskie *et al*., 1992; 2000). Additionally the rate of uranyl accumulation varied with the cellular phosphatase activity. The 300% uranyl ion immobilized on the cell might be due to the cellular ionisable groups present mainly within the cell wall and the membrane components or by phosphatase enzyme activity producing excess orthophosphate that biomineralizes uranium (Choudhary and Sar, 2011).

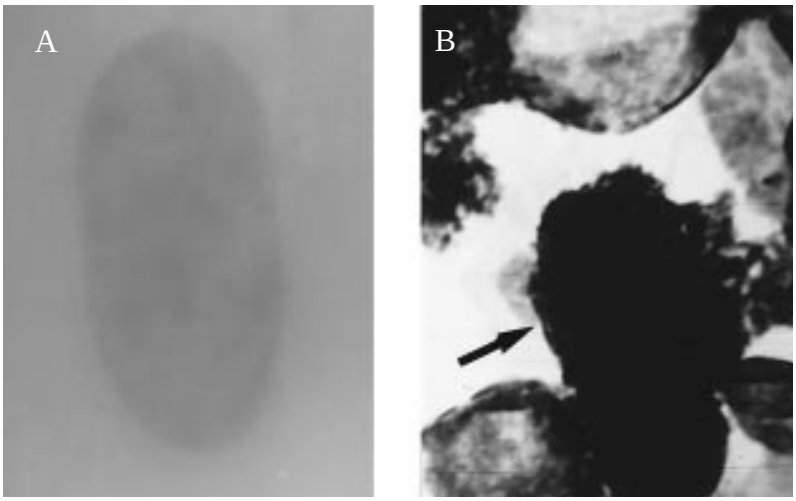

Figure 1.7: Uranyl ion accumulation by *Citrobacter* sp. N14. (A) Cells from a uranyl unchallenged preparation (control). (B) Cell (arrowed) prepared with uranyl ion to approximately 300% of bacterial dry weight (Taken from Macaskie *et al*., 1992).

1.2.4 Reduction

Metal bioreduction is generally the reduction of soluble metals to their less insoluble states, thereby decreasing their mobility depending on the type of metal and the oxidation state (Suzuki *et al*., 2005). An example of this is the transformation of hexavalent uranium and chromium to the tetra- and trivalent states respectively. As shown (Figure 1.8), the bioreduction of uranium is an important reaction influencing its mobility – as it is relatively soluble at a high oxidation state and is therefore susceptible to environmental transport. However, in the reduced lower oxidation states, it's solubility and mobility are limited due to the formation of black mineral precipitate, uraninite (Finneran *et al*., 2002a; Shelobolina *et al*., 2004; Gregory and Lovley, 2005; Lloyd and Renshaw, 2005; Suzuki *et al*., 2005; Martinez *et al*., 2007; Moon *et al*., 2010). There are several microbes that use U(VI) as an electron acceptor in dissimilatory anaerobic respiration (Gregory and Lovley, 2005). Usually in this type of mechanism a variety of short chained organic acids (lactate, acetate, and pyruvate) or hydrogen (H_2) in some instances serve as a carbon and energy source for the reduction of U(VI) (Nevin *et al*., 2003; Shelobolina *et al*., 2003).

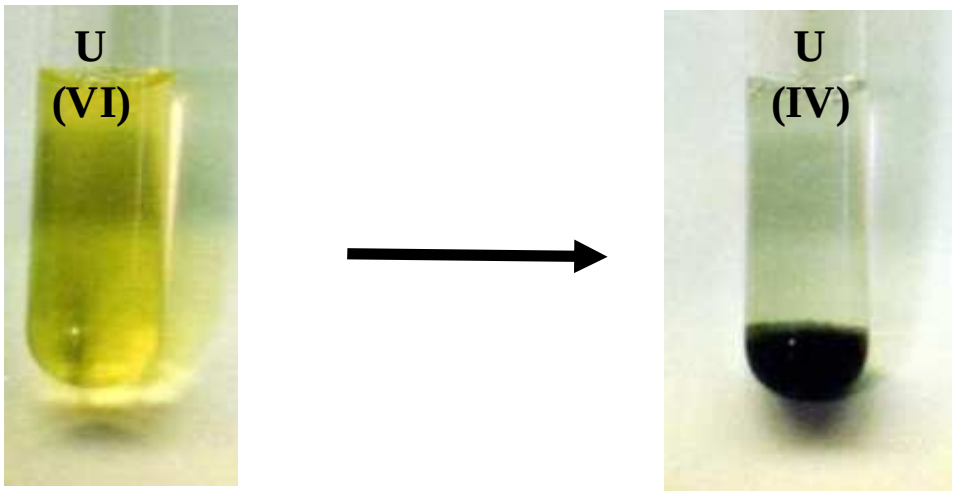

Figure 1.8: Schematic representation of uranium-reduction indicating the colour difference and a black mineral (uraninite) between the two redox states (Adapted from Payne, 2005).

Microbial uranium reduction was first reported in 1962 (Seyrig, 2010). However, it only received attention through the work of Lovely in the early 1990s (Lovley *et al*., 1991). It was before this time that the process was thought to be through an abiotic reaction, not the direct reduction by microbes (Lovley *et al.*, 1991). Since then, direct enzymatic U(VI) reduction is a well known mechanism and it's mostly notable among sulfate reducing bacteria (SRB) and iron reducing bacteria (IRB) (Beyenal *et al*., 2004; Cardenas *et al*., 2008). In addition, uranium reduction has also been reported for other groups of microorganisms such as the denitrifying bacteria, members of the deltaproteobacteria (Seyrig, 2010), hyperthermophilic archaea (Kashefi and Lovley, 2000), thermophilic bacteria (Cason *et al*., 2012) as well as fermentative bacteria from *Clostridium* spp. (Lloyd, 2003).

In contrast to enzymatic reduction, other microorganisms can reduce U(VI) indirectly through a non-enzymatic mechanism (Figure 1.9) (Tabak *et al*., 2005). In this type of reduction, soluble uranyl ion specie is immobilized (precipitated) by microbially formed complexing agents (Seyrig, 2010). This mechanism involves a reaction between a microbial end product and uranium (Seyrig, 2010). For example, the reduction of SO_4^{2-} yields hydrogen sulfide (H_2S) that is a by-product of sulphate reduction by SRB, which results in the reduction and precipitation of U(VI) (Seyrig, 2010). Also the ferrous iron produced in the reduction of ferric iron by IRB, results in the reduction of U(VI) as Fe(II) is re-oxidized and thus provides electrons for uranium reduction (Seyrig, 2010).

The first organisms found to catalyze the reduction of U(VI) was *Micrococcus lactilyticus* (reclassified as *Veillonella alcalescens*) (Woolfolk and Whiteley, 1962). Thereafter, the dissimilatory IRB were reported by Lovely and co-workers (1991) to carry out U(VI) reduction. A number of authors have also reported various SRB that are able to reduce U(VI) to U(IV) (Abdelouas *et al*., 1998). These SRB are ubiquitous in nature and fall under a group of anaerobic *Desulfovibrio* species, such as *D. vulgaris, D. desulfuricans*, *D. lulgaris* and *D. bacalatum* (Abdelouas *et al*., 1998; Elias *et al*., 2004; Chabalala and Chirwa, 2010a). Table 1.3 shows the mechanisms used by bacterium in the reduction and precipitation of U(VI) and with a growing number of bacteria reported to date able to reduce U(VI). Only the IRB, *Geobacter metallireducens* and *Shewanella putrefaciens*, have been reported to obtain energy for growth from using U(VI) as a terminal acceptor and this can be attributed to the outer membrane enzyme system that allows energy yield and growth (Beliaev *et al*., 2001). In

contrast, even though the SRB, especially the *Desulfovibrio* species contain the periplasmic cytochrome c_3 responsible for the reduction of U(VI), they cannot yield energy for growth (Lovley and Phillips, 1994; Chabalala and Chirwa, 2010a).

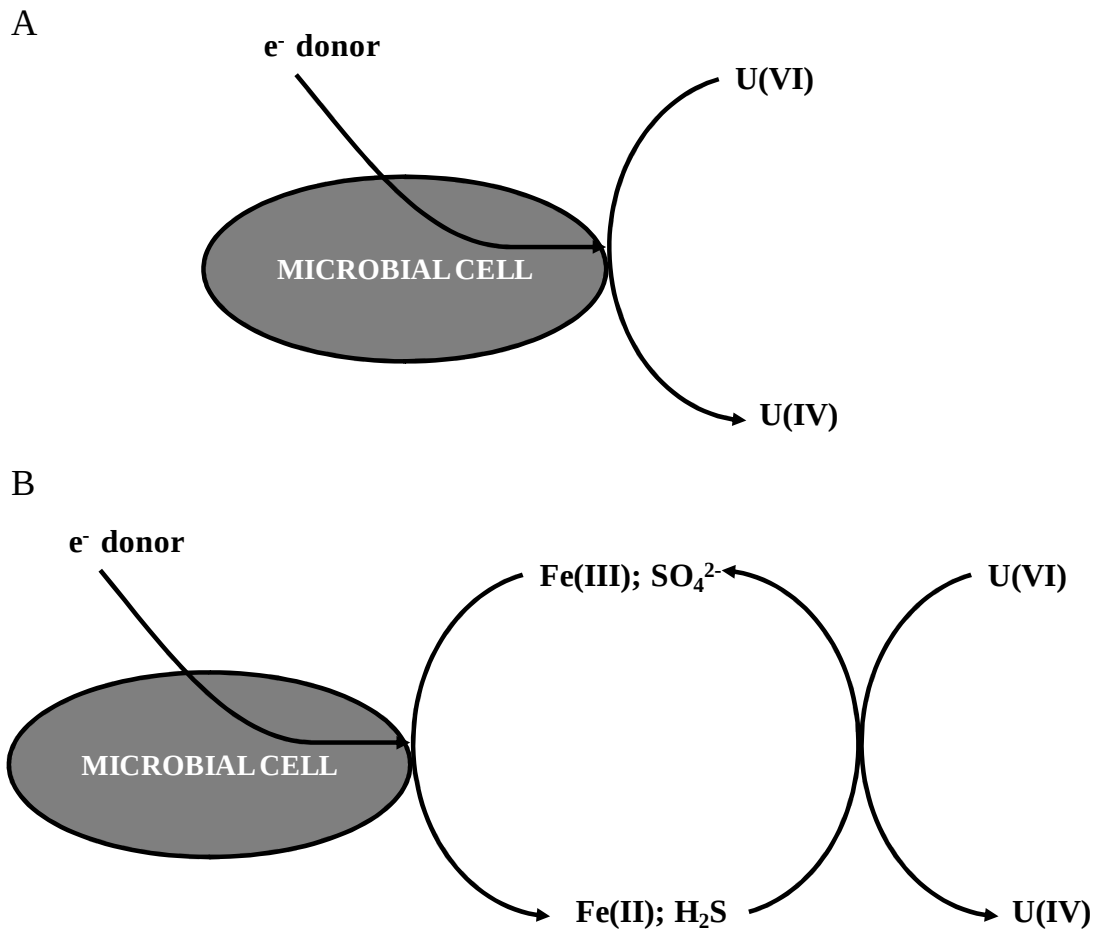

Figure 1.9: (A) Direct enzyme reduction vs. (B) Indirect immobilization of uranium (Tabak *et al*., 2005).

Table 1.3: Summary of uranium reducing bacteria (Adapted from Lloyd and Macaskie, 2000).

Organism	Comments
Micrococcus lactilyticus **(reclassified as *Veillonella alcalescens*)**	*M. lactilyticus c*ell extracts reduced U(VI) at the expense of molecular H_2; Hydrogenase activity implicated but not proven
Geobacter metallireducens **gen. nov. sp. nov. (formerly strain GS-15)**	Strict anaerobe; couples reduction of U(VI) with the oxidation of acetate or H_2 as electron donor, normally reduces Fe(III)
Geobacter argillaceus **sp. nov.**[i]	Reduces U(VI) in cell suspension; oxidizing different electron acceptors
Geobacter pickeringii **sp. nov.**[i]	Reduces U(VI) in cell suspension; oxidizing different electron acceptors
Geobacter sulfurreducens[ii]	Couples reduction of U(VI) to oxidation of acetate via cytochrome c_7
Shewanella putrefaciens	Facultative anaerobe; couples oxidation of H_2 to U(VI) reduction
Desulfovibrio desulfuricans	Couples reduction of U(VI) to oxidation of H_2 via cytochrome c_3 activity
Desulfovibrio vilgaris	Use of *in vitro* cytochrome c_3 coupled to hydrogenase for U(VI) reduction
Clostridium **sp.**	Strict anaerobe; bioreduction of U(VI) in waste
Thermus scotoductus **SA-01**[iii]	Whole cell reduction with lactate as an electron donor
Pyrobaculum isolandicum[iv]	Enzymatic reduction of uranium at 100^{o}C

[i] Shebolina *et al*., 2007 [ii] Yang *et al*., 2010 [iii] Cason *et al*., 2012 [iv] Kasheni and Lovley, 2000

Reduction through enzymatic reaction

One of the enzyme systems responsible for reduction of U(VI) is the *c*-type cytochrome, primarily present in *Desulfovibrio* species (Lovley *et al*., 1993; Merroun and Selenska-Pobell, 2008). This polyheme *c*-type enzyme cytochrome is present in the electron transport chain of all SRB (Lojou and Bianco, 1999). A specific feature for this enzyme is the low redox potential that ranges from – 200 to – 400 mV (Lojou and Bianco, 1999). Interestingly this enzyme is also capable of reducing Cr(VI) which is a analogue of U(VI) as they are hydrolyzed and relatively insoluble at low oxidation states (Lovley *et al*., 1993; Lovley and Phillips, 1994; Lojou and Bianco, 1999; Elias *et al*., 2004; Goulhen *et al*., 2006). A study by Lovley and co-workers (1993) suggested that the reduction of U(VI) by soluble cytochrome c_3 is a pathway of electron flow from hydrogen as an electron donor through hydrogenase (Figure 1.10). It has been established that reduced cytochrome c_3 from *D. vulgaris* Hildenborough could be oxidized by U(VI).

Figure 1.10 shows multiple pathways predicted for electrons from hydrogen supplied externally or produced in the cytoplasm. The protons generated from hydrogen oxidation could then be used to drive ATP synthesis through the F_1F_0 ATP synthase pictured in the cytoplasmic membrane (far left). The electrons generated from hydrogen oxidation are transferred into the *c*-type cytochrome network for delivery through the cytoplasmic membrane via membrane-bound electron carriers for reduction of the terminal electron acceptors sulfate or thiosulfate (Heidelberg *et al*., 2004).

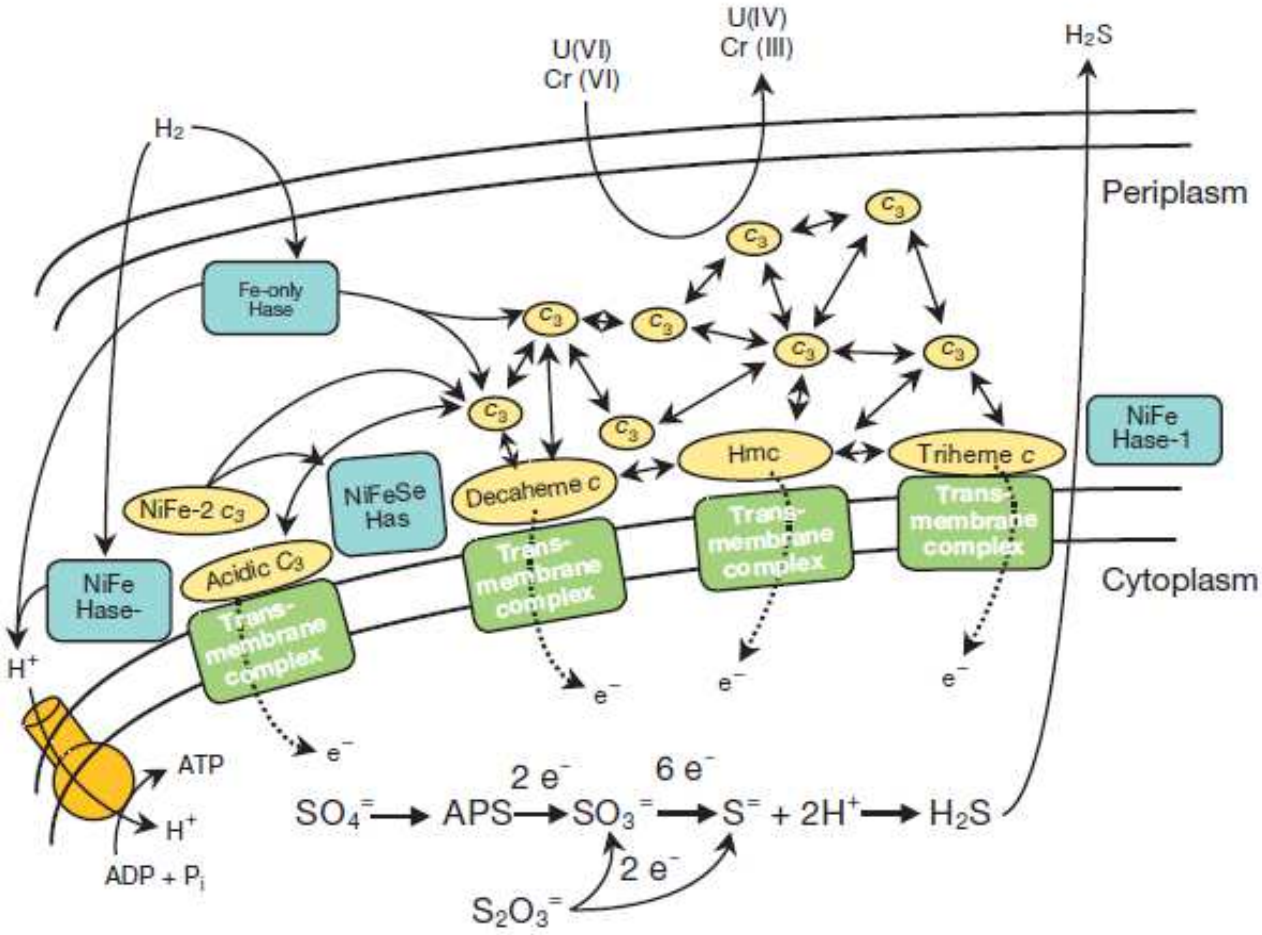

Figure 1.10: *Desulfovibrio vulgaris* c-type cytochrome network. Diagrammatic view of the c-type cytochrome network potentially present in the periplasm of *D. vulgaris* Hildenborough, and the associated periplasmic hydrogenases and transmembrane complexes (Taken from Heidelberg *et al*., 2004).

Lojou and Bianco (1999) showed that the efficiency of U(VI) reduction process originates in the presence of the heme-containing groups, such as the low redox-potential polyheme cytochromes. In 2000, Payne and co-workers developed a cytochrome c_3 mutant of *D. desulfuricans* to demonstrate that the enzyme was essential for U(VI) reduction. It was concluded that the parent strain *D. desulfuricans* G20 was able to reduce U(VI) enzymatically with various electron donors, however the mutant strain lacking cytochrome c_3 reduced U(VI) poorly with H_2 as the electron donor.

1.3 Conclusions

Uranium is ubiquitous in the environment as it can be found in soil, rocks, sediments and groundwater. It can be found in 4 oxidation states, namely U(III), U(IV), U(V) and U(VI). However, in aqueous solution it is primarily found in the IV and VI oxidation states. The U(VI) oxidation state is in the form of uranyl ions which is highly mobile and soluble in groundwater systems, in contrast the U(IV) is immobile and insoluble. Uranium can contaminate the environment through a number of processes; these include uranium mining, ore transportation and tailing disposals. However, in South Africa, it is mainly mined as a by-product through gold mining; as a result areas around the mining sites become contaminated with this heavy metal. Even though uranium is radioactive and toxic to the cells, many microbes can interact with it when encountered in the environment. This is because microbes have developed resistance mechanisms that allow them to thrive in such hostile environments. A number of interactions can occur between uranium and microbes, several of these interactions can be used in the bioremediation of uranium contaminated sites as they are able to immobilize/precipitate the uranyl ion, therefore limiting contamination. To date four mechanisms involved in uranium immobilization have been described and removal of uranium by these mechanisms is environmentally friendly and cost effective as compared to the available chemical methods in use.

1.4 References

- **Abdelouas, A., Lu, Y., Lutze, W. and Nuttall, H.E.** (1998) Reduction of U(VI) to U(IV) by indigenous bacteria in contaminated ground water. *Journal of Contaminant Hydrology*. **35**:217-233.

- **Ahalya, N., Ramachandra, T.V. and Kanamadi, R.D.** (2003) Biosorption of heavy metals. *Research Journal Of Chemistry And Environment*. **7**(4):71-78.

- **Ander, L. and Smith B.** (2002) 'Annexe F: Groundwater transport modelling' In The health hazards of depleted uranium part II. *The Royal Society*.

- **Ato, A.F., Samuel, O., Oscar, Y.D., Moi, P.A.N. and Akoto, B. (**2010) Mining and heavy metal pollution: Assessment of aquatic environments in Tarkwa (Ghana) using multivariate statistical analysis. *Journal of Environmental Statistics*. **1**(4):1-13.

- **Bajwa, I., Nawaz, H. and Bhatti, T.M.** (2003) Uranium solubilization from rock phosphate in carbonate leaching media. *International Journal Of Agriculture and Biology*. **1**(2):24-28.

- **Basnakova, G. and Macaskie, L.E.** (1997) Microbially enhanced chemisorption of nickel into biologically synthesized hydrogen uranyl phosphate: A novel system for the removal and recovery of metals from aqueous solutions. *Biotechnology and Bioengineering*. **54**(4):319-328.

- **Beliaev, A.S. and Saffarini, D.A.** (1998) *Shewanella putrefaciens mtrB* encodes an outer membrane protein required for Fe(III) and Mn(IV) reduction. *The Journal of Bacteriology*. **180**:6292-6297.

- **Beliaev, A.S., Saffarini, D.A., McLaughlin, J.L and Hunnicutt, D.** (2001) MtrC, an outer membrane decaheme *c* cytochrome required for metal reduction in *Shewanella putrefaciens* MR-1. *Molecular Microbiology*. **39**(3):722-730.

- **Bem, H. and Bou-Rabee, F.** (2004) Environmental and health consequences of depleted uranium use in the 1991 Gulf War. *Environment International*. **30**:123-134.

- **Beyenal, H., Sani, R.K., Peyton, B.M., Dohnalkova, A.C., Amonette, J.E. and Lewandowski, Z.** (2004) Uranium immobilization by sulfate-reducing biofilms. *Environ. Sci. Technol.* **38**:2067-2074.

- **Bhagure, G.R. and Mirgane, S.R.** (2011) Heavy metal concentrations in groundwaters and soils of Thane Region of Maharashtra, India. *Environ Monit Assess*. **173**:643-652.

- **Bleise, A., Danesi, P.R. and Burkart, W.** (2003) Properties, use and health effects of depleted uranium (DU): a general overview. *Journal of Environmental Radioactivity*. **64**:93-112.

- **Brady, D. and Duncan, J.R.** (1994) Bioaccumulation of metal cations by *Saccharomyces cerevisiae*. *Appl Microbiol Biotechnol*. **41**:149-154.

- **Brandl, H. and Faramarzi, M.A.** (2006) Microbe-metal-interactions for the biotechnological treatment of metal-containing solid waste. *China Particuology*. **4**(2):93-97.

- **Cardenas, E., W, W., Leigh, M.B., Carley,J., Carroll, S., Gentry, T., Luo, J., Watson, D., Gu, B., Ginder-Vogel, M., Kitanidis, P.K., Jardine, P.M., Zhou, J., Criddle, G.S., Marsh, T.L. and Tiedje, J.M.** (2008) Microbial communitities in contaminated sediments, associated with bioremediation of uranium to submicromolar levels. *Applied and Environmental Microbiology*. **74**(12):3718-3729.

- **Cason, E.D., Piater, L.A. and van Heerden, E.** (2012) Reduction of U(VI) by the deep subsurface bacterium, *Thermus scotoductus* SA-01, and the involvement of the ABC transporter protein. *Chemosphere*. **86**(6):572-577.

- **Chabalala, S. and Chirwa, E.M.N.** (2010a) Removal of uranium(VI) under aerobic and anaerobic conditions using indigenous mine consortium. *Minerals Engineering*. **23**:256-231.

- **Chabalala, S. and Chirwa, E.M.N.** (2010b) Uranium(VI) reduction by high performing purified anaerobic cultures from mine soil. *Chemospere*. **78**(1):52-55.

- **Choudhary, S. and Sar, P.** (2011) Uranium biomineralization by a metal resistant *Pseudomonas aerugenosa* strain isolated from contaminated mine waste. *Journal of Hazardous Material*. **186**(1):336-343.

- **Craft, E.S., Abu-Qare, A.W., Flaherty, M.M., Garofolo, M.C., Rincavage, H.L. and Abou-Donia, M.B.** (2004) Depleted and natural uranium: Chemistry and toxicological effects. *Journal of Toxicology and Environmental Health*. **7**:297-317.

- **Ehrlich, H.L.** (1997). Microbes and metals. *Appl Microbiol Biotechnology*. **48**:687-692.

- **El-Hendawy, H.H., Ali, D.A., El-Shatoury, E.H. and Ghanem, S.M.** (2009) Bioaccumulation of heavy metals by *Vibrio alginolyticus* isolated from waste of Iron and Steel Factory, Helwan, Egypt. *Egypt. Acad. J. Biolog. Sci.*, **1**(1)23-28.

- **Elias, D.A., Suflita, J.M., McInerney, M.J. and Krumholz, L.R.** (2004) Periplasmic cytochrome c_3 of *Desulfovibrio vulgaris* is directly involved in H_2-Mediated metal but not sulfate reduction. *Applied and Environmental Microbiology*. **70**(1):413-420.

- **Elles, M.P. and Lee, S.Y.,** (1998) Uranium solubility of carbonate-rich uranium-contaminated soils. *Water, Air and Soil Pollution*. **107**:147-162.

- **Finlay, J.A., Allan, V.J.M., Conner, A., Callow, M.E., Basnakova, G. and Macaskie, L.E.** (1998) Phosphate release and heavy metal accumulation by biofilm-immobilized and chemically-coupled cells of a *Citrobacter* sp. pre-grown in continuous culture. **63**(1):87-97.

- **Finneran, K.T., Housewright, M.E. and Lovley, D.R.** (2002a) Multiple influences of nitrate on uranium solubility during bioremediation of uranium-contaminated subsurface sediments. *Environmental Microbiology.* **4**(9):510-516.

- **Finneran, K.T., Forbush, H.M., VanPraagh, C.V.G. and Lovley, D.R.** (2002b) *Desulfitobacterium metallireducens* sp. nov., an anaerobic bacterium that couples growth to the reduction of metals and humic acids as well as chlorinated compounds. *International Journal of Systematic and Evolutionary Microbiology*. **52**:1929-1935.

- **Fredrickson, J.K., Kostandarithes, H.M., Li, S.W., Plymale, A.E. and Daly, M.J.** (2000) Reduction of Fe(III), Cr(VI), U(VI), and Tc(VII) by *Deinococcus radiodurans* R1. *Applied and Environmental Microbiology*. **66**(5):2006-2011.

- **Gadd, G.M.** (2010) Metals, minerals and microbes: geomicrobiology and bioremediation. *Microbiology*. **156**:609-643.

- **Galperin, A. (1992) Nuclear Energy, Nuclear Waste. Image adapted from (website reference) (Accessed 4 October 2012).**

- **Goulhen, F., Gloter, A., Guyot, F. and Bruschi, M. (2006)** Cr(VI) detoxification by *Desulfovibrio vulgaris strain Hilden*borough: microbe-metal interactions studies. *Appl Microbiol Biotechnol.* **71**:892-897.

- **Gregory, K.B. and Lovley, D.R.** (2005) Remediation and recovery of uranium from contaminated subsurface environments with electrodes. *Environ. Sci. Technol*. **39**:8943-8947.

- **Heidelberg, J.F., Seshadri, R., Haveman, S.A., Hemme, C.L., Paulsen, I.T., Kolonay, J.F., Eisen, J.A., Ward, N., Methe, B., Brinkac, L.M., Daugherty, S.C., Deboy, R.T., Dodson, R.J., Durkin, A.S., Madupu, R., Nelson, W.C., Sullivan, S.A., Fouts, D., Haft, D.H., Selengut, J., Peterson, J.D., Davidsen, T.M., Zafar, N., Zhou, L., Radune, D., Dimitrov, G., Hance, M., Tran, K., Khouri, H., Gill,J., Utterback, T.R., Feldblyum, T.V., Wall, J.D., Voordouw, G. and Fraser, C.M.** (2004) The genome sequence of anaerobic, sulphate-

reducing bacterium *Desulfovibrio vulgaris* Hildenborough. *Nature Biotechnology*. **22**(5):554-559.

- **Heshmati-Rafsanjani, M.** (2009) Comparitive studies on the solubility of uranium and phosphorus in phosphate-ferilisers and their uranium transfer to plants. Ph.D *Thesis*. Technical University Carolo-Wilhelmina zu Braunschweig.

- **Hu, P., Brodie, E.L., Suzuki, Y., McAdams, H.H. and Andersen, G.L.** (2005) Whole-Genome transcriptional analysis of heavy metal stresses in *Caulobacter crescentus*. *Journal of Bacteriology*. **187**(24):8437-8449.

- **Kalin, M., Wheeler, W.N. and Meinrath, G.** (2005) The removal of uranium from mining waste water using algal/microbial biomass. *Journal of Environmental Radioactivity*. **78**:151-177.

- **Kashefi, K. and Lovley, D. R.** (2000) Reduction of Fe(Ill), Mn(IV), and toxic metals at 100°C by *Pyrobaculum islandicum*. *Applied and Environmental Microbiology*. **66**:1050-1056.

- **Khani, M.H.** (2011) Uranium biosorption by *Padina* sp. Algae biomass: kinetic and thermodynamics. *Environ Sci Pollut Res.* **18**:1593-1605.

- **Kilincarslan, A. and Akylin, S.** (2004) Uranium adsorption characteristic and thermodynamic behaviour of clinoptilolite zeolite. *Journal of Radioanalytical and Nuclear Chemistry*. **264**(3):541-548.

- **Kumar, A., Rout, S., Narayanan, U., Mishra, M.K., Tripathi, R.M., Singh, J., Kumar, S. and Kushwaha, H.S. (**2011) Geochemical modelling of uranium speciation in the subsurface aquatic environment of Punjab State in India. *Journal of Geology and Mining Research.* **3**(5):137-146.

- **Lloyd, J.R.** (2003) Microbial reduction of metals and radionuclides. *FEMS Microbiology Reviews*. **27**:411-425.

- **Lloyd, J.R. and Lovley, D.R.** (2001) Microbial detoxification of metals and radionuclides. *Current Opinion in Biotechnology*. **12**:248-253.

- **Lloyd, J.R. and Macaskie, L.E.** (2000) 'Bioremediation of radionuclides' In **Lovley, D.R.** (ed.) *Environmental microbe-metal interactions*. Washington: ASM press.

- **Lloyd, J.R. and Renshaw, J.C.** (2005) Bioremediation of radioactive waste: radionuclide-microbe interactions in laboratory and field-scale studies. *Current Opinion in Biotechnology*. **16**:254-260.

- **Lofty, S.M., Mostafa, A.Z. and Abdel-Sabour, M.F.** (2012) Fractionation of uranium forms as affected by spiked soil treatment and soil type. *Arab Journal of Nuclear Sciences and Applications*. **42**(2):516-522.

- **Lojou, E. and Bianco, P.** (1999) Electron reduction of uranium by bacterial cytochromes: biochemical and chemical factors influencing the catalytic process. *Journal of Electroanalytical Chemistry*. **471**:96-104.

- **Lovley, D.R. and Coates, J.D.** (1997) Bioremediation of metal contamination. *Current Opinion in Biotechnology*. **8**:285-289.

- **Lovley, D.R. and Phillips, E.J.P.** (1994) Reduction of chromate by *Desilfovibrio vulgar* and its c_3 cytochrome. *Applied and Environmental Microbiology*. **60**(2):726-728.

- **Lovley, D.R., Phillips, E.J.P., Gorby, Y.A. and Landa, E.R.** (1991) Microbial reduction of uranium. *Nature*. **350**:413-416.

- **Lovley, D.R., Roden, E.E., Phillips, E.J.P. and Woodward, J.C.** (1993) Enzymatic iron and uranium reduction by sulfate-reducing bacteria. *Marine Geology*. **113**:41-53.

- **Macaskie, L.E., Empson, R.M., Cheetham, A.K., Grey, C.P. and Skarnuliss, A.j.** (1992) Uranium bioaccumulation by a *Citrobacter* sp. as a result of

enzymatically mediated growth of polycrystalline HUO_2PO_4. *Science*. **257**:782-784.

- **Macaskie, L.E., Bonthrone, K.M., Yong, P. and Goddard, D.T.** (2000) Enzymatically mediated bioprecipitation of uranium by a *Citrobacter* sp.: a concerted role for exocellular lipopolysaccharide and associated phosphatase in biomineral formation. *Microbiology*. **148**:1855-1867.

- **Martinez, R.J., Beazley, M.J., Taillefert, M., Arakaki, A.K., Skolnick, J. and Sobecky, P.A.** (2007) Aerobic uranium(VI) bioprecipitation by metal-resistant bacteria isolated from radionuclide-and metal-contaminated subsurfaces soils. *Environmental Microbiology*. **9**(12):3122-3133.

- **Merroun, M.L. and Selenska-Pobell, S.** (2008) Bacterial interactions with uranium: An environmental perspective. *Journal of Contaminant Hydrology*. **102**:285-295.

- **Moon, H.S., McGuinness, L., Kukkadopu, R.K., Peacock, A.D., Komlos, J., Kerkhof, L.J., Long, P.E. and Jaffe, P.R.** (2010) Microbial reduction of uranium under iron- and sulphate-reducing conditions: Effect of amended goethite on microbial community composition and dynamics. *Water Research*. **44**:4015-4038.

- **Murr, L.E.** (2006) Biological issues in materials science and engineering: interdisciplinarity and the bio-materials paradigm. *JOM*. **58**(7):23-33.

- **Nagy, A.S., Zavodska, L., Matel, L. and Lesny, J.** (2009) Geochemistry and determination possibilities of uranium in natural waters. *Acta Technica Jaurinesis*. **2**(1):19-34.

- **Nevin, K.P., Finneran, K.T. and Lovley, D.R.** (2003) Microorganisms associated with uranium bioremediation in a high-salinity subsurface sediment. *Applied and Environmental Microbiology*. **69**(6):3672-3675.

- **Parameswari, E., Lakshmanan, A. and Thilagavathi, T.** (2009) Biosorption of chromium(VI) and nickel(II) by bacterial isolates from an aqueous solution. *Electronic Journal of Environment, Agricultural and Food Chemistry*. **8**(3):150-156.

- **Payne, R.B.** (2005) Energy metabolism and uranium(VI) reduction by *Desulfovibrio*. *Thesis*. University of Missouri-Columbia.

- **Payne, R.B., Gentry, D.M., Rapp-Giles, B.J., Casalot, L. And Wall, J.D.** (2005) Uranium reduction by *Desulfovibrio desulfuricans* strain G20 and a cytochrome c_3 mutant. *Applied and Environmental Microbiology*. **68**(6):3129-3132.

- **Rathnayake, I.V.N., Megharaj, M., Bolan, N. and Naidu, R.** (2010) Tolerance of heavy metals by gram positive soil bacteria. *International Journal of Civil and Environmental Engineering*. **2**(4):191-195.

- **Seyrig** (2010). Uranium bioremediation: current knowledge and trends. *Basic Biotechnology*. **6**:19-24.

- **Shelobolina, E.S., O'Neil, K., Finneran, K.T., Hayes, L.A. and Lovley, D.R.** (2003) Potential for *In Situ* bioremediation of a low-pH, high-nitrate uranium-contaminated groundwater. *Soil and Sediment Contamination*. **12**:865-884.

- **Shelobolina, E.S., Sullivan, S.A., O'Neill, K.R., Nevin, K.P. and Lovley, D.R.** (2004) Isolation, characterization, and U(VI)-reducing potential of a facultatively anaerobic, acid-resistant bacterium from low-pH, nitrate- and U(VI)-contaminated subsurface sediment and description of *Salmonella subterranean* sp. nov. *Applied Environmental Microbiology*. **70**:2959-2965.

- **Shebolina, E.S., Nevin, K.P., Blakeney-Hayward, J.D., Johnsen, C.V., Plaia, T.W., Krader, P., Woodard, T., Holmes, D.E., VanPraagh, C.G. and Lovley, D.R.** (2007) *Geobacter pickeringii* sp. nov., *Geobacter argillaceus* sp. nov., sp. nov., isolated from subsurface kaolin lenses. *International Journal of Systematic and Evolutionary Microbiology*. **57**:126-135.

- **Suzuki, Y. and Banfield, J.F.** (2004) Resistance to, and accumulation of, uranium by bacteria from a uranium-contaminated sites. *Geomicrobiology Journal*. **21**:113-121.

- **Suzuki, Y., Kelly, S.D., Kemner, K.M. and Banfield, J.F.** (2005) Direct microbial reduction and subsequent preservation of uranium in natural near-surface sediment. *Applied and Environmental Microbiology*. **71**(4):1790-1797.

- **Tabak, H.H., Lens, P., van Hullebusch, E.D. and Dejonghe, W.** (2005) Development in bioremediation of soils and sediments polluted with metals and radionuclides – 1. Microbial processes and mechanisms affecting bioremediation of metal contamination and influencing metal toxicity and transport. **4**:115-156.

- **Tripathi, R.M., Sahoo, S.K., Jha, V.N., Khan, A.H. and Puranik, V.D.** (2008) Assessment of environmental radioactivity at uranium mining, processing and tailings management facility at Jaduguda, India. *Applied Radiation and Isotopes.* **66**:1666-1670.

- **Udofia, G.E., Essien, J.P., Eduok, S.I. and Akpan, B.P.** (2009) Bioaccumulation of heavy metals by yeast from Qua Iboe estuary mangrove sediment ecosystem, Nigeria. *African Journal of Microbiology Research*. **3**(12):862-869.

- **Vaughan, D.J. and Lloyd, J.R.** (2011) Mineral-organic-microbe interactions: Environmental impacts from molecular to macroscopic scales. *C. R. Geoscience*. **343**(2-3):140-159.

- **Volesky, B. and May-Phillips, H.A.** (1995) Biosorption of heavy metals by *Saccharomyces cerevisiae*. *App Microbiol Biotechnol*. **42**:797-806.

- **Wall, J.D. and Krumholz, L.R.** (2006) Uranium reduction. *Annual Review of Microbiology*. **60**:149-66.

- **Wang, B.E. and Hu, Y.Y.** (2008) Bioaccumulation versus adsorption of reactive dye by immobilized growing *Aspergillus fumigatus* beads. *Journal of Hazardous Materials*. **157**:1-7.

- **Winde, F., Wade, P. and van der Walt, I.J.** (2004) Gold tailings as a source of waterborne uranium contamination of streams – The Koekemoerspruit[#] (Klerksdorp goldfields, South Africa) as a case study. Part I of III: Uranium migration along the aqueous pathway. *Water SA*. **30**(2):219-225.

- **Woolfolk, C.A. and Whitely, H.R.** (1962) Reduction of inorganic compounds with molecular hydrogen by *Micrococcus lactilyticus*. *J. Bacteriol.* **84**:647-658.

- **Yang, T.H., Coppi, M.V., Lovley, D.R. and Sun, J.** (2010) Metabolic response of *Geobacter sulfurreducens* towards electron donor/acceptor variation. *Microbial Cell Factories*. **9**(90):1-15.

Chapter 2

2.1 Introduction to the present study

Uranium can occur in the environment either due to natural or anthropogenic sources, and in South Africa (S A) particularly, uranium is mainly in the environment as a result of anthropogenic sources (tailings) through gold mining (Robertson and Feather, 2004; Winde *et al.*, 2004). Since the early 1950s, about 240 000 t of uranium was exported by uranium-producing gold mines in S A, however, it is estimated that approximately 600 000 t is still contained in gold mining tailings (Winde, 2010). Groundwater plays a vital role in the transportation of uranium and usually this is an uncontrolled migration in the environment (Winde, 2010). It is thus not surprising that slimes dams and areas around former gold-uranium mines, are contaminated with uranium. One of many areas contaminated by uranium is the Wonderfonteinspruit catchment, which is located in the North West Province, S A. During mining in this area, approximately 100 000 t of U_3O_8 was obtained through gold mining at depths of up to 3 000 m (Winde, 2010).

Uranium is one of the most toxic and radioactive metals (Fairlie, 2009; Khani, 2011). The presence of uranium in the environment is a concern and is hazardous to humans in four ways, namely (a) as a toxic heavy metal, (b) as a chemical carcinogen (c) as an endocrine disruptor and (d) as a radiation carcinogen (Fairlie, 2009). Although studies of uranium health effects are mostly based on animal experiments, in S A, a study was reported which linked uranium levels in groundwater to higher incidences of atypical lymphocytes related to leukaemia in the community involved, hence providing some direct epidemiological health effects on humans (Winde, 2010). The presence of uranium in the environment is a great health concern, and thus important to minimize its spread in the environment. A number of methods are utilized for the removal of uranium from wastewater and process effluents (Konstantinou *et al*., 2007). However, the technologies are both costly and ineffective, particularly when the concentration of uranium is very low (Konstantinou *et al*., 2007). As a result, the use of microbial agents such as bacteria is widely used for the removal of uranium (Ahemad, 2012; Viladi, 2001), not only is this process economical but it is more effective for the removal of uranium especially at low concentrations. Uranium can still have significant adverse health effects even at these low concentrations and that is why it is important to remediate as much as possible uranium from contaminated sites (Bleise *et al*., 2003).

Microorganisms are ubiquitous in the environment, thus they offer a potentially enormous pool to select from when looking for enzymes that can help treat metal contamination (Lloyd, 2002). These microorganisms are those that exist from indigenous environments contaminated with metals, such as uranium. The indigenous microorganisms can be used as a remediation strategy for contaminated uranium environments because they have evolved a wide range of biochemical mechanisms to protect themselves from potentially toxic metals (Lloyd, 2002). As stated in section 1.2.4, one of the enzyme mechanisms responsible for reduction of U(VI), is the *c*-type cytochrome. Interestingly this enzyme is also capable of reducing Cr(VI), which is a analogue of U(VI) as they are hydrolyzed and relatively insoluble at low oxidation states.

2.2 The aims of the present study

- To use and adapt Cr(VI) reduction studies from earlier work performed in the research group as a model for U(VI) reduction studies.
- To characterize microbial uranium bioreduction and metal-microbe interactions.

2.3 References

- **Ahemad, M.** (2012) Implications of bacterial resistance against heavy metals in bioremediation: a review. *IIOABJ*. **3**(3):39-46.

- **Bleise, A., Danesi, P.R. and Burkart, W.** (2003) Properties, use and health effects of depleted uranium (DU): a general overview. *Journal of Environmental Radioactivity*. **64**:93-112.

- **Fairlie, I.** (2009) Depleted uranium: properties, military use and health risks. *Medicine, Conflict and Survival*. **25**(1):41-64.

- **Khani, M.H.** (2011) Uranium biosorption by *Padina* sp. Algae biomass: kinetic and thermodynamics. *Environ Sci Pollut Res.* **18**:1593-1605.

- **Konstantinou, M., Demetriou, A. and Pashalidis, I.** (2007) Adsorption of hexavalent uranium on dunite. *Global NEST Journal*. **9**(3):229-236.

- **Lloyd, J.R.** (2002) Bioremediation of metals; the application of micro-organisms that make and break minerals. *Microbiology Today*. **29**(5):67-69.

- **Robertson, M. E. A. and Feather, C.E.** (2004) Determination of gold, platinum and uranium in South African ores by high-energy XRF spectrometry. *X-Ray Spectrom.* **33**:164-173.

- **Vidali, M.** (2001) Bioremediation. An overview. *Pure Appl. Chem.* **73**(7):1163-1172.

- **Winde, F.** (2010) Uranium pollution of the Wonderfonteinspruit, 1997-2008. Part 2: Uranium in water – concentrations, loads and associated risks. *Water SA.* **36**(3):257-278.

- **Winde, F., Wade, P. and van der Walt, I.J.** (2004) Gold tailings as a source of waterborne uranium contamination of streams – The Koekemoerspruit[#] (Klerksdorp goldfields, South Africa) as a case study. Part I of III: Uranium migration along the aqueous pathway. *Water SA.* **30**(2):219-225.

Chapter 3

3.1 Introduction

Chromium (Cr) is the 21st most abundant element in the earth crust and was discovered in 1797 (Zou *et al*., 2006). It is the 24th element in the periodic table with a relative atomic mass of 51.97 (Owlad *et al*., 2009). Chromium exists in several oxidation states (Table 3.1), ranging from Cr(-II) to Cr(VI), with Cr(III) and Cr(VI) being the most common and stable (Kim *et al*., 2001; Farag and Zaki, 2010). These two oxidation states have widely contrasting and transport characteristics: Cr(VI) is more water soluble and mobile, while Cr(III) less soluble in water and less mobile (Silva *et al*., 2009).

Cr(III) is considered a trace nutrient for humans and is sometimes specifically included as a dietary supplement (Beukes *et al*., 1999; Hininger *et al*., 2007). In contrast, Cr(VI) is approximately 1 000 folds more toxic than Cr(III) and is considered to be carcinogenic (Beukes *et al*., 1999). In addition, Cr(VI) induces oxidative stress, DNA damage and apoptotic cell death (Hininger *et al*., 2007). Cr(VI) is mainly introduced in the environment as a result of anthropogenic activities, such as chrome plating, leather-tanning, wood preservation, welding, pigment production and thermonuclear weapons manufacturing (Ackerley *et al*., 2004; Zou *et al*., 2006; Wang *et al*., 2008). Like many other metals in the environment, chromium is subjected to microbial interaction. For instance, the reductive biotransformation influences chromium mobility and solubility in the environment. Similar to chromium, uranium can be reduced by the cytochrome c_3 enzyme system (Figure 1.10).

Table 3.2 shows the four oxidation states in which uranium can exist. In aqueous systems, uranium is mainly found in the U(IV) and U(VI) oxidation states (Suzuki *et al*., 2005). These oxidation states have contrasting and transport characteristics: U(IV) is less soluble in water and less mobile, as a result, does not move with the flow. In contrast, U(VI) compounds are highly soluble and mobile within aqueous systems, therefore moves with groundwater flow, spreading contamination (Suzuki *et al*., 2005).

The current pattern of industrial activity allows the natural flow of soluble metals and introduces novel toxic chemicals in the environment (Ravichandran *et al*., 2011). Fortunately, recent advances in biotechnology have made it possible to open up a window for new applications, this includes the use of microbes to remediate the soluble metals such as Cr(VI)

and U(VI) from impacted environments through a process called bioremediation (Martins *et al*., 2010).

Bioremediation is a process that exploits biological agents, mainly microorganisms, e.g. yeast, fungi or bacteria to eliminate toxic material from environments and as such is an option that offers the possibility to render harmless various contaminants using natural biological activity (Vidali, 2001; Ahmed, 2010). Bioremediation is mainly classified as *ex situ* and *in situ*, the former are those technologies which involve the physical removal of the contaminated material for treatment (Boopathy, 2000). In contrast, the latter technology involves the treatment of the contaminated material in place (Boopathy, 2000). Some examples of bioremediation include *in situ* bioaugmentation and biostimulation. Bioaugmentation is defined as the addition of bacterial cultures to a contaminated medium while the latter can be defined as the stimulation of indigenous microbial population in soil or groundwater by providing necessary nutrients/electron donors (Boopathy, 2000).

Table 3.1: Chemical species of chromium in the environment according to its oxidation state (Taken from Vasilatos *et al*., 2008).

Chemical species	Oxidation state	Examples	Comments
Elemental Cr	Cr(0)		Does not occur naturally
Divalent Cr	Cr(II)	$CrBr_2$, $CrCl_2$, CrF_2, CrSe, Cr_2Si	Relatively unstable and is readily oxidized to the trivalent state
Trivalent Cr	Cr(III)	CrB, CrB_2, $CrBr_3$, $CrCl_3.6H_2O$, $CrCl_3$, CrF_3, CrN	Forms unstable compounds and occurs in nature in ores, such as ferrochromite ($FeCr_2O_4$)
Tetravalent Cr	Cr(IV)	CrO_2, CrF_4	Does not occur naturally. The Cr(IV) ion and its compounds are not very stable and because of short half−lives, defy detection as reaction intermediates between Cr(VI) and Cr(III)
Pentavalent Cr	Cr(V)	CrO_4^{3-}, potassium perchromate	Does not occur naturally. Chromium (V) species are derived from the anion CrO_4^{3-} and are long-lived enough to be observed directly. However, there are relatively few stable compounds containing Cr(V)
Hexavalent Cr	Cr(VI)	$(NH_4)_2CrO_4$, $BaCrO_4$, $CaCrO_4$, K_2CrO_4, $K_2Cr_2O_7$	The second most stable state of Cr. However, Cr(VI) rarely occurs naturally, but is produced from anthropogenic sources. It occurs naturally in the rare mineral crocoite ($PbCrO_4$)

Table 3.2: Chemical species of uranium in the environment according to its oxidation state.

Chemical species	Oxidation state	Examples	Comments
Trivalent U	U(III)		The trivalent state of uranium can only be found in very reducing conditions in acidic solutions, pH less than 3. In oxygen-free aqueous solution, while kinetically stable, will eventually reduce water.
Tetravalent U	U(IV)	UO_2	Stable form of uranium. Occurs mainly as a black mineral precipitate uraninite.
Pentavalent U	U(V)	UO_2^+, UOX_5^{21}, UX_5 and UX_6^- (X = halide)	Occurs in small proportions over a limited redox potential range and disproportionates to U(IV) and U(VI) states. This instability also reflects the extreme air and water sensitivity of pentavalent uranium and its easy conversion/oxidation to U(VI) in the presence of trace amounts of oxygen or water.
Hexavalent U	U(VI)	UO_2^{2+}, UO_3, UF_6, UCl_6	Most stable state of uranium. Occurs mainly as uranyl ion, which is highly mobile and soluble in groundwater at pH less than 5.5. This state of uranium readily forms complexes with carbonate and calcium.

Background on the study

Earlier work performed in the research group dealt with water and soil collected from a Cr(VI) impacted site. Through the study, microbial diversity analysis of the site water indicated the presence of several different types of bacteria (predominantly *Pseudomonas* and *Bacillus* sp.). Isolation and characterisation of individual bacterial isolates revealed that some bacteria were resistant to Cr(VI). As a selection process each of the isolates were evaluated for Cr(VI) reducing ability to Cr(III) in the presence and absence of oxygen with a variety of commonly used electron donors. The *Pseudomonas mendocina* MH 50/1 isolate was successfully used in small scale laboratory bioreactors to demonstrate the applicability of Cr(VI) bioreduction. However, over time there was a shift in microbial population within the column due to the selective pressures, suggesting the dominance of indigenous bacteria within the bioreactor as a result of the external electron donor (biostimulation).

3.2 Aims

- To standardize upflow column treatment using Cr(VI) bioreduction as a model.
- To understand/benchmark uranium contaminated water by adapting the above mentioned system for small scale upflow bioreactors.

3.3 Materials and Methods

3.3.1 Sample collection and characterization

3.3.1.1 Chromium source water site description

During the early 1940's, Marble Lime and associated industries, who at that time were the lease-holders of the mine area, were commissioned by the South African Government to use their facilities to produce chrome-based tanning salts for the production of military footwear. Unlined dumps of waste material, including solid waste dumps and slimes dams containing Cr(VI) were formed during this period. Despite efforts to prevent groundwater contamination, extensive leaching of Cr(VI) into the water table has taken place during the 80-year history of the site.

The current mine, actively mines and processes marble and dolomite stone. Material extracted from an open pit quarry is transported to a central processing facility where it is crushed, graded, and washed in preparation for retail sale. This wash water is sourced from a water filled quarry and circulated via a cement holding dam at a higher elevation.

Contractual agreement prohibited full disclosure of sampling locations, thus for the purpose of this thesis generic sample names or locations of catchments were chosen and global position satellite (GPS) co-ordinates were omitted.

Water was collected from a Cr(VI) impacted mining site, Limpopo. The collected water samples were stored at 4^{o}C and sent to the Institute of Groundwater Studies (IGS), University of the Free State (UFS) for geochemistry analysis. Both water and biofilm were obtained from inside a reservoir (holding tank) containing Cr(VI) contaminated water on site, and soil samples were collected near the edge of a pond heavily impacted with Cr(VI) as core samples (Figure 3.1).

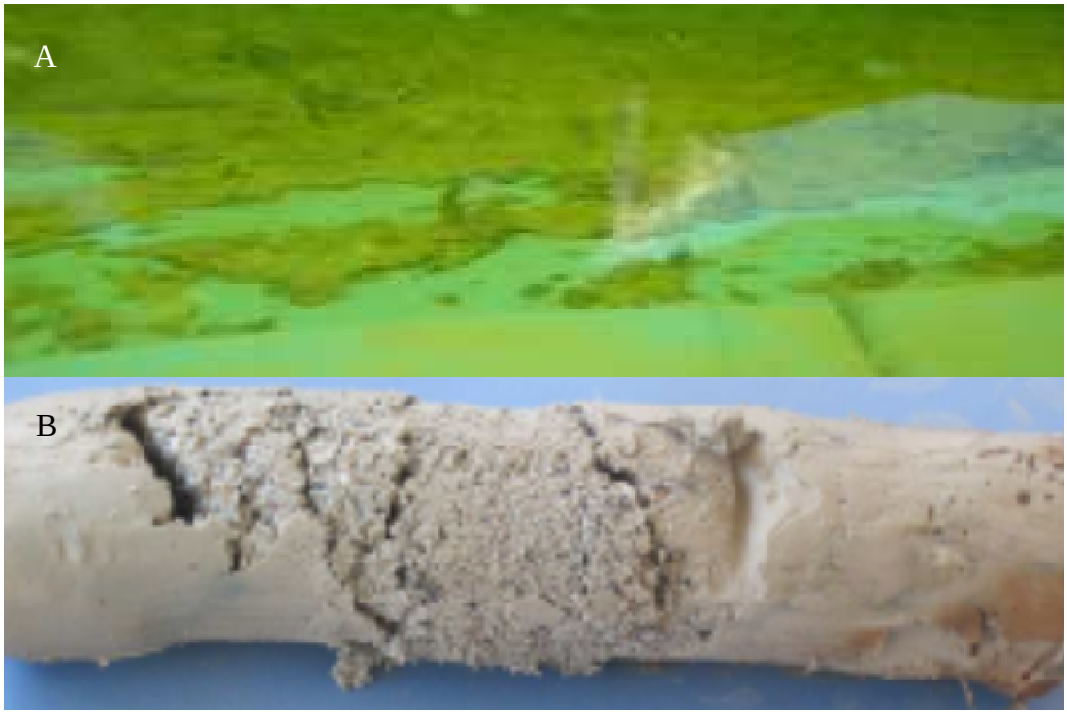

Figure 3.1: (A) Biofilm formation in a storage/holding reservoir with Cr(VI) contaminated water, (B) core soil sample obtained from Cr(VI) contaminated water.

3.3.1.2 Uranium source water site description

The Wonderfonteinspruit catchment is shown in Figure 3.2. Draining a catchment area of approximately 1 600 km^2, the Wonderfonteinspruit runs through two major mining areas, the West Rand, covering almost the entire headwater region, and the Far West Rand in the lower central part. Gold mining started in the area as early as 1887, one year after gold was discovered approximately 25 km east at the present day Johannesburg. Up until 1992, the West Rand produced a total of 1 990 t of gold, mainly from small bands of auriferous conglomerates embedded in outcropping quartzites of the Witwatersrand Supergroup. These weathering resistant rocks form part of an east-west running range of hills known as the Witwatersrand, after which the basin with the richest gold deposit on earth was named.

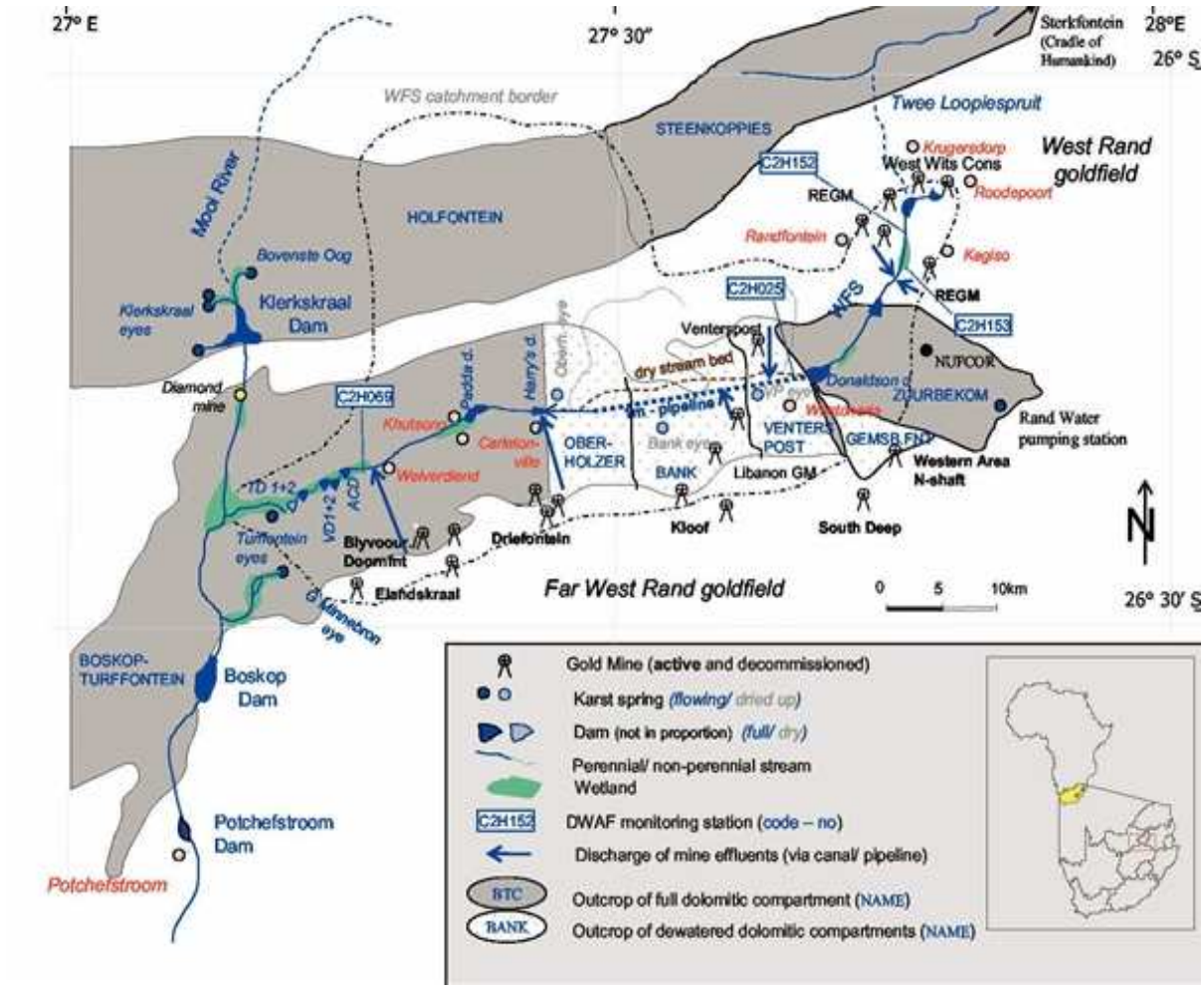

Figure 3.2: Sampling location at the Coetzee dam within the Wonderfonteinspruit catchment (Winde, 2010).

The sample water used for this research was collected in containers from an area in catchment, with the sludge collected at a depth of approximately 10 cm below the surface of the sediment on site holding's dam for wash bay distribution. The collected samples were stored at $4^{o}C$ and sent to IGS, UFS for geochemistry analysis.

3.3.2 Electron donor evaluation

In 2009, earlier work performed in the research group by Robert Jordan (M.Sc) showed effective indigenous bacteria for Cr(VI) bioreduction. The study demonstrated that several electron donors are accepted in their metabolism. After visits and investigation of the local farming industries, citric acid was selected as electron donor for Cr(VI) reduction, since it was effectively close to the site, readily available and cost effective (approximately R13/kg at the local farmer's store).

In order to test different donors that would be effective for U(VI) anaerobic reduction, 0.5 gram of the sludge from the site was used as an inoculum for various serum vials and incubated at 25°C, 45°C and 65°C for 72 h. Electron donor experiments were carried out in serum vials containing 50 ml freshwater medium inoculated with 0.5 g of the sludge from the site and a nitrogen headspace of 100 ml The media used consisted of 2.5 g/l $NaHCO_3$, 0.25 g/l NH_4Cl, 0.6 g/l $NaH_2PO_4.H_2O$, 0.1 g/l KCl, 10 ml/l Vitamin solution and 1mM Na_2SeO_3 (1 ml/l). The Vitamin solution consisted of 0.01 g/l Biotin, 0.05 g/l ρ-Aminobenzoic acid, 0.05 g/l Vitamin B_{12} and 0.1 g/l Thiamine. U(VI) in the form of uranyl acetate ($C_4H_6O_6U.2H_2O$) served as the electron acceptor, a 100 mg/l stock solution was added to a final concentration of 35 mg/l U(VI) to each vial. The electron donors added individually are: Pyruvate (1 g/l sodium pyruvate), lactate (1 g/l sodium lactate) and citric acid (2 g/l). Vials were incubated at 25°C, 45°C and 65°C for 72 h without shaking.

This media was subsequently bubbled with N_2/CO_2 (80:20). The final pH was approximately 6.7, buffered with bicarbonate and NaOH in the case of citric acid. Resazurin (0.1%) was added to each serum vial as a redox indicator to ensure no oxygen remained after preparation.

3.3.3 Bioreactor set-up

Polyvinyl chloride (PVC) columns (500 mm height X 110 mm inner diameter) were used to construct laboratory scale bioreactors with an empty bed volume of approximately 5 l (Figure 3.3). Each column had an inlet port at the bottom and outlet port at the top of the column. The PVC columns were packed with dolerite gravel, leaving a 1 cm head space at the top of the column. The columns were then filled with water and allowed to stand overnight in order to saturate and stabilize the matrix. The column was drained to determine the drainage volume. A conservative tracer breakthrough was constructed to determine pore volume of the column by pumping 200 ml of 100 mM NaCl in water into the column and measuring electrical conductivity (EC) at the outlet ports. The column was characterized to determine the static and effective porosity according to equations 3.1 and 3.2.

$$\textit{Static Porosity} = \frac{\textit{Drainage Volume (ml)}}{\textit{Empty Bed Volume (ml)}} \; X\,100 \qquad \textbf{Equation 3.1}$$

$$\textit{Efficiency Porosity} = \frac{\textit{Pore Volume (ml)}}{\textit{Empty Bed Volume (ml)}} \; X\,100 \qquad \textbf{Equation 3.2}$$

3.3.4 Bioreactor start-up and operation

The seeding material (20% w/v) was pumped at low speed in their respective columns. To allow adherence of the cells to the matrix, the columns were allowed to stand for 24 hrs without any disturbance. Consequently, the columns were operated in continuous upflow mode for the *in situ* reduction of Cr(VI) and U(VI) separately. Influent source water, amended with electron donor concentrations according to the Table 3.3 was fed into the bioreactor to achieve a hydraulic retention time (HRT) of 24 – 48. Upon citric acid addition to Cr(VI) influent source water, the pH of the water dropped from 8.31 to below 5, as a result the pH was adjusted to 6 with 1 M NaOH. The citric acid added to U(VI) column was proportionally less based on the theoretical donor demand calculation and therefore no pH adjustment needed.

Table 3.3: Bioreactors operational parameter and composition of influents.

	Chromium Bioreactor	**Uranium Bioreactor**
HRT	24 – 48 (h)	24 – 48 (h)
Electron donor	Citric acid (370 mg/l)	Citric acid (200 mg/l)

Once metal reducing conditions were established, the amount of electron donor fed to the column could be gradually decreased to correspond with the calculated electron donor demand based on the chemical composition of the source water.

3.3.5 Sampling and analysis

Two laboratory scale bioreactors were operated in a continuous upflow mode (Figure 3.3) under reducing conditions. Influent water was prepared in batches of 25 l, citric acid was added to each batch and kept at 4^{o}C during the time it was pumped into the bioreactor. Samples were taken from the effluent port for the immediate measurement of physical parameters, such as oxidation reduction potential (ORP) using the Oakton ORP Tester 10 meter, while electrical conductivity (EC), pH and temperature were measured with the ExStik II pH, Conductivity/TDS meter.

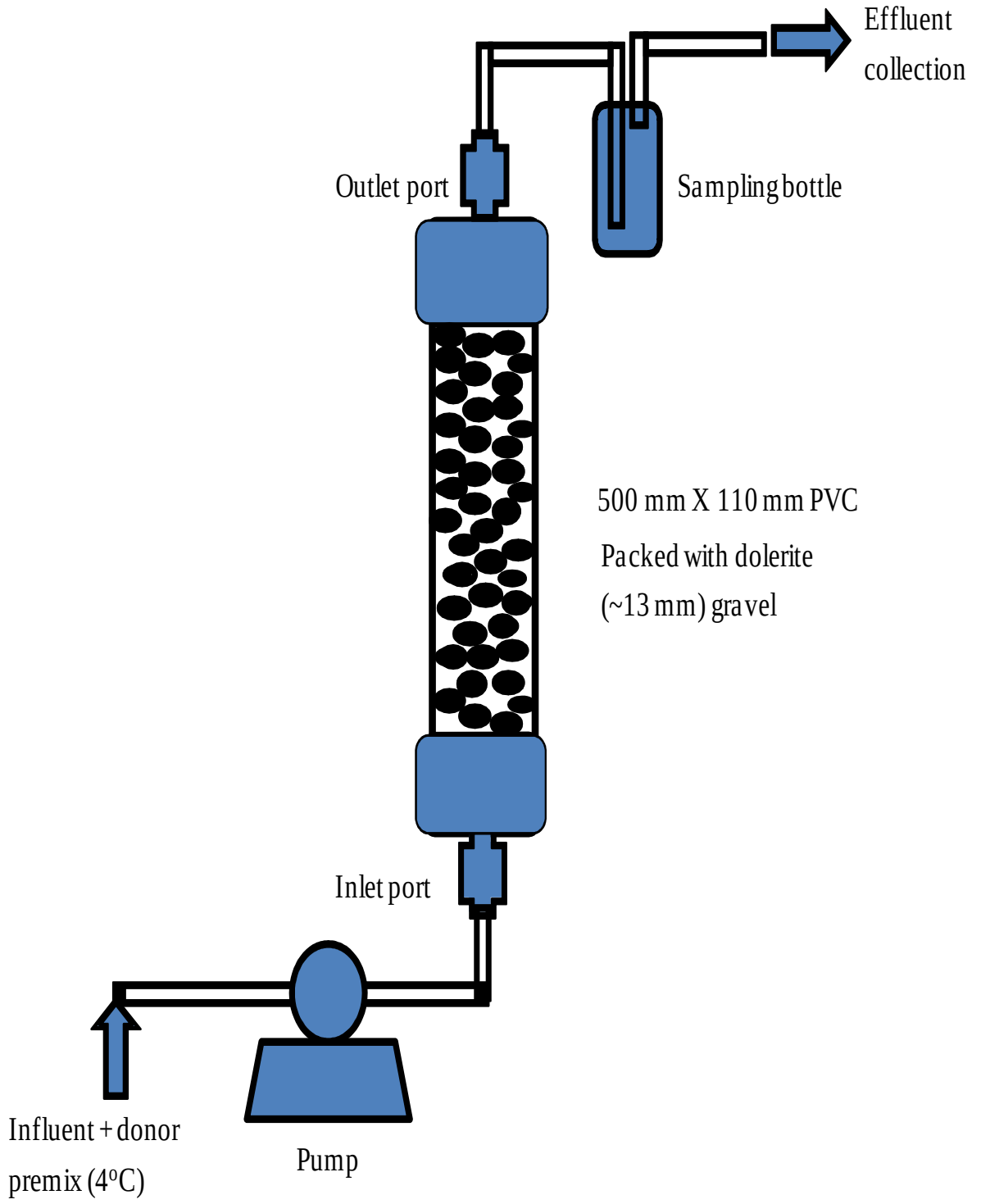

Figure 3.3: Schematic representation of the continuous upflow bioreactor.

3.3.5.1 Spectrophotometric chromium(VI) determination

Cr(VI) was analyzed by a *s*-diphenylcarbazide method as described by Urone, 1955. A stock solution of Cr(VI) of concentration 1000 mg/l was prepared by dissolving analytical grade $K_2Cr_2O_7$ in distilled water. *S*-diphenylcarbazide was used to prepare a 0.15% solution by dissolving the reagent in acetone, wrapped in foil and stored at 4^oC. A 0.12 M H_2SO_4 stock solution was prepared by dissolving 1.2 ml acid in 40 ml water, and made up to 100 ml.

Cr(VI) dilutions were made by diluting the stock solution with distilled water. 100 µl of the Cr(VI) was taken into a 2.0 ml eppendorf tube. To the above, 1000 µl of the 0.12 M H_2SO_4 solution and 100 µl of *s*-diphenylcarbazide solution were added. The resulting pink coloured solution was measured using a Spectronic® Genesys™ 5 spectrophotometer (Milton Roy Company) at 540 nm against distilled water blank. A Cr(VI) standard curve was constructed by plotting the absorbance reading against the known Cr(VI) concentration (Figure 3.4).

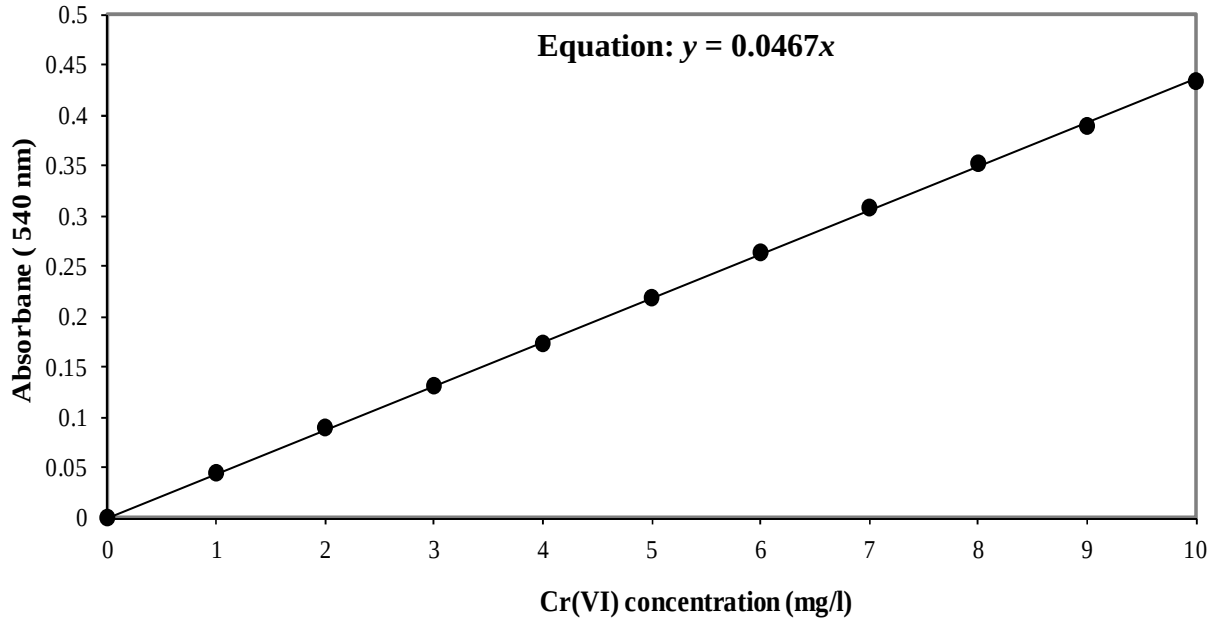

Figure 3.4: Standard curve for the determination of hexavalent chromium with the s−diphenylcarbazide method using $K_2Cr_2O_7$ as standard. The standard deviations are smaller than symbols used with $R^2 = 0.9998$.

3.3.5.2 Uranium(VI) determination by inductively coupled plasma mass spectrometry (ICP-MS) and Br-PADAP spectrophotometric method

U(VI) was analyzed by a Br-PADAP method by Johnson and Florence (1970). A stock solution of U(VI) of concentration 1000 mg/l was prepared by dissolving analytical grade $UO_2(CH_3COO)_2.2H_2O$ in distilled water. Br-PADAP was used to prepare a 0.05% solution by dissolving the reagent in ethanol, wrapped in foil and stored at 4^oC. 14 g of TEA was used to prepare a buffer solution by dissolving the reagent in 80 ml distilled water, the pH of the solution was adjusted to 7.8 with perchloric acid, left to stand overnight and made up to 100 ml. The complexing solution was prepared by dissolving 1 g NaF and 13 g sulphosacyclic acid in 40 ml distilled water, the pH of the solution was adjusted to 7.8 with NaOH, made up to 100 ml, wrapped in foil and stored at 4^oC.

U(VI) dilutions were made by diluting the stock solution with distilled water. 200 µl of the U(VI) was taken into a 2.0 ml eppendorf tube. To the above, 50 µl of the complexing solution, 200 µl Buffer solution, 160 µl Br-PADAP, 1 240 µl 100% ethanol and 150 µl distilled water were added. The resulting purple coloured solution was allowed to stand for 20 minutes and absorbance was measured using a Spectronic® Genesys™ 5 spectrophotometer (Milton Roy Company) at 578 nm against a water blank. However, a U(VI) standard curve could not be constructed due to the detection limit of the assay which was below the environmental levels of samples, as a result the assay was not used for U(VI) determination. Therefore, ICP-MS was used instead.

Effluent samples were taken in 15 ml falcon tubes for the measurement of U(VI) concentration. U(VI) was measured using an ICP-MS system at the Institution of Groundwater Studies (UFS, Free State, South Africa) with a detection limit of 0.005 mg/l (El Himri *et al*., 2012).

3.3.6 Bioreactor termination

After continuous operation for 8 weeks for the chromium bioreactor and 10 weeks for the uranium bioreactor, the reactors were terminated after maximum reduction levels were achieved. Each bioreactor was drained in timed 500 ml fractions (F1 – F4) from the inlet port and the corresponding section of the column marked (Figure 3.5). Each bioreactor was cut open and the matrix sample collected for fraction 1 was evaluated for biofilm formation and elemental composition by SEM-EDX since the most characterizing activity could be observed (Figure 3.5 C).

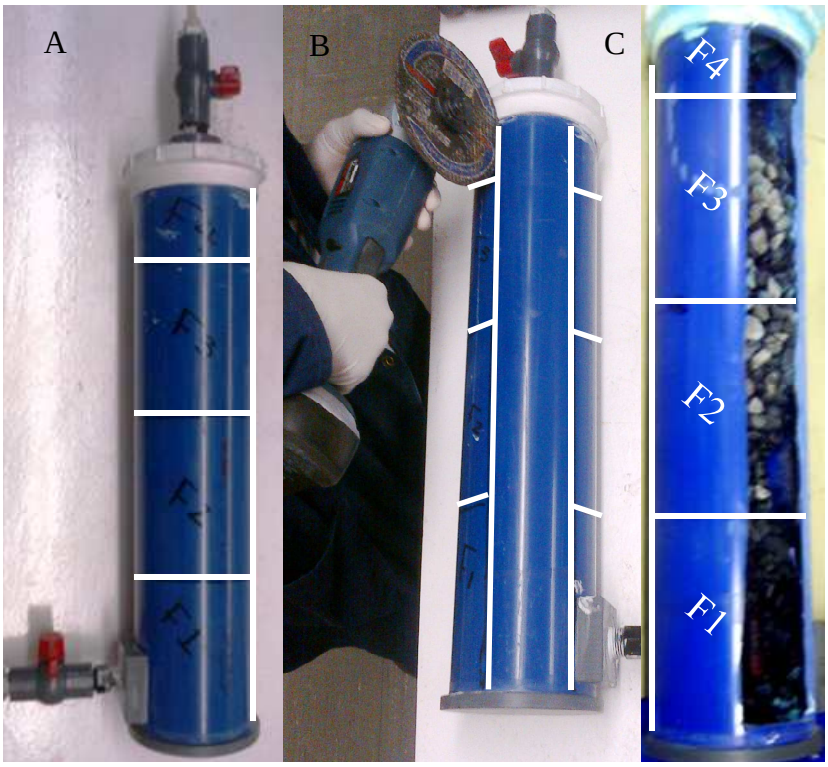

Figure 3.5: Bioreactor termination. (A) Marked bioreactor with corresponding water fraction, (B) bioreactor to be sacrificed by cutting it open with grinder and (C) an open bioreactor with black precipitate formation on fraction 1. (Note for future reference the color of matrix for harvested column).

3.3.6.1 Cell counts

DAPI (4',6-diamidino-2-phenylindole) staining was performed according to the method of Porter and Feig (1980), in which samples were fixed by adding 4% (v/v) final concentration formaldehyde solution to 1 ml of the water sample and stored at $4^{o}C$ for 20 min. The fixed samples were filtered through a 0.20 µm pore size membrane filters. A piece of membrane filter was then excised with a sterile blade and stained with 10 µl of DAPI solution (10 µg/ml) and left in the dark for 2 min at room temperature. The filter was rinsed with water, embedded with 10 µl citifluor on a glass slide and analyzed with an epifluorescence microscope.

Stained cells were enumerated under the epifluorescence microscope under 1 000X magnification. The number of cells were determined by counting 10 fields on the slide and determining the average number of cells for the fixed counting areas. The equations below were used to determine the final number of cells:

$$\text{Area (Filter)} = \pi r^2$$

$$= \pi \times 8000^2 \text{ (radius of DAPI filter = 8000)}$$

$$= 2.01 \times 10^8 \mu m^2 \qquad \textbf{Equation 3.3}$$

$$\therefore \text{No. of cells/ml} = \frac{\text{(Area of filter / Counted area) x Average no. of cells}}{\text{Volume of water filtered (ml)}} \qquad \textbf{Equation 3.4}$$

3.3.6.2 Genomic DNA (gDNA) extraction and 16S rDNA amplification

The collected water fractions from column (F1 – F4) were filtered through a membrane filter with a 0.20 μm pore size. The filters were then cut using a sterile blade and gDNA was extracted from the filters using NucleoSpin® Soil kit (Pro) according to the manufacturer's instructions. Subsequently, the gDNA extracts were visualized on a 0.8% (w/v) agarose gel stained with ethidium bromide under UV illumination.

Partial 16S rDNA fragments were amplified from the gDNA extracts using the two set of primers outlined in Table 3.4.

Table 3.4: Nucleotide sequence of primers used to amplify 16S rDNA.

Primer	Sequence	Reference
341F	5'-CCT ACG GGA GGC AGC A -3'	Muyzer et al., 1993
907RM	5'- CCG TCA ATT CMT TTG AGT TT -3'	Muyzer et al., 1993
GC clamp[a]	5'-CGCGCGCCGCGCCCCGCGCCCGTCCCGCCGCCCCCGCCCG-3'	Muyzer et al., 1993

[a] GC clamp attached to the 5'end of the primer 341F.

F= Forward primer, R = Reverse primer and M=A/C.

Each PCR reaction was performed in a total volume of 50 μl (Table 3.5), using a Thermal Cycler (PxE 0.2, Thermo Electron Corporation). PCR cycling started with an initial denaturation step at 95^{o}C for 3 min and ended with a final extension step at 72^{o}C for 10 min. Amplification was carried out at 12 cycles at 95 ^{o}C for 1 min, followed by annealing at 55 ^{o}C for 1 min and primer extension at 72 ^{o}C for 1:30 min. Then 13 additional cycles were carried out at 94 ^{o}C for 1 min, 50^{o}C for 1 min and primer extension at 72 ^{o}C for 1:30 min.

The PCR products were visualised on 1% (w/v) agarose gel UV illumination by running the amplicons against a DNA standard (Gene rulerTM DNA Ladder, Fermentas), then subsequently subjected to denaturing gradient gel electrophoresis (DGGE).

Table 3.5: PCR reaction composition.

Reagents	Volume
10X Buffer	5 µl
10 mM dNTP mix	1 µl
10 µM Forward primer	1 µl
10 µM Reverse primer	1 µl
10 µg/µl BSA	1 µl
Taq DNA polymerase	0.25 µl
Template DNA	1 µl*
Sterile water	39.75 µl
Total volume	**50 µl**

* Concentration (25ng/µl – 50ng/µl)

3.3.6.3 Denaturing gradient gel electrophoresis

DGGE is a technique used to separate PCR amplicons of the same length but different sequences by chemical denaturation. DGGE detects melting patterns of small DNA fragments (200 – 700 bp) that differs by as little as a single base substitution. Theoretically, each band within a DGGE profile is a representative of a related group of organisms, and if primer specificity is high enough, each band may represent a species or even an isolate (Muyzer *et al*., 1993; Muyzer and Smalla, 1998).

After obtaining the resulting PCR product (Section 3.3.6.2), they were then separated using DGGE, which used the Bio-Rad DCode system for casting of the gel and electrophoresis. The prepared 7% acrylamide/bis denaturing solutions are outlined in Table 3.6. To each 15 ml denaturing solution, 12.5 % (w/v) APS (100 µl) and TEMED (10 µl) were added in order to catalyze the gel polymerization. The gel was cast, allowed to polymerize for 30 min at room temperature and stored in the dark, the polymerized gel released from the casting stand and placed into the pre-heated buffer (140 ml 50X TAE filled up to 7 l with water). The PCR amplicons were loaded and allowed to run according to the conditions in Table 3.7.

Table 3.6: Urea-formamide composition.

Component	40% denaturing solution	60% denaturing solution
40% acrylamide/bis 37.5:1	8.75 ml	8.75 ml
50X TAE	1 ml	1 ml
Formamide (deionised)	8 ml	12 ml
Urea	8.4 g	12.6 g
Ultrapure water	Fill up to 50 ml	Fill up to 50 ml

Table 3.7: Operating conditions of DGGE.

Acrylamide/bis concentration	7%
Denaturing concentration gradient	40% ⟶ 60%
Temperature	60^{o}C
Voltage	100 V
Time	16 h

The gel was stained with SYBR Gold solution (Diluted 1:10 000 in 1X TAE buffer) for 15 min, washed with distilled water and subsequently examined using ChemDoc XRS (Biorad Laboratories) gel documentation system under a UV transilluminator. Dominant bands were excised; autoclaved milliQ water (50 µl) was added to each band in a 1.5 ml tube and incubated at 55^{o}C overnight to elute the DGGE bands. The resolved DGGE bands were re-amplified using the primer set 341 F and 907 RM. The PCR conditions were as follows: initial denaturation step at 95^{o}C for 5 min, followed by 25 cycles at 95^{o}C for 1 min, annealing at 53^{o}C for 1 min and primer extension at 72^{o}C for 1 min. Final extension was performed at 72^{o}C for 10 min.

The PCR products were the separated on a 1% (w/v) agarose gel and the bands corresponding to the expected size of ~600 bp were excised and purified using the Biospin Gel Extraction Kit (Bioflux) according to the manufacturer's instructions.

Table 3.8: Sequencing PCR reaction composition.

Reagents	Volume
1X Dilution Buffer	2 µl
Premix	0.5 µl
3.2 pmol Primer	1 µl
Template	6.5 µl
Total volume	**10 µl**

Sequencing was performed by using the ABI BigDye Terminator v3.1 Ready Reaction Sequencing Kit (Applied Biosystems). The reactions were made up to a total volume of 10 µl as outlined in Table 3.8. The PCR cycling consisted of 25 cycles of denaturation at 96^{o}C for 10 sec, followed by annealing at 50^{o}C for 5 sec and primer extension at 60^{o}C for 4 min.

The resulting sequencing PCR products were purified using the EDTA/Ethanol precipitation protocol. Briefly, autoclaved distilled water (10 µl) was added to PCR products to adjust the volume to 20 µl and transferred to a 1.5 ml eppendorf that contained 60 µl absolute ethanol and 5 µl EDTA (pH8.0, 125 mM) solution. This mixture was vortexed for 5 sec and allowed to precipitate at room temperature for 15 min. The 1.5 ml tubes were centrifuged for 15 min at 20 000 x g (4 ^{o}C) and the supernatant aspirated. The pellet was washed twice with a 70% (v/v) ethanol solution (100 µl), centrifuged for 5 min at 20 000 x g (4 ^{o}C) each time. The supernatant was completely aspirated and dried in the Speedvac Concentrator (Eppendorf Concentrator 5301) for 5 min. Sequencing was performed with capillary sequencer 3130xl ABI Genetic Analyzer (Applied Biosystems) at the Department of Microbial, Biochemical and Food Biotechnology (UFS, Free State, South Africa).

3.3.6.4 Scanning electron microscope and energy dispersive x-ray spectrometry

Fraction 1 matrixes were chosen for analysis since the most characterizing activity was observed in this fraction (Figure 3.5C). Matrix from the terminated bioreactors was allowed to air dry overnight, and then gradually dehydrated in a graded series of ethanol solution (50%, 70% and 100% v/v) for 15 min per solution. The ethanol-dehydrated matrix was critical-point dried, mounted, and coated with gold to make the matrix electrically conductive. Energy Dispersive X-ray spectrometry (EDX) was used to identify the chemical composition of the inorganic compounds present on the biofilm and their relative amounts, and was performed using a Thermoscientific Ultradry detector energy dispersive X-ray spectrometry system, coupled to JEOL JSM-6610 SEM, at the Department of Geology (UFS, Free State, South Africa).

3.4 Results and discussions

3.4.1 Characteristics of collected samples

Physicochemical composition of the contaminated water was obtained from IGS (UFS, Free State, South Africa). Results are outlined in Table 3.9.

The results of the physicochemical analysis indicate 7.19 mg/l Cr(VI) [highlighted in green] was present in the water samples obtained from the impacted site, and 15 µg/l of U(VI) [highlighted in yellow] were detected for the Wonderfonteinspruit water. According to the Department of water affairs (DWA, 2011), these concentrations are higher than the acceptable drinking water limit. Chromium(VI) is 14 times higher than the accepted limit, while U(VI) is 2 times higher than the accepted 15 µg/l. The results also show the presence of other metals, in summary Cr(VI) contaminated water contained nitrates, high sulphate and calcium (80.6 mg/l), while the source water contained 1.1 x 10^4 cells/ml (Figure 3.6 (A)) On the other hand Wonderfonteinspruit water contained very low concentrations of nitrates (<0.05 mg/l), a sulphate concentration of 297 mg/l and calcium (79.19 mg/l), while the water contained 2.4 × 10^5 cells/ml (Figure 3.6 (B)). The pH of the water samples for chromium and uranium containing water was 8.13 and 9.1 respectively, indicating that the contaminated sites are slightly alkaline. The alkaline pH values are in accordance with Ramenshkumar *et al.* (2010) and Bondici *et* al., (2013) who reported alkaline pH for Cr(VI) and U(VI) contaminated water respectively.

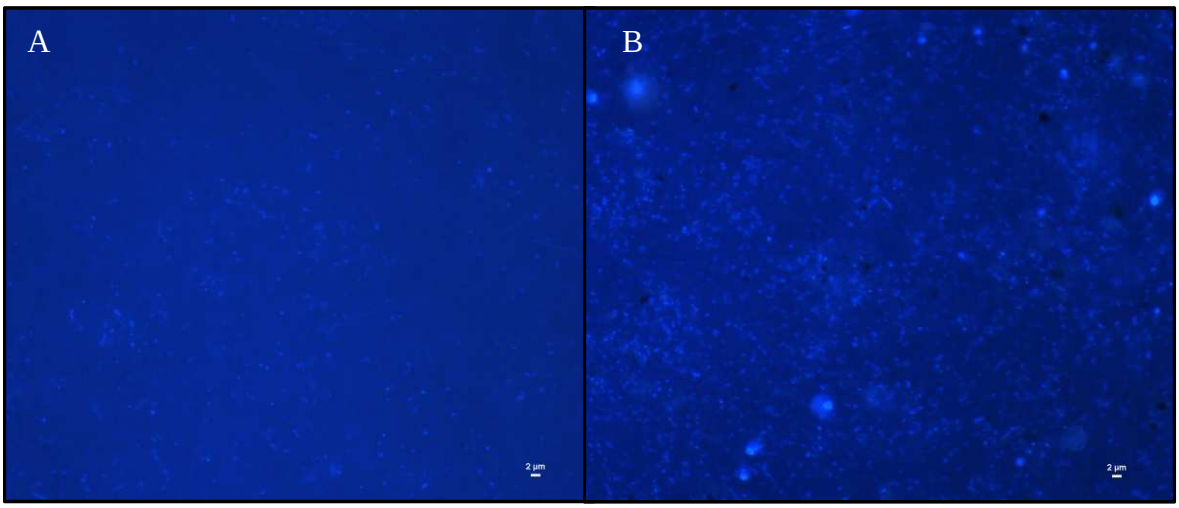

Figure 3.6: DAPI staining of influent water. (A) Cr(VI) source water and (B) U(VI) source water, 10 ml filtered.

Table 3.9: Physiochemical parameter results of the collected water samples (Values in mg/l and EC in mS/cm).

Parameters	Chromium water	Uranium water
pH	8.31	9.1
EC	162	96.7
Ca	80.6	79.19
Mg	86.5	43.04
Na	131.4	65.56
K	5.2	5.62
PAlk	0	29.6
MAlk	167	168
Cl	165.2	67.5
NO_3(N)	19.2	<0.05
PO_4	-0.1	<0.1
SO_4	434	297
Al	0.011	0.03
Cr(VI)	7.19	<0.05
Cu	0.011	0.016
Co	0.005	0.006
Li	0	0.025
Ni	<0.010	0.046
U(VI)	0.001	0.037
Zn	0.020	0.015
TOC	2.57	6.09
DOC	1.99	5.87

3.4.2 Electron donor evaluation and balancing

The source water from Cr(VI) and U(VI) impacted sites were chemically analyzed at IGS to allow stoichiometric balancing of electron donor with terminal electron acceptors to achieve an ORP that will allow maximal Cr(VI) and U(VI) reduction, respectively. In section 3.3.2 the electron donor for Cr(VI) reduction was directed by availability. Uranium resistance was followed with various electron donors and conditions described in section 3.3.2.

By stoichiometrically balancing terminal electron acceptors present in the feed water with the chosen electron donor, it is possible to calculate the theoretical amount of electron donor required to affect complete metal reduction/removal. For this purpose, oxygen, nitrate, Cr(VI)/U(VI) and a portion of available sulphates (15 mg/l) was taken into consideration. From Table 3.10 it can be seen that approximately 50 mg/l of citric acid is required to obtain 100% Cr(VI) reduction.

The results shown in Figure 3.7 shows that citric acid and pyruvate can be effective electron donors for U(VI) reduction. Citric acid was chosen to standardise as the electron donor since it was also effective for the reduction Cr(VI). Another consideration was that citric acid is a widely used food-grade additive that would have high public acceptance if the bioreactors were to be considered for up scaling.

From Table 3.11, it can be seen that half the concentration of electron donor used for Cr(VI) is required to obtain 100% U(VI). However, as stated in section 3.3.4, the start up donor feed was 200 mg/l citric acid to establish biofilm. Once metal reducing conditions were established, the amount of electron donor feed was gradually decreased to correspond with the calculated e^- donor demand in Table 3.11.

Table 3.10: Electron donor demand calculator for Cr(VI) reduction.

Electron acceptor	**Formula**	**Balanced Redox Reaction**	**Molar Ratio**
Oxygen	O_2	$2C_6H_8O_7 + 9O_2 = 8H_2O + 12CO_2$	2/9
Nitrate	NO^-_3	$5C_6H_8O_7 + 18NO_3^- + 18\ H^+ = 29H_2O + 30CO_2 + 9N_2$	5/18
Chromium(VI)	Cr^{6+}	$C_6H_8O_7 + 3CrO_3 = H_2O + 6CO_2 + 3CrOH_2$	1/3
Sulphate	SO^{2-}_4	$4C_6H_8O_7 + 9SO_4^{2-} + 18H^+ = 16H_2O + 24CO_2 + 9H_2S$	4/9
	MW (g/mol)	**Water Concentration (mg/l)**	**Donor Demand (mg/l)**
Citric acid	192.10		
Oxygen	32.00	8.00	10.67
Nitrate	62.01	19.2	16.52
Chromate	50.00	7.19	9.21
Sulphate	96.07	15.00	13.33
Total Donor Demand			**~50**
	MW (g/mol)		
Nitrate conversion	N = 14.01		
	NO^-_3 = 62.01	Ratio = 0.22593	0.15

Table 3.11: Electron donor demand calculator for U(VI) reduction.

Electron acceptor	**Formula**	**Balanced Redox Reaction**	**Molar Ratio**
Oxygen	O_2	$2C_6H_8O_7 + 9O_2 = 8H_2O + 12CO_2$	2/9
Nitrate	NO^-_3	$5C_6H_8O_7 + 18NO_3^- + 18\ H^+ = 29H_2O + 30CO_2 + 9N_2$	5/18
Uranium(VI)	U^{6+}	$C_6H_8O_7 + 9UO_3 = 4H_2O + 6CO_2 + 9UOH_2$	1/9
Sulphate	SO^{2-}_4	$4C_6H_8O_7 + 9SO_4^{2-} + 18H^+ = 16H_2O + 24CO_2 + 9H_2S$	4/9
	MW (g/mol)	**Water Concentration (mg/l)**	**Donor Demand (mg/l)**
Citric acid	192.10		
Oxygen	32.00	8.00	10.67
Nitrate	62.01	0.05	0.0043
Uranium	238.03	0.037	0.001
Sulphate	96.07	15.00	13.33
Total Donor Demand			**~24**
	MW (g/mol)		
Nitrate conversion	N = 14.01		
	NO^-_3 = 62.01	Ratio = 0.22593	0.15

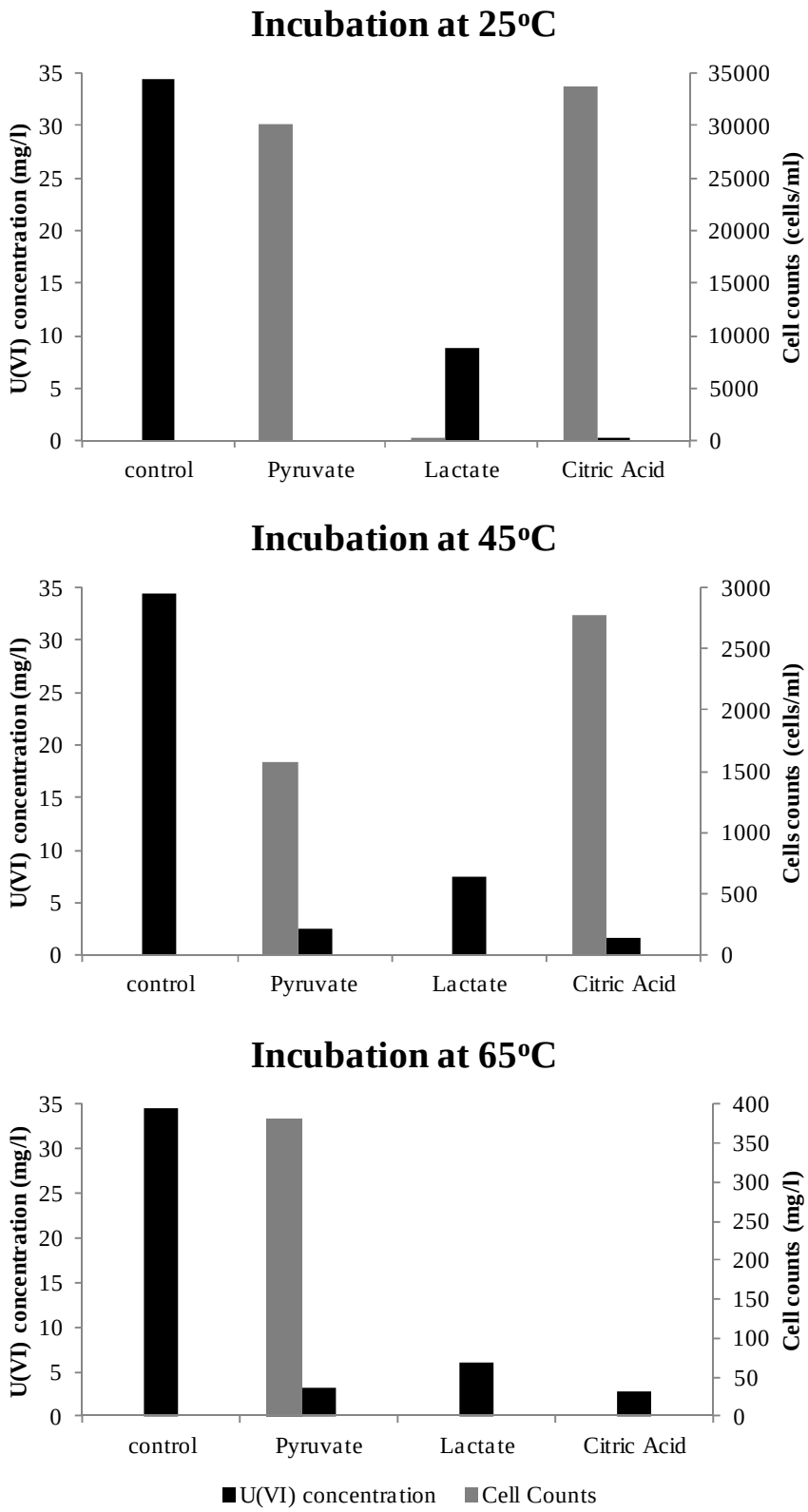

Figure 3.7: Electron donor comparison for U(VI) reduction incubated at different temperatures.

3.4.3 Column characterization

Subsequent to column packing and tracer conditioning, the conservative tracer (NaCl) breakthrough curves were constructed according to section 3.3.3.

From the conservative tracer peaks it was possible to determine the pore volume of each of the columns. A pore volume in this case can be defined as the volume of a liquid required to completely displace the same volume of liquid from a fully hydrated bioreactor. The empty bed volume (BED) of the columns was calculated to be 4.95 l.

The Cr(VI) bioreactor had a drainage volume and pore volume of 2.11 l and 2.16 l (Figure 3.8), respectively. Using equation 3.1 and 3.2, the static porosity and efficiency porosity were calculated to be 43% and 44 %, respectively.

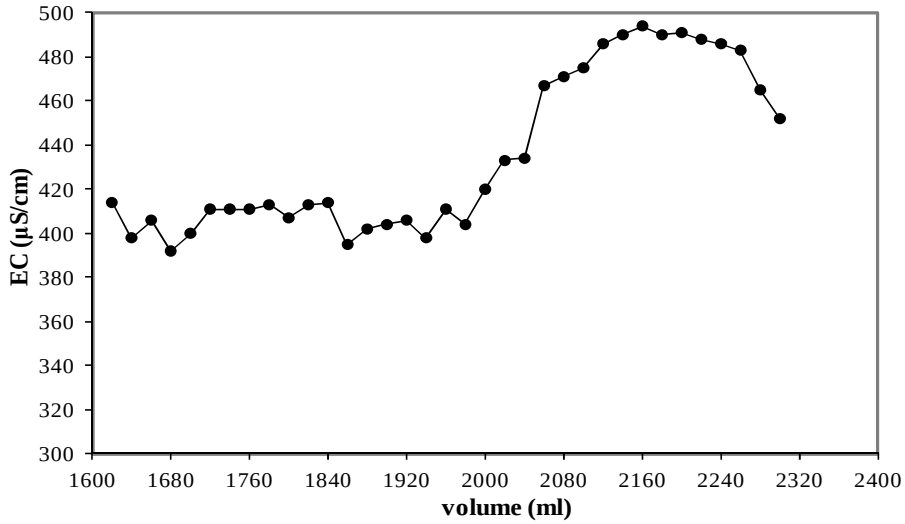

Figure 3.8: Conservative tracer breakthrough for Cr(VI) continuous upflow bioreactor packed with dolerite rock.

The U(VI) bioreactor had a drainage volume and pore volume of 1.84 l and 1.96 l (Figure 3.9), respectively. Using equation 3.1 and 3.2, the static porosity and effective porosity were calculated to be 37% and 40%, respectively. The slight differences in both the drainage/pore volume of the columns packed with dolerite can be attributed to mass loading of matrix or particle sizes.

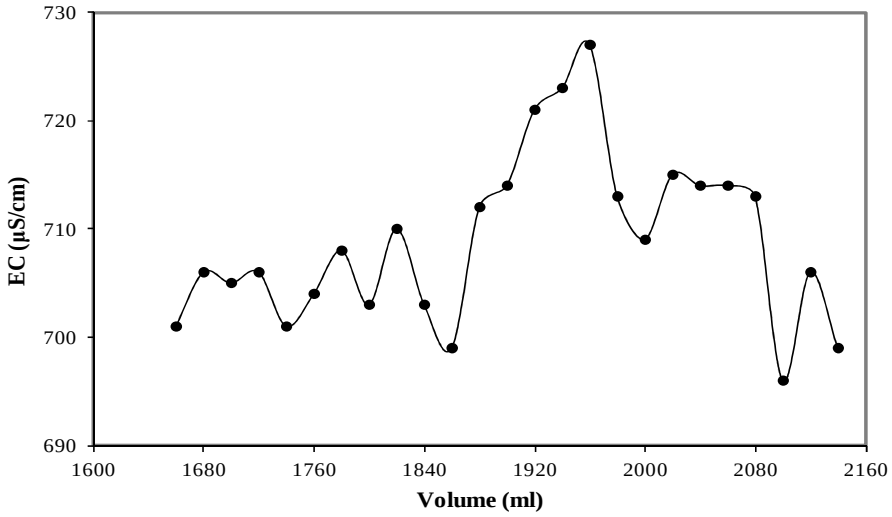

Figure 3.9: Conservative tracer breakthrough for U(VI) continuous upflow bioreactor packed with dolerite rock.

3.4.4 Sampling and *In situ* bioreduction analysis

The two bioreactors were operated in continuous upflow mode with citric acid as an electron donor, care was taken to correct for any pH changes and columns inlet influent always had a pH between 6 and 7.5. Samples were taken from the effluent port for the immediate measurement of physical parameters, such as ORP, EC, pH and temperature according to section 3.3.5.

From Figure 3.10 EC started at a high, however it stabilized after day 6 and it remained constant throughout the operational period. Temperature of the bioreactor was influenced by the ambient temperature while the pH remained fairly constant through a range (between 6.5 and 8.5) throughout the operational period. As stated by Kumar and co-workers (2010) metal precipitation is good at pH range of 5 – 8 and this may be because at low pH the H^+ is high thus competing with metal resulting in the decrease of the cell's removal capacity. As previously discussed in section 3.3.4, upon Cr(VI) influent source water premix (citric acid 370 mg/l) preparation the pH of the water dropped from 8.31 to below 5, as a result the pH was adjusted to 6 with 1 M NaOH. Cr(VI) was reduced, this was confirmed by colorimetric Cr(VI) assay (Section 3.3.5.1) and a change of a greenish colour from the influent source water compared to the clear effluent. Considering chemical properties it is thus expected that Cr(III) would precipitated as $Cr(OH)_3$ in the bioreactor (Ramakrishnaiah and Prathima, 2012).

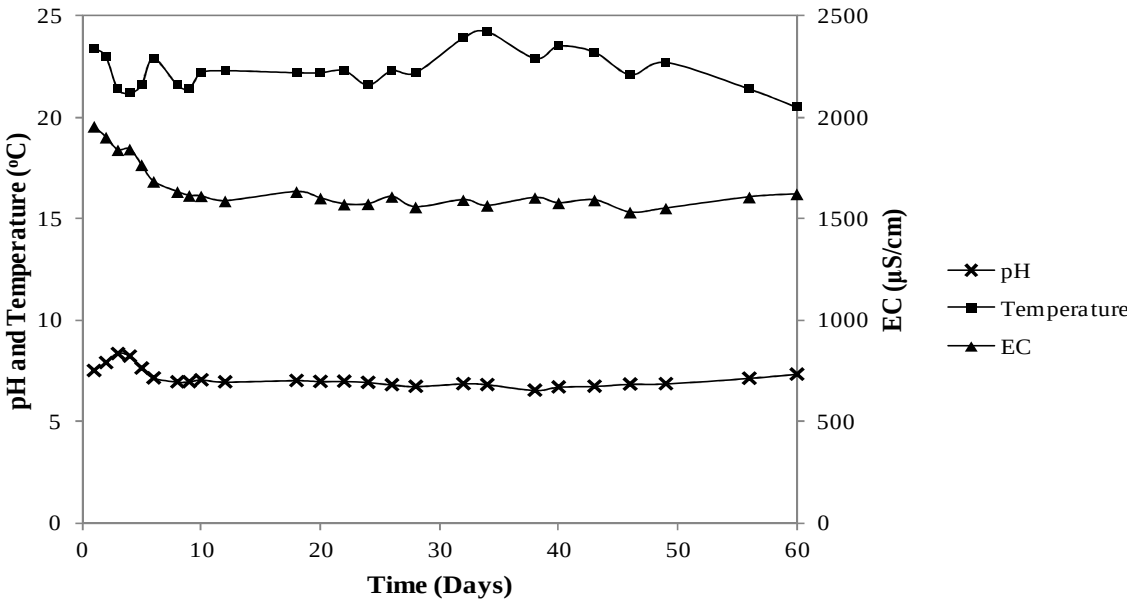

Figure 3.10: Cr(VI) bioreactor effluent physical parameters.

According to Gomez-Sjoberg and co-workers (2002) during bacterial growth there is an increase in EC due to the ionic metabolites from live cells. In contrast to the chromium bioreactor, EC from the uranium bioreactor (Figure 3.11) was inconsistent during the operational period and this can be attributed to the different electron donor concentration feed to the bioreactor. The ambient temperature influenced the temperature of the U(VI) bioreactor with the pH in the range that corresponds to those of the Cr(VI) bioreactor.

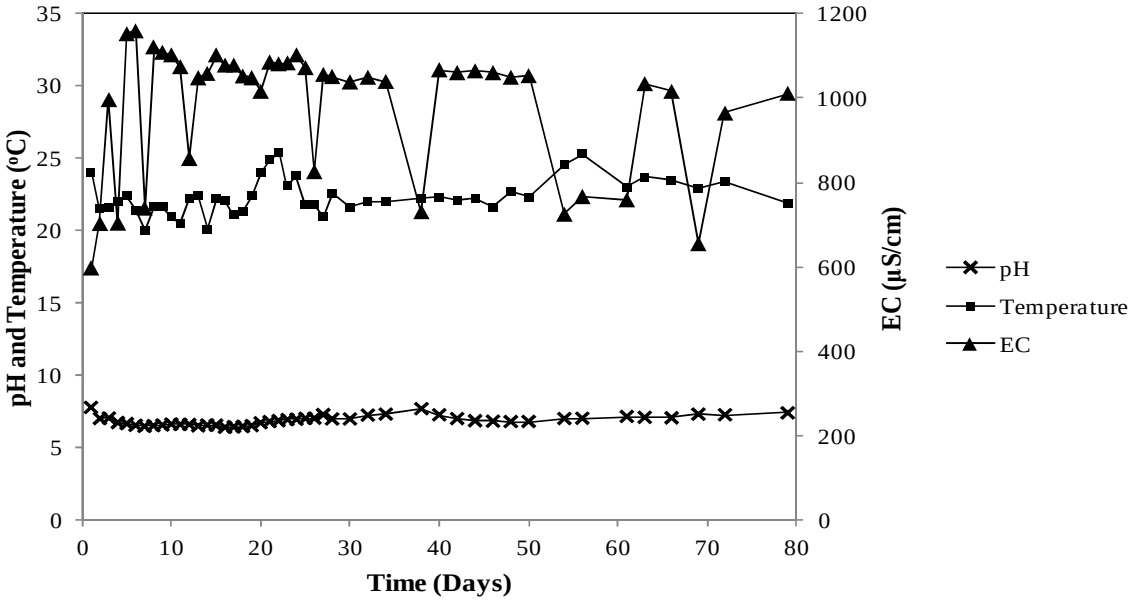

Figure 3.11: U(VI) bioreactor effluent physical parameters.

The effluent samples were taken in 15 ml falcon tubes and analysed for the measurement of soluble Cr(VI) and U(VI) concentration according to section 3.3.5.1 and 3.3.5.2 respectively.

The results of the continuous upflow bioreactors are summarized and depicted in Figure 3.12 and Figure 3.13.

Successful Cr(VI) reduction was achieved over the 60 days of operation. The adapted biofilm/sludge collected from the Cr(VI) impacted site was able to reduce a total of 100% Cr(VI) from the influent source water amended with citric acid as an electron donor (370 mg/l). A change in oxidation-reduction potential (ORP) that coincides with the Cr(VI) reduced was observed. After 5 days of operation the bioreactor reached anoxic conditions as indicated by the negative ORP, it was during this time where 100% Cr(VI) reduction was obtained. The bioreactor went back to a positive ORP unexpectedly between day 5 - 9, however this change in ORP did not have any effect on the Cr(VI) removed as it remained 100%. As shown by Opperman and van Heerden (2007) microbial Cr(VI) reduction can take place even in oxic conditions, however this is a two or three step process were Cr(VI) is initially reduced to the short-lived intermediates Cr(V) and/or Cr(IV) before further reduction to the thermodynamically stable end product, Cr(III) (Barrera-Diaz *et al*., 2012). A number of authors have also reported bacterial Cr(VI) reduction in anaerobic conditions. In absence of oxygen, Cr(VI) can serve as a terminal electron acceptor in the electron transport chain (Barrera-Diaz *et al*., 2012). It is thus not a surprise that Cr(VI) was reduced in a broad ORP range (+116 to – 148 mV). Furthermore, Wang and Shen (1995) stated that the best ORP range for Cr(VI) reduction has not yet been well established.

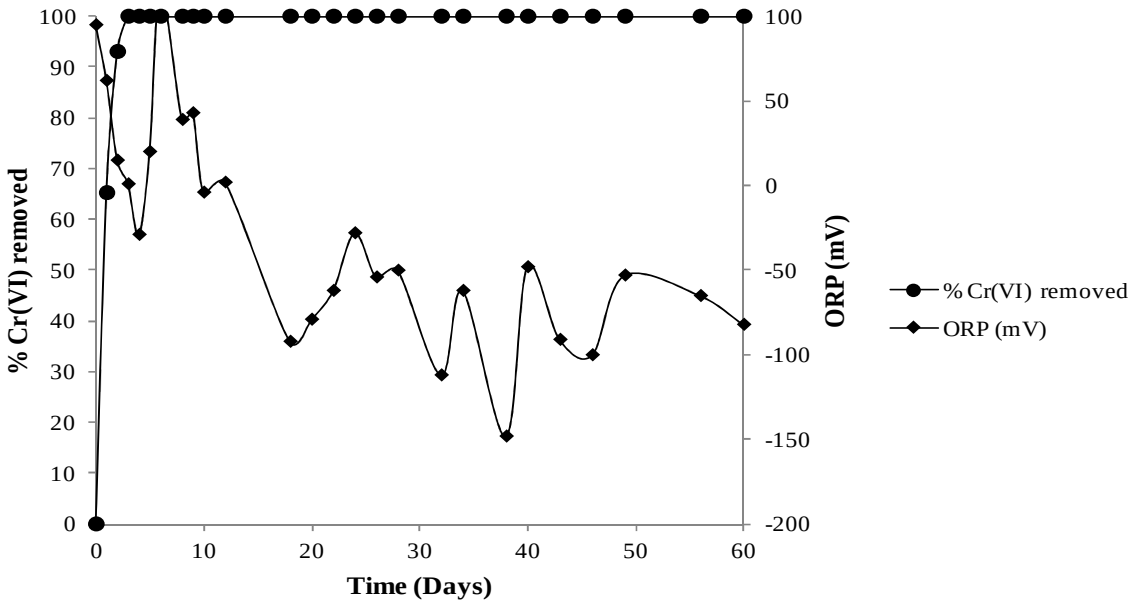

Figure 3.12: *In situ* Cr(VI) reduction by adapted biofilm in an upflow bioreactor with citric acid as electron donor.

The U(VI) bioreactor reached anoxic conditions after 7 days of operation as indicated by the negative ORP. After 20 days of operating the bioreactor, the electron donor concentration was lowered from 200 mg/l to 150 mg/l and then to 100 mg/l at day 27. After 25 days of operation the HRT of the bioreactor was increased to 48 h to allow more contact time between the bacterial cells and influent premix. As a result, the ORP decreased from -150 to -215 mV, and remained stable until day 40. Thereafter the ORP dropped into sulphate reducing conditions (-250 mV). As seen in Figure 3.13, up to 87% U(VI) reduction was observed at this conditions, the results are in contrast with Moon and co-workers (2010), who reported that upon commencement of sulphate reducing conditions, U(VI) reduction decreased. Even so, our results indicate that sulphate reducing conditions permit U(VI) reduction, this is in accordance with a number of authors (Beyenal *et al*., 2004; Sani *et al*., 2004; Sitte *et al*., 2010; Lee *et al*., 2013). A possible explanation as stated by Beyenal and co-workers (2004) is that during sulphate reducing conditions bacterial cells remove U(VI) enzymatically as well as chemically as explained in section 1.2.4. Thus the stable microbial community was able to reduce the low levels of U(VI) from the influent premix with citric acid as an electron donor. An expected relationship between ORP and % U(VI) reduced was observed, a decrease in the ORP resulted in an increase in the % U(VI) removed. However, as seen from Figure 3.13 when the ORP is between 0 to – 100, U(VI) removal is poor.

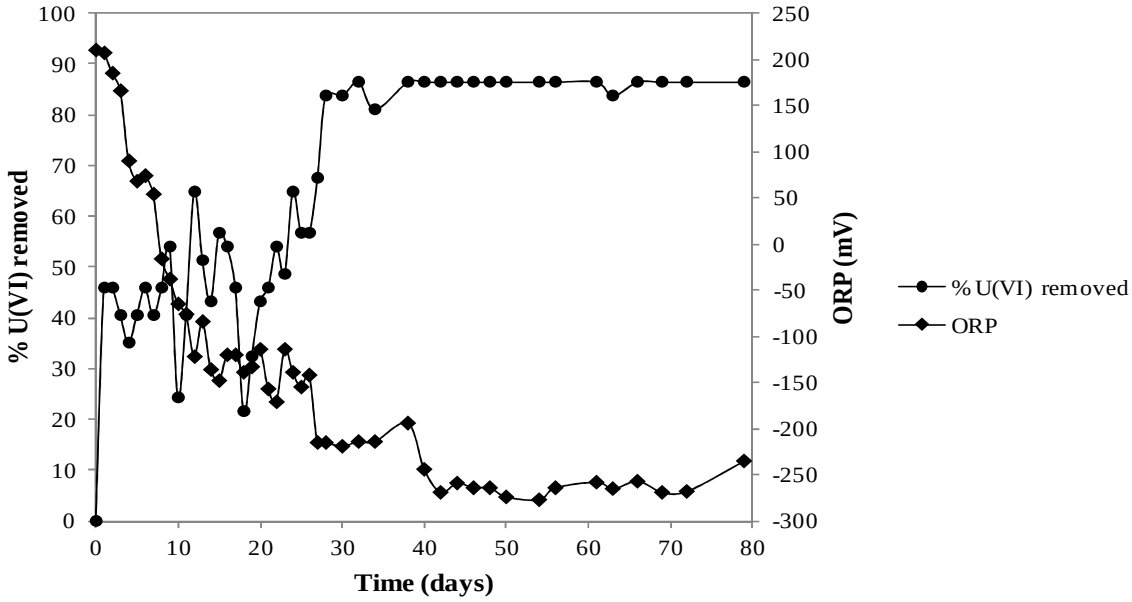

Figure 3.13: *In situ* U(VI) reduction by adapted biofilm in an upflow bioreactor with citric acid as electron donor.

After continuous operation [60 days for Cr(VI) and 79 days for U(VI)], the bioreactors were drained and cut open according to section 3.3.6. The collected water fractions were subjected to molecular assessment and the matrix examined with scanning electron microscope coupled to EDX for biofilm formation.

3.4.5 Bioreactor termination

3.4.5.1 Cell counts

The four water fractions from the bioreactors were DAPI stained according to the section 3.3.6.1. The DAPI staining confirmed that the collected water fractions contained cells, with a decreasing gradient of cells obtained from fraction 1 to 4, as expected since this is an upflow bioreactor.

Using DAPI staining it was possible to count the number of cells for each fraction according to equation 3.4. Cr(VI) column fractions gave values of 10^4 cells counted, in contrast 10^3 cells were counted for U(VI) bioreactor (Table 3.12). This is not surprising since the amount of electron donor feed to the U(VI) bioreactor was lower to that fed to the Cr(VI) bioreactor.

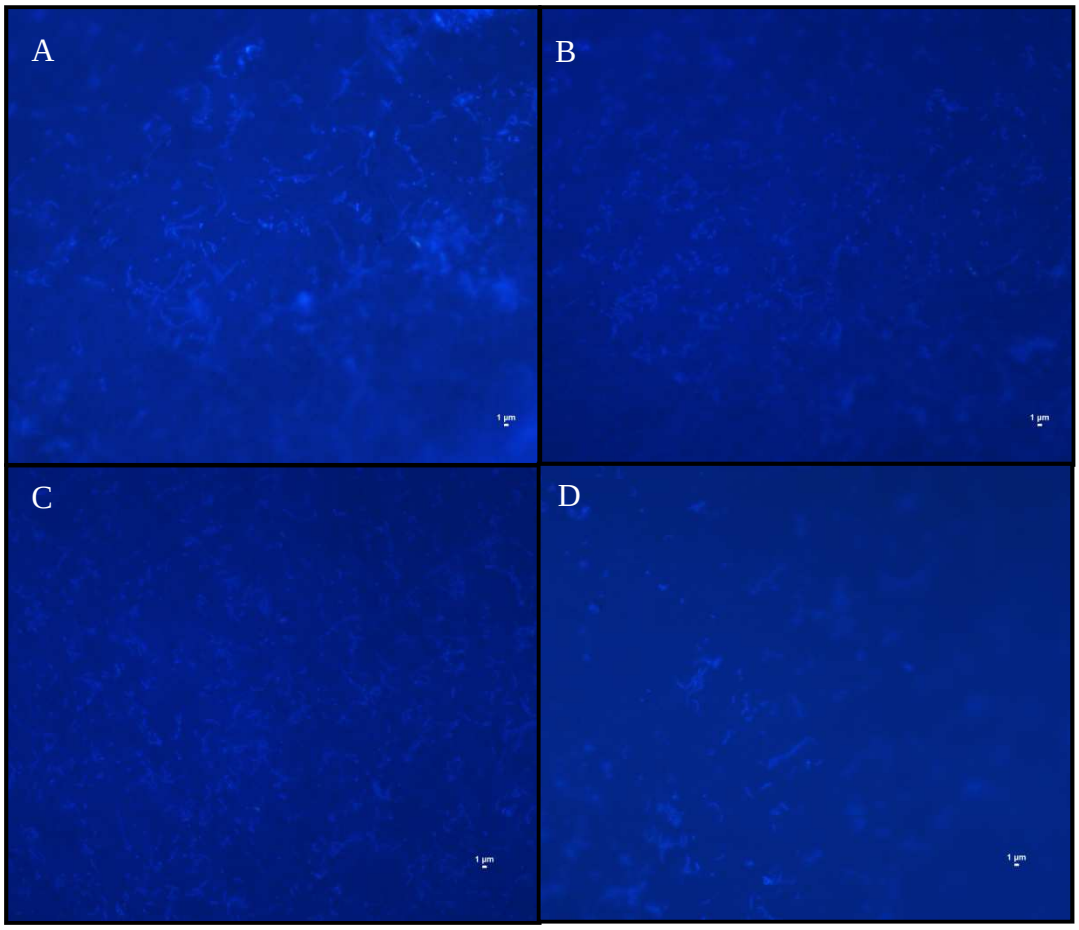

Figure 3.14: DAPI staining of the water fractions collected from the Cr(VI) bioreactor. (A) Fraction 1, (B) Fraction 2, (C) Fraction 3 and (D) Fraction 4.

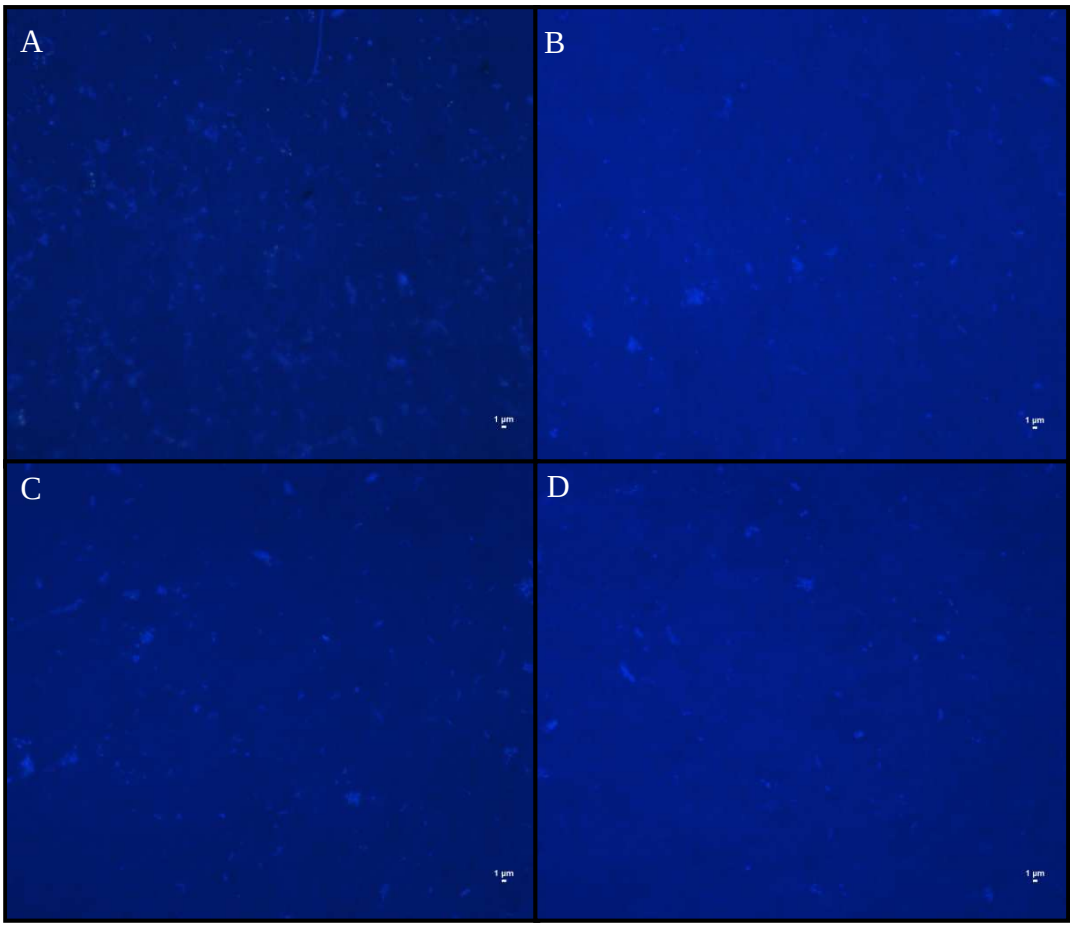

Figure 3.15: DAPI staining of the water fractions collected from the U(VI) bioreactor. (A) Fraction 1, (B) Fraction 2, (C) Fraction 3 and (D) Fraction 4.

Table 3.12: DAPI cell counts for the Cr(VI) and U(VI) bioreactor.

Bioreactor	**Sample**	**Cells/ml**
Chromium(VI)	Fraction 1	1.5×10^4
	Fraction 2	1.2×10^4
	Fraction 3	1.2×10^4
	Fraction 4	0.6×10^4
Uranium(VI)	Fraction 1	8.4×10^3
	Fraction 2	4.6×10^3
	Fraction 3	4.3×10^3
	Fraction 4	2.8×10^3

3.4.5.2 Genomic DNA extraction and 16S rDNA amplification

Genomic DNA (gDNA) was successfully extracted from the water fractions as described in section 3.3.6.2. The gDNA extracts showed low integrity with shearing as indicated in Figure 3.16. The resulting gDNA was then used in a 16S rDNA PCR thermal cycling reaction.

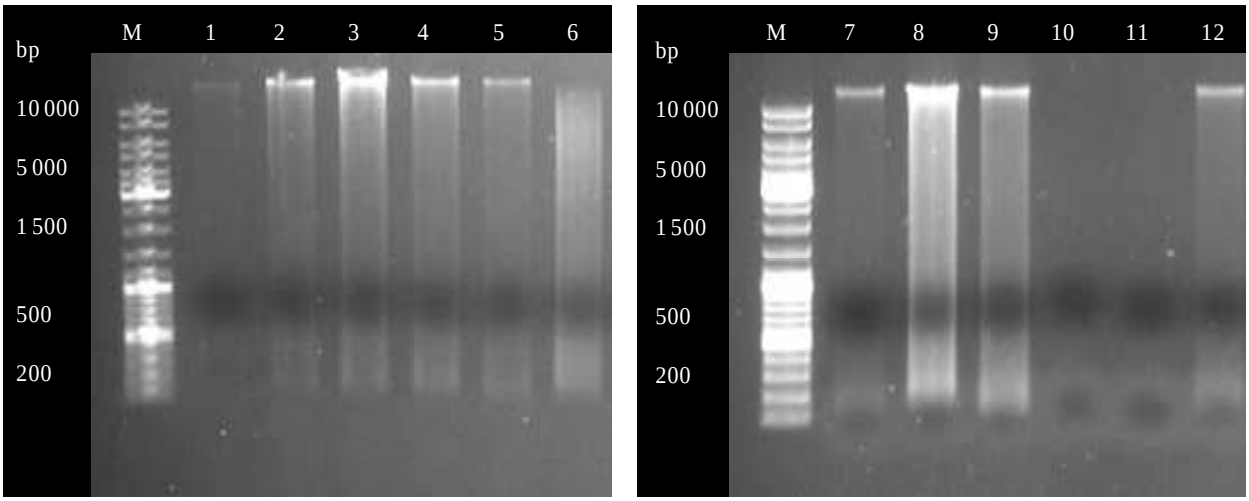

Figure 3.16: Genomic DNA extraction Cr(VI) bioreactor (left) and U(VI) bioreactor (right). Lane M: GeneRulerTM DNA ladder, Lane 1: Cr(VI) Influent water, Lane 2: Cr(VI) Seeding material, Lane 3: Fraction 1, Lane 4: Fraction 2, Lane 5: Fraction 3, Lane 6: Fraction 4, Lane 7: U(VI) Influent water, Lane 8: U(VI) Seeding material, Lane 9: Fraction 1, Lane 10: Fraction 2, Lane 11: Fraction 3 and Lane 12: Fraction 4.

Partial 16S rDNA was amplified as described in section 3.3.6.2, using primers described in section 3.3.6.2. Band amplicons of approximately 700 bp (Figure 3.17) were obtained which confirmed amplification irrespective of the low gDNA extracted. The PCR amplicons were then subsequently loaded onto the DGGE gel.

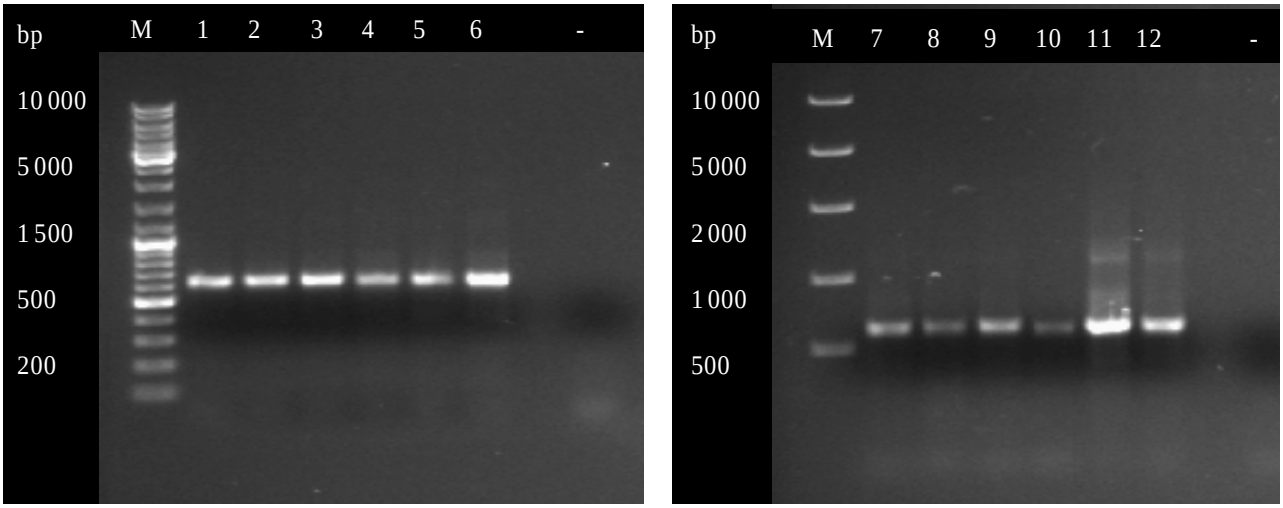

Figure 3.17: 16S rDNA amplification products from Cr(VI) bioreactor (left) and U(VI) bioreactor (right). Lane M: GeneRuler^{TM} DNA ladder, Lane 1: Cr(VI) Influent water, Lane 2: Cr(VI) Seeding material, Lane 3: Fraction 1, Lane 4: Fraction 2, Lane 5: Fraction 3, Lane 6: Fraction 4, Lane 7: U(VI) Influent water, Lane 8: U(VI) Seeding material, Lane 9: Fraction 1, Lane 10: Fraction 2, Lane 11: Fraction 3, Lane 12: Fraction 4 and Lane -: Negative control.

3.4.5.3 Denaturing gradient gel electrophoresis (DGGE)

DGGE gel that was run with PCR products amplified using 16S rDNA primers (Table 3.4). The DGGE gel was operated at 100V for 16 hours at 60^{o}C. Bacterial phylogenetic identification was determined by sequencing dominant bands from the resulting DGGE profiles (Figure 3.18). From theoretical description of DGGE (section 3.3.6.3), one band represent one bacterial specie, therefore it can be seen that there is a great biodiversity in the bioreactor fractions. The water fractions from the Cr(VI) bioreactor shows a shift in microbial community in the column. In contrast, the U(VI) bioreactor shows a constant biodiversity in all the bioreactor fractions. Even so, there is a microbial shift of abundance from the band indicated with a red arrow, a stated that the intensity of the band represents the abundance of specie; this is seen by the change in relative intensity from the individual band (Campell *et al*., 2009).

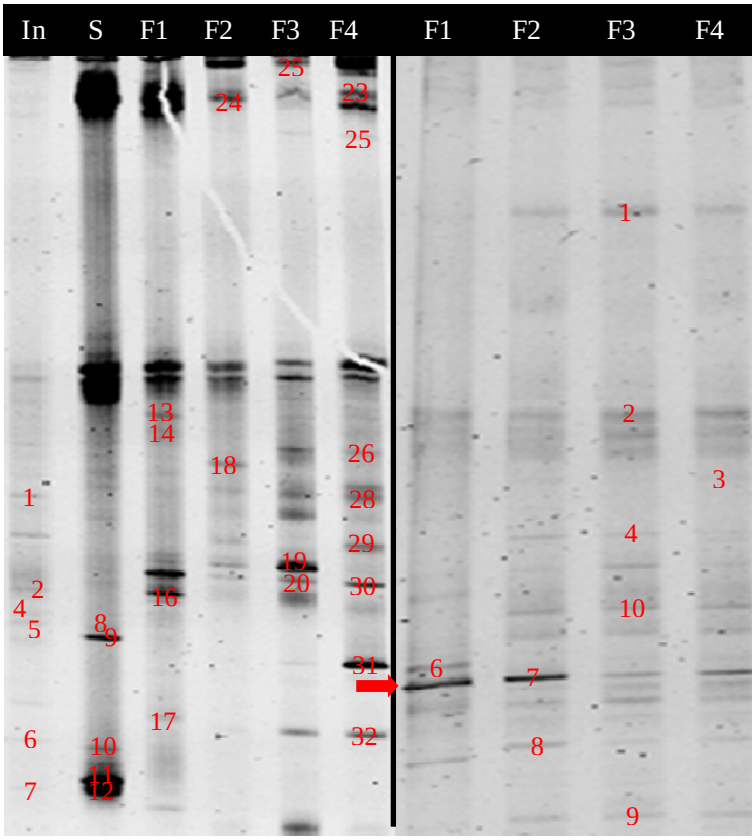

Figure 3.18: DGGE profile of the Cr(VI) bioreactor (left) and the U(VI) bioreactor water fractions (right). In: Cr(VI) influent water, S: Seeding material, F1: Fraction 1, F2: Fraction 2, F3: Fraction 3 and F4: Fraction 4.

The partial 16S rDNA sequencing results (Table 3.13 and Table 3.14) show a number of uncultured bacteria which indicates the novelty in the biodiversity present in the water fractions from the bioreactors. However, most of the sequences retrieved for both bioreactors from NCBI BLAST database (http://blast.ncbi.nlm.nih.gov/Blast.cgi) show bacterial sequences reported for the reduction of the following metals: chromium, uranium, sulphate, and iron or nitrate reduction.

Table 3.13: Sequencing results retrieved from BLASTN algorithm for the Cr(VI) bioreactor water fractions.

Band	Accession number	Closest sequences with BLASTN	E-value	Maximum Identity (%)
1	HQ75046.1	Uncultured organism clone ELU0035-T194-S-NIPCRAMgANb_000398 small subunit ribosomal RNA gene, partial sequence	0.0	98%
2	FN555649.1	Uncultured Hydrogenophaga sp. partial 16S rRNA gene, clone D-K46	0.0	95%
4	FN868340.1	Uncultured *Pedobacter* sp. partial 16S rRNA gene, clone clone 54	1e-75	78%
5	AM421802.1	*Pandoraea* sp. PVC(14d)6 partial 16S rRNA gene, strain PVC(14d)6	2e-153	88%
6	JQ660307.1	*Cellulomonas* sp. S9-651 16S ribosomal RNA gene, partial sequence	1e-43	78%
7	HE614774.1	Uncultured *Chloroflex*i bacterium partial 16S rRNA gene, clone F09L-1	2e-71	74%
8	JN162435.1	*Aeromonas* sp. PHAs048 16S ribosomal RNA gene, partial sequence	1e121	82%
9	JF736645.1	Uncultured *Azospira* sp. clone CFC11 16S ribosomal RNA gene, partial sequence	0.0	97%
10	JQ934230.1	*Microvirgula aerodenitrificans* strain OPU2012/1 16S ribosomal RNA gene, partial sequence	2e-149	85%
11	JX393048.1	*Laribacter hongkongensis* strain ZW18-1 16S ribosomal RNA gene, partial sequence	0.0	91%
12	KC211019.1	*Enterobacter* sp. ALL-3 16S ribosomal RNA gene, partial sequence	0.0	99%
13	JF151159.1	Uncultured bacterium clone ncd1729h10c1 16S ribosomal RNA gene, partial sequence	1e-43	70%
14	GQ072767.1	Uncultured bacterium clone nbw200h10c1 16S ribosomal RNA gene, partial sequence	5e-61	75%

16	AB696880.1	*Zoogloea* sp. UNPF89 gene for 16S rRNA, partial sequence	5e-140	84%
17	FN669649.1	Uncultured *Firmicutes* bacterium partial 16S rRNA gene, isolate DGGE band SP_MBR15	5e-23	70%
18	JF139347.1	Uncultured bacterium clone ncd1622g02c1 16S ribosomal RNA gene, partial sequence	3e-101	78%
19	JX994135.1	*Sphingomonas* sp. A2-S10 16S ribosomal RNA gene, partial sequence	0.0	99%
20	FM877976.1	*Geobacter* sp. IST-3 partial 16S rRNA gene, isolate ALISIMBF42R42	0.0	95%
22	JF958153.1	*Cytophaga* sp. JSC-P2-223-10 16S ribosomal RNA gene, partial sequence	0.0	98%
23	NR 041374.1	*Pedobacter ginsengisoli* strain Gsoil 104 16S ribosomal RNA, partial sequence	5e-73	74%
24	NR 041374.1	*Pedobacter ginsengisoli* strain Gsoil 104 16S ribosomal RNA, partial sequence	0.0	97%
25	KC352895.1	*Legionella* sp. 5E50 16S ribosomal RNA gene, partial sequence	0.0	99%
26	EF649780.1	*Citrobacter* sp. stain DBM 16S ribosomal RNA gene, partial sequence	1e-115	99%
28	HQ830175.1	*Brevundimonas* sp. cp05 16S ribosomal RNA gene, partial sequence	0.0	100%
29	FJ887893.1	Uncultured *Pseudomonas* sp. clone BAM 4 16S ribosomal RNA gene, partial sequence	2e-144	98%
30	HM124374.1	*Ferribacterium* sp. 24-19 16S ribosomal RNA gene, partial sequence	0.0	99%
31	JQ217279.1	Uncultured *Burkholderiale*s bacterium clone OTU9 16S ribosomal RNA gene, partial sequence	0.0	98%
32	KC237428.1	*Mesorhizobium* sp. ICMP 19540 16S ribosomal RNA gene, partial sequence	1e-101	98%

Table 3.14: Sequencing results retrieved from BLASTN algorithm for the U(VI) bioreactor water fractions.

Band	Accession number	Closest sequences with BLASTN	E-value	Maximum identity (%)
1	GQ148878.1	*Flavobacteria* bacterium HMD1033 16S ribosomal RNA gene, partial sequence	0.0	98%
2	DQ168182.1	Uncultured *Clostridium* sp. clone T146 16S ribosomal RNA gene, partial sequence	1e-157	84%
3	HQ377330.1	*Paenibacillus* sp. On11 16S ribosomal RNA gene, partial sequence	2e-73	81%
4	GU979450.1	Uncultured *Legionella* sp. clone B28/SB1 16S ribosomal RNA gene, partial sequence	0.0	94%
6	JQ288653.1	Uncultured *Ferribacterium* sp. clone 16S ribosomal RNA gene, partial sequence	0.0	97%
7	JQ288706.1	Uncultured *Dechloromonas* sp. clone Depth_12to24-62 16S ribosomal RNA gene, partial sequence	0.0	98%
8	EU642133.1	Uncultured *Alcaligenaceae* bacterium clone Gap-2-74 16S ribosomal RNA gene, partial sequence	0.0	99%
9	HM346348.1	Uncultured *Micrococcineae* bacterium clone Jab PL2W1G8 16S ribosomal RNA gene, partial sequence	0.0	99%
10	AM056026.1	*Desulfovibrio* sp. A-1 16S rRNA gene, isolate A-1	0.0	99%

3.4.5.4 Scanning electron microscope and energy dispersive x-ray spectrometry

The PVC bioreactors were packed with dolerite rocks to provide a surface to which the bacteria could adhere for *in situ* bioreduction in these studies (section 3.3.3).

The SEM micrograph (Figure 3.19) reveal that bacterial cells were able to form biofilm onto the matrix, and these cells are elongated rod shaped. This phenomenon was observed by Yoon and co-workers (2011) on an anaerobically grown *Pseudomonas aeruginosa*. Their results suggest that during anaerobic respiration, the bacterium will elongate in the contribution of biofilm formation.

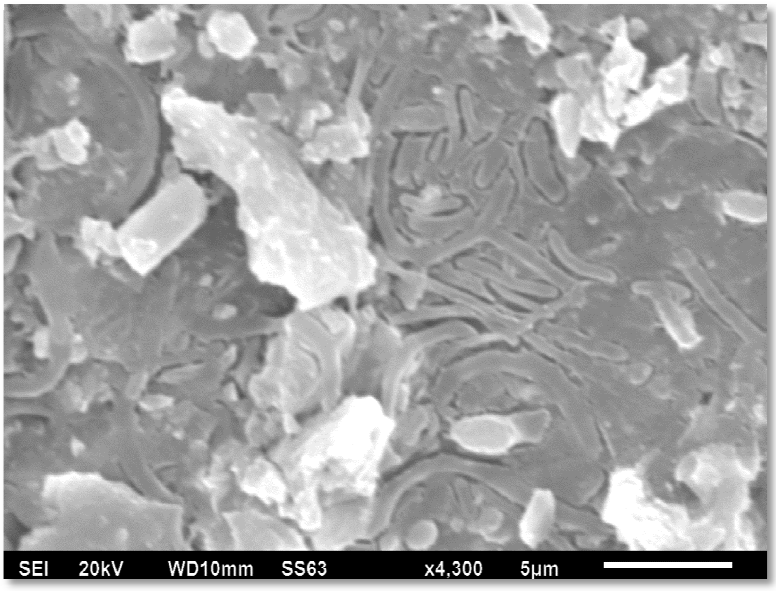

Figure 3.19: Scanning electron microscopy imaging of a matrix obtained from the first fraction of the Cr(VI) bioreactor showing biofilm formation.

The EDX was done on the first fractions of the matrix and for the Cr(VI) bioreactor it reveals traces of chrome as shown in Figure 3.20.

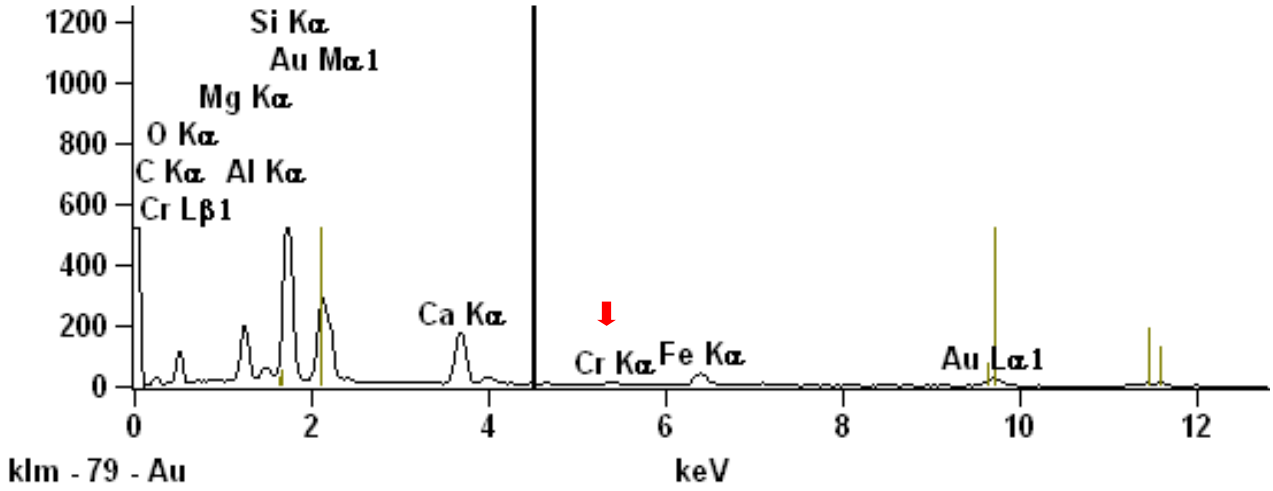

Figure 3.20: EDX spectrum recorded for the Cr(VI) matrix.

The initial investigation of the Cr(VI) bioreactor matrix revealed that the biofilm collected from the holding tank (reservoir) could adhere to the matrix rock. However, the SEM micrograph (Figure 3.21) does not show any biofilm formation/adherence onto the matrix and this can be attributed to the amount of electron acceptors available to the U(VI) bioreactor being low, with the exception of sulphates, to establish biofilm on the matrix.

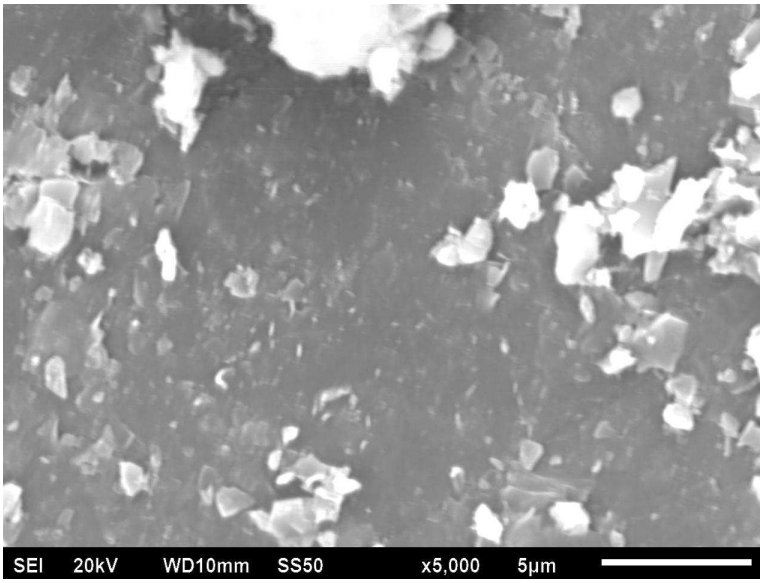

Figure 3.21: Scanning electron microscopy imaging of a matrix obtained from the first fraction of the U(VI) bioreactor.

3.5 Conclusions

Water samples were collected from Cr(VI) impacted environment which harbour indigenous microorganisms. The water was confirmed to contain Cr(VI) by ICP-MS and through Cr(VI) assay as described in section 3.3.5.1.

The Cr(VI) bioreactor was packed, conditioned and ran successfully for 8 weeks. At day 5, the Cr(VI) spectrometric assay indicated that 100% Cr(VI) was removed. It can be seen that a decrease in ORP into anoxic conditions results in an increase in Cr(VI) reducing abilities. The immediate Cr(VI) reduction observed in the Cr(VI) bioreactor suggests that the collected biofilm/sludge has a natural adaptation to support biological Cr(VI) reduction. This phenomenon might be due to the indigenous Cr(VI) reducing bacteria that occur in the sludge/biofilm, as a result through biostimulation with the addition of an electron donor. The pH range of the Cr(VI) bioreactor is ideal for metal precipitation, which suggest that Cr(VI) is being precipitated to Cr(III), in addition the end product can be assumed to be $Cr(OH)_3$.

DAPI staining of the terminated Cr(VI) bioreactor water fractions confirmed the presence of bacterial cells, with counts of 10^4 cells/ml. On the other hand, the DGGE profile shows a great diversity with a microbial shift in population observed between the water fractions and the collected sludge. The sequenced bands reveal sequences which are not only related to chromium reducing bacteria but also to other metal reducing bacteria. The Cr(VI) bioreactor matrix evaluation suggests that the sludge collected attached to the matrix as elongated biofilm.

Successful U(VI) reduction was achieved over the operational period of the bioreactor. Therefore it can be concluded that the indigenous bacteria were able to effectively remove the U(VI) from the impacted water with maximum removal ability obtained in sulphate reducing conditions. These finding suggest that sulphate reducing conditions permit U(VI) removal. The pH range of the U(VI) bioreactor resembles that of Cr(VI) bioreactor that was reported by Kumar and Co-workers (2010) to be ideal for metal precipitation, with the temperature of the bioreactor influenced by the ambient temperature.

DAPI staining of the collected water fractions also preliminarily confirmed the presence of bacterial cells, however, cell counts were lower than those of the Cr(VI) bioreactor at 10^3 cells/ml. The DGGE profile of the U(VI) bioreactor shows a uniform distribution of bacterial species between the fractions, however there is a shift in abundance in one particular specie shown in Figure 3.18 which shows a change in relative intensity. The sequencing results reveal a number of bacteria that have been reported for U(VI) reduction and other metals. In contrast to the Cr(VI) bioreactor matrix, the U(VI) matrix showed no biofilm formation.

Overall, the system works as a remediation strategy for impacted water with low levels of U(VI) and thus can be evaluated for water impacted with high levels of U(VI). From the results, it can be seen that the addition of an external electron donor results in the biostimulation of indigenous bacteria which results in the removal of U(VI).

3.6 References

- **Ackarley, D.F., Gonzalez, C.F., Keyhan, M., Blake II, R. and Matin, A.** (2004) Mechanism of chromate reduction by the *Escherichia coli* protein, NfsA, and the role of different chromate reductases in minimizing oxidative stress during chromate reduction. *Environmental Microbiology*. **6**(8):851-860.

- **Ahemad, M.** (2012) Implications of bacterial resistance against heavy metals in the bioremediation: a review. *IIOABJ*. **3**(3):39-46.

- **Barrera-Diaz, C.E., Lugo-Lugo, V. and Bilyeu, B.** (2012) A review of chemical, electrochemical and biological methods for aqueous Cr(VI) reduction. *Journal of Hazardous Material*. **223-224**:1-12.

- **Beukes, J.P., Pienaar, J.J., Lachmann, G. and Giesekke, E.W.** (1999) The reduction of hexavalent chromium by sulphite in wastewater. *Water SA*. **25**(3):363-370.

- **Beyenal, H., Sani, R.K., Peyton, B.M., Dohnalkova, A.C., Amonette, J.E. and Lewandowski, Z.** (2004) Uranium immobilization by sulfate-reducing biofilms. *Environ. Sci. Technol*. **38**:2067-2074.

- **Bondici, V.F., Lawrence, J.R., Khan, N.H., Hill, J.E., Yergeau, E., Wolfaardt, G.M., Warner, J. and Korber, D.R.** (2013) Microbial communities in low permeability, high pH uranium mine tailings: characterization and potential effects. *Journal of Applied Microbiology*. **114**:1671-1686.

- **Boopathy, R.** (2000) Factors limiting bioremediation technologies. *Bioresource Technology* . **74**:63-67.

- **Campbell, J.H., Clark, J.S. and Zak, J.C.** (2009) PCR-DGGE comparison of bacterial community structure in fresh and archived soils sampled along a Chihuahuan desert elevational gradient. *Microb Ecol*. **57**:261-266.

- **Department of Water Affairs (DWA)** (2011) South African national standard – Drinking water. Part 1: Microbiological, physical, aesthetic and chemical determinants.

- **El Himri, M., El Himri, A., Pastor, A. and De la Guardia, M.** (2012) Evaluation of method for uranium determination in waters by ICP-MS. *Journal of Applied Technology in Environmental Sanitation*. **2**(2):115-120.

- **Farag, S. and Zaki, S.** (2010) Identification of bacterial strains from tannery effluent and reduction of hexavalent chromium. *Journal of Environmental Biology*. **31**(5):877-882.

- **Finneran, K.T., Housewright, M.E. and Lovley, D.R.** (2002) Multiple influences of nitrate on uranium solubility during bioremediation of uranium-contaminated subsurface sediments. *Environmental Microbiology*. **4**(9):510-516.

- **Gomez-Sjoberg, R., Morisette, D.T. and Bashir, R.** (2002) Impedance microbiology-on-a-chip: microfluidic bioprocessor for rapid detection of bacterial metabolism. *Journal of Microelectromechanical Systems*.

- **Hininger, I., Benaraba, R., Osman, M., Faure, H., Roussel, A.M. and Anderson, R.A.** (2007) Safety of trivalent chromium complexes: No evidence for DNA damage in human HaCaT keratinocytes. *Free Radical Biology & Medicine*. **42**:1759-1765.

- **Johnson, D.A. and Florence, T.M.** (1970) Spectrophotometric determination of uranium(VI) with 2-(5-bromo-2-2pyridylazo)-5-diethylaminophenol. *Anal. Chim. Acta*. **53**:73-79.

- **Jordan, R.** (2009) Hexavalent chromium removal by novel site-specific bacteria – modeling and optimization for pollution reduction. *M.Sc*. University of the Free State.

- **Kalin, M., Wheeler, W.N. and Meinrath, G.** (2005) The removal of uranium from mining waste water using algal/microbial biomass. *Journal of Environmental Radioactivity*. **78**:151-177.

- **Kim, C., Zhou, Q., Deng, B., Thornton, E.C. and Xu, H.** (2001) Chromium(VI) reduction by hydrogen sulfide in aqueous media: Stoichiometry and kinetics. *Environ. Sci. Technol.* **35**:2219-2225.

- **Kumar, A., Bisht, B.S. and Joshi, V.D.** (2010) Biosorption of heavy metals by four acclimated microbial species, *Bacillus* spp., *Pseudomonas* spp., *Staphylococcus* spp. and *Aspergillus niger*. *J. Biol. Environ. Sci*. **4**(12):97-108.

- **Lee, S.Y., Baik, M.H., Cho, H., Jung, E.C., Jeong, J.T., Choi, J.W., Lee, Y.B. and Lee, Y.J.** (2013) Abiotic reduction of uranium by mackinawite (FeS) biogenerated under sulfate-reducing condition. *J. Radioanal. Nucl. Chem.* **296**:1311-1319.

- **Martins, M., Faleiro, M.L., Chaves, S., Tenreiro, R., Santos, E. and Costa, M.C.** (2010) Anaerobic bio-removal of uranium(VI) and chromium(VI): Comparison of microbial community structure. *Journal of Hazardous Material*. **176**:1065-1072.

- **Moon, H.S., McGuinness, L., Kukkadapu, R.K., Peacock, A.D., Komlos, J., Kerkhof, L.J., Long, P.E. and Jaffe, P.R.** (2010) Microbial reduction of uranium under iron- and sulfate-reducing conditions: Effects of amended goethite on microbial community composition and dynamics. *Water Research*. **44**:4015-4028.

- **Muyzer, G., De Waal, E. and Uitterlinden, A.G.** (1993) Profiling of complex microbial populations by denaturing gradient gel electrophoresis analysis of polymerase chain reaction-amplified genes coding for 16S rRNA. *Applied and Environmental Microbiology*. **59**(3):695-700.

- **Muyzer, G. and Smalla, K.** (1998) Application of denaturing gradient gel electrophoresis (DGGE) and temperature gradient gel electrophoresis (TGGE) in microbial ecology. *Antonie van Leeuwenhoek*. **73**:127-141.

- **Opperman, D.J. and van Heerden, E.** (2007) Aerobic Cr(VI) reduction by *Thermus scotoductus* strain SA-01. *Journal of Applied Microbiology*. **103**:1907-1913.

- **Owlad, M., Arouna, M.K., Daud, W.A.W. and Baroutian, S.** (2009) Removal of hexavalent chromium-contaminated water and wastewater: a review. *Water Air Soil Pollut*. **200**:59-77.

- **Porter, K.S. and Feig, Y.S.** (1980) The use of DAPI for identifying and counting aquatic microflora. *Society of Limnology and Oceanography*. **25**:943-948.

- **Ramakrishnaiah, C.R. and Prathima, B.** (2012) Hexavalent chromium removal from industrial wastewater by chemical precipitation method. *International Journal of Engineering Research and Applications*. **2**(2):599-603.

- **Ravichandran, S.** (2011) Possible natural ways to eliminate toxic heavy metals. *International Journal of ChemTech Research*. **3**(4):1886-1890.

- **Sani, R.K., Peyton, B.M., Amonette, J.E. and Geesey, G.G.** (2004) Reduction of uranium(VI) under sulfate-reducing conditions in the presence of Fe(III)-(hydr)oxides. *Geochimica et Cosmochimica Acta*. **68**(12):2639-2648.

- **Silva, B., Figueiredo, H., Neves, I.C. and Tavares, T.** (2009) The role of pH on Cr(VI) reduction and removal by *Arthrobacter viscosus*. *International Journal of Chemical and Biological Engineering*. **2**(2):100-103.

- **Sitte, J., Akob. D.M., Kaufmann, C., Finster, K., Banerjee, D., Burhardt, E., Kostka, J.E., Scheinost, A.C., Buchel, G. and Kusel, K.** (2010) Microbial links between sulphate reduction and metals retention in uranium- and heavy metal-contaminated soil. *Applied and Environmental Microbiology*. **76**(10):3143-3152.

- **Suzuki, Y. and Banfield, J.F.** (2004) Resistance to, and accumulation of, uranium by bacteria from a uranium-contaminated sites. *Geomicrobiology Journal*. **21**:113-121.

- **Suzuki, Y., Kelly, S.D., Kemner, K.M. and Banfield, J.F.** (2005) Direct microbial reduction and subsequent preservation of uranium in natural near-surface sediment. *Applied and Environmental Microbiology*. **71**(4):1790-1797.

- **Urone, P.F.** (1955) Stability of colorimetric reagent for chromium, *s*-diphenylcarbazide, in various solvents. *Anal Chem*. 27:1354-1355.

- **Vasilatos, C., Megremi, I., Conomou-Eliopoulos, M. and Mitsis, I.** (2008). Hexavalent chromium and other toxic elements in natural waters in theThiva – Tanagra – Malakasa Basin, Greece. *Hellenic Journal of Geosciences*. **43**:57-66.

- **Wall, J.D. and Krumholz, L.R.** (2006) Uranium reduction. *Annual Review of Microbiology*. **60**:149-66.

- **Wang, G., Huang, L. and Zhang, Y.** (2008) Cathodic reduction of hexavalent chromium [Cr(VI)] coupled with electricity generation in microbial fuel cells. *Biotechnol Lett*. **30**:1959-1966.

- **Yoon, M.Y., Lee, K., Park, Y. and Yoon, S.S.** (2011) Contribution of cell elongation to the biofilm formation of *Pseudomonas aeruginosa* during anaerobic respiration. *PLoS One*. **6**(1):1-11.

- **Zou, J., Wang, M., Jiang, W. and Liu, D.** (2006) Chromium accumulation and its effect on other mineral elements in *Amaranthus viridis* L. *Acta Biologica Cracoviensia Series Botanica*. **48**(1):7-12.

Chapter 4

4.1 Introduction

Uranium (U) is a radionuclide and heavy metal that forms part of our natural environment (Schnug *et al*., 2005). However, recent anthropogenic activities such as uranium mining, milling and nuclear power generation have elevated uranium concentrations in the environment (Tripathi *et al*., 2008). Once the uranium is mined, it is transported and processed. The ore processed during milling emerges as waste (Tripathi *et al*., 2008).

Uranium exists in four oxidation states, ranging from U(III) to U(VI), with U(IV) and U(VI) being the most common. Uranium in the U(VI) oxidation state is mainly in the form of uranyl ions (UO_2^{2+}) which is highly mobile and soluble in aqueous environments (Finneran *et al*., 2002). In contrast, the U(IV) oxidation state as uraninite precipitate (UO_2) is insoluble and immobile in aqueous environments (Suzuki *et al*., 2005). Once uranium enters the organism, it is transferred to the extracellular fluids and transported through the blood to other organs (Shnug *et al*., 2005). The soluble form, UO_2^{2+} is transported and forms complexes with proteins and ions (Schnug *et al*., 2005). The risks associated with the exposure of uranium are thus chemical and radiological (Schnug *et al*., 2005). Untreated inhalation of uranium from contaminated substrates may cause leukaemia (Shnug *et al*., 2005; Winde, 2010).

A number of physiochemical methods have been used for the removal of U(VI) from impacted sites (Chabalala and Chirwa, 2010b). These methods include ion exchange, chemical clarification that uses ferric sulphate or aluminium sulphate, membrane filtration and reverse osmosis (Camacho *et al*., 2010). Amongst these methods, ion exchange is the most efficient removal method removing about 98% of the uranium from the groundwater; however, the resin material generates concentrated liquids that must be disposed of (Camacho *et al*., 2010). Major limitations of the other methods are the proper disposal of the resulting sludge and the disposal cost thereof (Camacho *et al*., 2010). Biological remediation processes have been developed as an alternative to the physiochemical methods. Several microorganisms have been reported for U(VI) immobilization/precipitation. To date, four mechanisms involved in the removal of have been described, namely (a) biosorption, (b) bioaccumulation, (c) biomineralization and (d) bioreduction (Chabalala and Chirwa, 2010a, b).

Studies have shown that *Saccharomyces cerevisiae* (Volesky and May-Phillips, 1995) and *Bacillus subtilis* (Fowle *et al*., 2000) are capable of uranium biosorption. Dead cells of *S. cerevisiae* have been reported to absorb approximately 40% more uranium than their living counterparts (Volesky and May-Phillips, 1995). As a result, the best absorbants of uranium are non-living cells. In contrast to biosorption, bioaccumulation is a process in which metabolically active microbe will immobilize U(VI) (Brandl and Faramarzi, 2006). *Citrobacter* sp. N14 has been reported for the accumulation of UO_2^{2+} via precipitation with phosphate ligand liberated by the bacterium (Macaskie *et al*., 2000). Bacteria such as *Shewanella putrefaciens*, *Geobacter metallireducens*, *G. sulfurreducens*, bacterial groups in *Desulfovibrio*, *Pseudomonas*, *Thermus*, *Clostridium* and hyperthermophilic archaea, among others have been reported for U(VI). These interactions of microbes and U(VI) can be used in the bioremediation of contaminated sites with uranium (Goulhen *et al*., 2006).

4.2 Aims

- To establish a microbial community suitable in the bioreactor for U(VI) reduction.
- To assess the performance of the upflow bioreactor for the removal of increasing levels of U(VI) with the established microbial community.

4.3 Materials and Methods

4.3.1 Uranium source waste collection and characterization

The sample water used for this research was collected from U(VI) impacted site (Figure 3.3). Over time, new source was collected in containers according to section 3.3.1.2 and each batch sent to IGS, UFS for geochemistry analysis.

4.3.2 Biological oxygen demand test

Biological oxygen demand (BOD) is a test applied to measure of the amount of dissolved oxygen which is required for the biochemical oxidation of the organic compounds (Kumlanghan *et al*., 2008). The standard BOD method (BOD_5) is a measure of BOD in 5 days from the time when the microorganisms are inoculated to the sample water (Brookman, 1997; Kumlanghan *et al*., 2008).

BOD experiments were carried out in 300 ml schott bottles with various electron donors reported to be effective for U(VI) anaerobic reduction. The theoretical electron donor concentration for U(VI) bioreduction was calculated as described in section 3.4.2. Each schott bottle was filled with impacted site water, electron donor and 0.5 g of the seeding material. The electron donors added individually are: Acetate (18 mg/l), citric acid (25 mg/l), ethanol (9 mg/l), glucose (18 mg/l), glycerol (9.5 mg/l), lactate (18 mg/l) and pyruvate (21 mg/l).

BOD_5 was reported as the amount of oxygen consumed in air tight 300 ml sample of water incubated in the dark at ~20°C (ambient room temperature) for 5 days. Incubations were conducted in the dark. The BOD was then calculated from the initial and final dissolved oxygen (DO) concentration. All dissolved oxygen measurements were measured in mg/l with the ExStik II dissolved oxygen meter.

4.3.3 Bioreactor set-up

Polyvinyl chloride (PVC) column was used to construct laboratory bioreactor with an empty bed volume of approximately 5 l according to section 3.3.3. Quartzite is available on site therefore the PVC column was packed with quartzite gravel as inert matrix, leaving a 1 cm head space at the top of column as stated in section above. The column was filled with water and allowed to stand overnight and drained to determine the drainage volume. A conservation tracer breakthrough was constructed by pumping 200 ml of 100 mM NaCl in water into the column and measuring electrical conductivity (EC) at the outlet port. The column was characterized to determine the static and effective porosity as described in section 3.3.3.

4.3.4 Bioreactor start-up and operation

The seeding material was diluted with influent water, 20% (w/v) and pumped at low speed as described in section 3.3.4. Subsequently, heterotrophic media outlined in Table 4.1 was pumped into the bioreactor. To allow adherence of the cells to the matrix, the bioreactor was allowed to stand for 24 hrs without any disturbance.

Table 4.1: Media used to stimulate the indigenous bacteria.

Component	Amount (g/l)
Glucose	0.1
Yeast extract	0.1
Peptone	0.05
Tryptone	0.05
$MgSO_4 7H_2O$	0.6
$CaCl_2 2H_2O$	0.07
MOPS	0.1

The bioreactor was operated in continuous upflow for *in situ* bioreduction of U(VI). Once the community was established the influent source water, amended with citric acid (250 mg/l) as an electron donor was fed into the bioreactor to achieve a HRT of 24 – 48. The ORP gradually dropped as the bioreactor was conditioning until U(VI) reducing conditions corresponding to – 250 mV were established. Since the source water contained only low

concentrations of U(VI) the bioreactor was spiked with uranyl acetate stepwise, after each increase the bioreactor and the community was allowed to adjust and U(VI) reduction monitored. The stoichiometric balance was always considered and thus the acceptor could be increased steadily. The outflow was monitored and until the U(VI) levels reached a very high level of 10 mg/l then the balance was adjusted to optimal by decreasing the electron donor concentrations to find the maximum concentration the bioreactor could accommodate.

4.3.5 Sampling and analysis

Laboratory scale bioreactor was operated in a continuous upflow mode under U(VI) reducing conditions. Influent water was prepared in batches of 10 l as described in section 3.3.5, citric acid and uranyl acetate were added to each batch and kept at 4^{o}C during the time it was pumped into the bioreactor. Samples were collected for diversity assessment to estimate population diversity and the immediate measurements of physical parameters as described in section 3.3.5. U(VI) bioreduction was followed continuously.

4.3.5.1 Uranium(VI) determination by inductively coupled plasma mass spectrometry (ICP-MS) and Br-PADAP spectrophotometric method

U(VI) was analyzed by a Br-PADAP method with several modifications to the original procedure. A 1 000 mg/l U(VI) stock solution prepared by dissolving analytical grade $UO_2(CH_3COO)_2.2H_2O$ in distilled water. Br-PADAP was used to prepare a 0.1 mM solution by dissolving the reagent in ethanol, wrapped in foil and stored at 4^{o}C. Sodium phosphate (1 M) buffer was prepared by dissolving the reagent in 80 ml distilled water, the pH of the solution was adjusted to 8.0 and diluted to 100 ml. Each solution of EHDMA (50 mM), sodium citrate (100 mM) and EDTA (100 mM) was prepared by dissolving each reagent in distilled water.

U(VI) dilutions were made by diluting the stock solution with distilled water. 1 000 µl of the U(VI) was taken into a 2.0 ml eppendorf tube. To the above, 200 µl sodium phosphate buffer, 200 µl EHDMA, 200 µl sodium citrate, 200 µl EDTA, 10 µl Br-PADAP and 190 µl were added. The resulting purple coloured solution was allowed to stand for 20 minutes and absorbance was measured using a Spectronic® Genesys™ 5 spectrophotometer (Milton Roy Company) at 578 nm against a water blank. A U(VI) standard curve was constructed by plotting the absorbance reading against the known U(VI) concentration (Figure 4.1).

Effluent samples were collected in 15 ml falcon tubes according to section 3.3.5.2 and sent to IGS (UFS, Free Sate, S A) for the measure of U(VI) concentration.

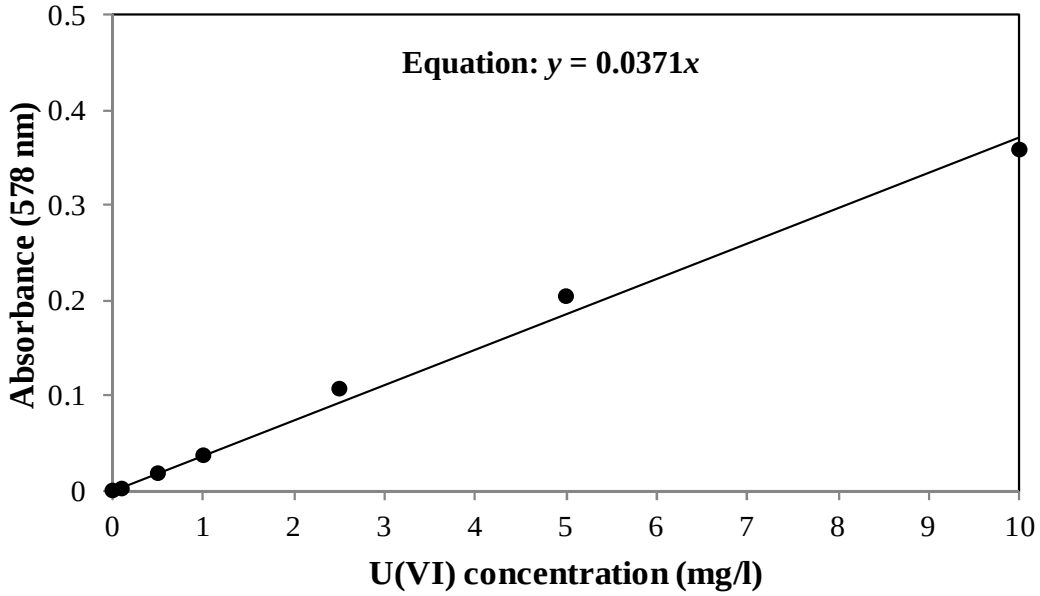

Figure 4.1: Standard curve for the determination of hexavalent uranium with the Br-PADAP method using $UO_2(CH_3COO)_2.2H_2O$ as standard with $R^2 = 0.9933$.

4.3.6 Genomic DNA extraction and 16S rDNA amplification

The selected effluent samples were filtered through a membrane filter with a 0.20 µm pore size. The filters were then cut using a sterile blade and gDNA was extracted from the filters using NucleoSpin® Soil kit (Pro) according to the manufacturer's instructions. Subsequently, the gel was visualized as described in section 3.3.6.2.

Partial 16S rDNA fragments were amplified from the gDNA extracts using primer set 341F-GC and 907RM. The PCR reaction mixture was performed in a total volume of 50 µl (Table 3.5) according to PCR conditions described in section 3.3.6.2. The PCR products obtained were visualized on 1% (w/v) agarose gel by running amplicons against a DNA standard (Gene ruler^{TM} DNA ladder, Fermentas), then subsequently subjected to denaturing gradient gel electrophoresis (DGGE).

4.3.7 Denaturing gradient gel electrophoresis

DGGE was performed as described in section 3.3.6.3, the gel was stained with SYBR Gold solution for 15 min, washed with distilled water and evaluated using ChemDoc XRS (Biorad Laboratories) gel documentation system under short UV light. Dominant bands obtained from DGGE profile were excised; autoclaved milliQ water (50 µl) was added to each band in a 1.5 ml tube and incubated at 55^{o}C overnight. The eluted DGGE bands were re-amplified using primer set 341F and 907RM (Table 3.4) according to PCR conditions described in section 3.3.6.3.

The resulting PCR products were separated on a 1% (w/v) agarose gel and bands corresponding to the expected size of ~600 bp were excised and purified using the Biospin Gel Extraction Kit (Bioflux) according to the manufacturer's instructions.

Subsequent to gel extraction, sequencing PCR was carried out in a total volume of 10 µl (Table 3.8) with the PCR cycle conditions as follows: 25 cycles of denaturation at 96^{o}C for 10 sec, followed by annealing at 50^{o}C for 5 sec and primer extension at 60^{o}C for 4 min. The resulting products were purified and sequenced on a capillary sequencer 3130xl ABI Genetic Analyzer (Applied Biosystems) at the Department of Microbial, Biochemical and Food Biotechnology (UFS, Free State, S A).

4.3.8 Bioreactor termination

After continuous operation for 10 weeks, the bioreactor was terminated according to section 3.3.6. The corresponding bioreactor fractions were collected for diversity assessment to estimate population diversity and the matrix sample collected was evaluated for biofilm formation and elemental composition using scanning electron microscope coupled to energy dispersive x-ray spectrometry.

4.3.8.1 Cell counts

DAPI staining was performed as described in section 3.3.6.1 to confirm the presence and number of cells from the collected bioreactor fractions.

4.3.8.2 Molecular analysis of the fractions

Subsequent to DAPI staining, gDNA was extracted from the collected bioreactor fractions as described in section 3.3.6.2. This was followed by partial PCR amplification of the 16S rDNA fragment using primer sets 341 F and 907RM. The PCR conditions were as described in section 3.3.6.2. The resulting PCR products were evaluated on a 1% (w/v) agarose gel stained with ethidium bromide, followed by DGGE and downstream molecular analysis.

4.3.8.3 Scanning electron microscopy and energy dispersive x-ray spectrometry

Matrix from the terminated bioreactor was allowed to air dry overnight, and then gradually dehydrated in a graded series of ethanol solutions as described in section 3.3.6.4. The ethanol-dehydrated matrix was critical point dried, mounted, and coated with gold. The resulting preparation was analysed using a Thermoscientific Ultradry detector energy dispersive X-ray spectrometry system, coupled to JEOL JSM-6610 SEM, at the Department of Geology (UFS, Free State, S A).

4.3.8.4 X-ray fluorescence analysis

An X-ray fluorescence measurement on the matrix sample was used to determine the presence of trace elements as well as uranium at the Department of Geology (UFS, Free State, S A).

4.3.8.5 Transmission electron microscopy

Bacteria cells were harvested from effluent water with centrifugation (6,000×g for 10 min at 25^{o}C). The collected cells were fixed, dehydrated and polymerized. Blocks were trimmed using an ultramicrotome and then cut into thin sections of approximately 0.2µm. Sections were collected on a copper grid, subjected to staining and electron micrographs taken with a TEM at the Center of Microscopy (UFS, Free State, S A).

4.3.8.6 Uranium qualitative analysis

Effluent water as well as matrices from fraction 1 and fraction 2 was collected for qualitative analysis of uranium. Effluent water was filtered through a membrane filter with a 0.20 µm pore size. The samples were leached with 10 ml 32% (v/v) hydrochloric acid and 1 ml 65% nitric acid in an Anton Paar Multiwave 3000 microwave reaction system for 30 min at 220^{o}C and 60 bar pressure. The resulting solvent was transferred quantitatively to a 100 ml volumetric flask and diluted to the mark. Uranium was analysed using Shimadzu ICPS-7500 ICP-OES spectrometer at the Department of Chemistry (UFS, Free State, S A).

4.4 Results and Discussions

4.4.1 Characteristics of collected samples

The four water samples were collected and sent to IGS (UFS, Free State, S A) for geochemistry analysis. The physiochemical parameters presented in Table 4.2 shows a pH range of 8.47 – 8.67, i.e., once again indicating an alkaline pH of uranium containing water. The U(VI) levels (highlighted in yellow) for all the batch samples were detected to be approximately 2 times higher than the acceptable drinking water limit set out by the Department of water affairs (DWA, 2011). The results also show the presence of other heavy metals. In summary the U(VI) contaminated water contained nitrates, calcium, magnesium and high levels of sulphate concentration at a range of 308 mg/l to 310 mg/l. The differences in nitrates within the sampled batches of water are in accordance with Islam and co-workers (2011). The total N results of their collected samples ranged from 0.02 to 0.4. The number of cells counted for the collected water was 10^5 cells/ml (Figure 4.2).

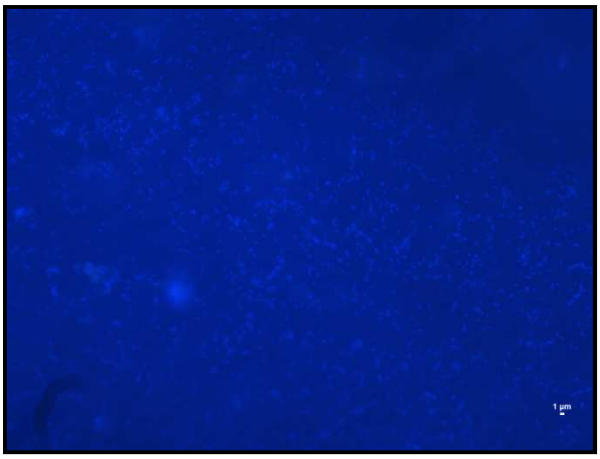

Figure 4.2: DAPI staining of the U(VI) source water, 10 ml filtered.

Table 4.2: Physiochemical parameter results of the collected U(VI) contaminated water samples (Values in mg/l and EC in mS/cm).

Parameters	Batch 1	Batch 2	Batch 3	Batch 4
pH	8.67	8.54	8.58	8.47
EC	103	104	104	103
Ca	93.9	95.0	93.2	93.3
Mg	45.6	46.0	45.3	45.3
Na	85.1	85.0	84.5	84.7
K	7.8	8.4	7.9	8.1
PAlk	9.3	7.0	8.3	5.8
MAlk	154	153	153	152
Cl	73.5	66.9	67.9	73.0
NO_3(N)	0.70	0.02	0.01	0.60
PO_4	<1	<1	<1	<1
SO_4	310.47	308.39	310.34	310.06
Al	0.041	0.047	0.047	0.046
Cr(VI)	<0.005	<0.005	<0.005	<0.005
Cu	0.013	0.014	0.012	0.013
Co	0.015	0.015	0.015	0.015
Fe	0.041	0.043	0.046	0.047
Mn	0.035	0.037	0.037	0.037
Ni	0.041	0.038	0.040	0.037
U(VI)	0.028	0.027	0.029	0.028
Zn	0.034	0.027	0.023	0.015
TOC	13.16	11.15	5.08	4.59
DOC	9.14	4.15	3.76	2.63

4.4.2 Biological oxygen demand

BOD tests were performed as described in section 4.3.2. Table 4.3 suggest that the indigenous bacteria prefer to use glucose as an electron donor; this is not surprising since bacteria are well known to use glucose as an electron donor. The BOD results also suggest that glycerol and acetate can be used as alternative electron donors for the reduction of U(VI). All of the electron donors tested are relatively good however a change in electron donor might introduce more parameters that could influence the bioreactor population, therefore in order to compare these aspects, the donor was kept constant. Additionally, because of the successful U(VI) bioreduction achieved in the previous chapter, citric acid was used as the electron donor of choice although in the future one might consider glucose for U(VI) bioreduction.

Table 4.3: BOD results for different electron donors.

Donor	**Initial DO**	**Final DO**	**BOD_5**
Glucose	2.15	0.22	1.93
Glycerol	2.02	0.25	1.77
Acetate	1.98	0.28	1.7
Citric acid	1.9	0.26	1.64
Pyruvate	1.79	0.18	1.61
Lactate	1.85	0.31	1.54
Ethanol	1.8	0.34	1.46
Influent + Seeding material	1.96	0.74	1.22

4.4.3 Column characterization

Subsequent to column packing and tracer conditioning, the conservative tracer (NaCl) breakthrough curves were constructed according to section 3.3.3.

From the conservative tracer peaks it was possible to determine the pore volume of the column. The Empty Bed Volume of the bioreactor was calculated to be 4.80 l. The bioreactor had a drainage volume and pore volume of 1.58 l and 1.66 l (Figure 4.3), respectively. Using equation 3.1 and 3.2, the static porosity and efficiency porosity were calculated to be 33% and 35 %, respectively.

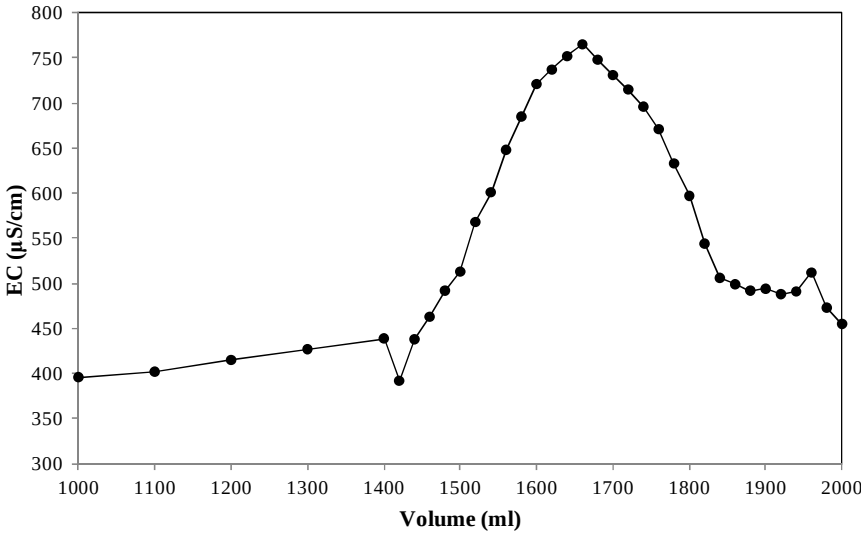

Figure 4.3: Conservative tracer breakthrough for U(VI) continuous upflow bioreactor packed with quartzite rock.

4.4.4 Sampling and analysis

All data are shown below in Figure 4.4, the EC started at a high level, however it stabilized after 10 days of operation. The increase in EC can be attributed to the media added to the bioreactor, as a result of media addition and nutrients available in the media, bacterial growth will cause an increase in EC due to the ionic metabolites from live cells. While slight changes in the EC during the operational period can be attributed to the gradual electron donor decrease fed to the bioreactor, as seen in the previous chapter (Figure 4.4). Similar trends in pH and temperature were observed to those discussed in section 3.4.4. The temperature of the bioreactor was also influenced by the ambient temperature, while the pH was in the range of 5 – 7.5 which was reported by Kumar and co-workers (2010) to permit metal precipitation.

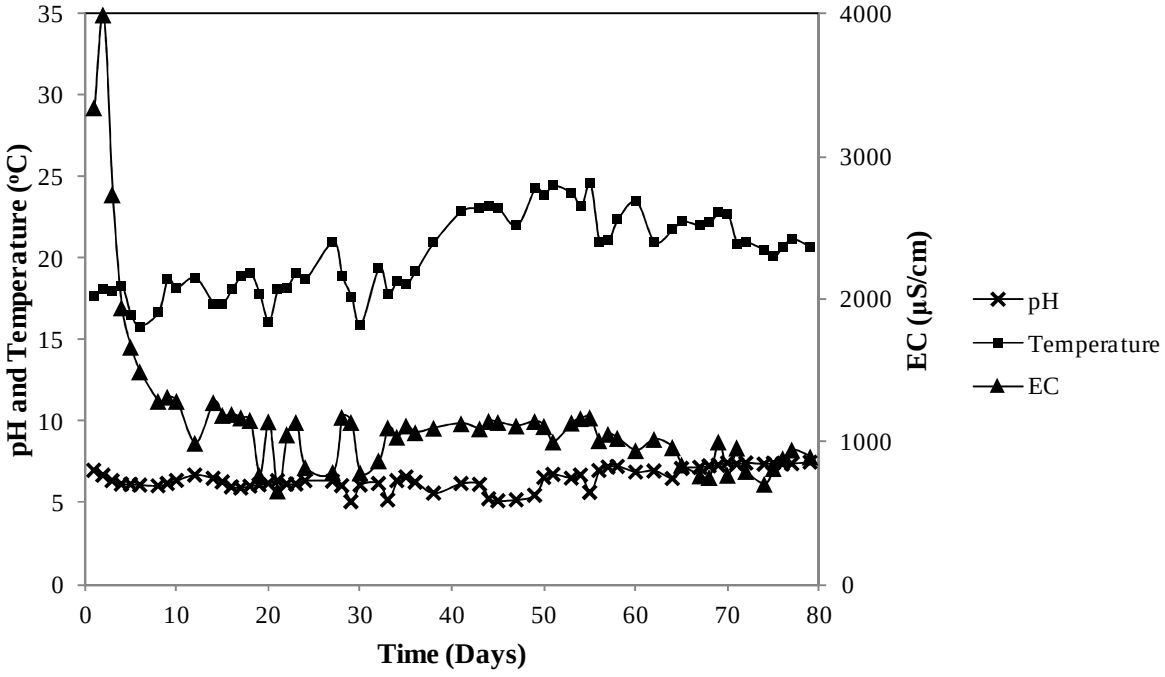

Figure 4.4: U(VI) bioreactor effluent physical parameters.

The effluent samples were taken in 15 ml falcon tubes and analysed for the measurement of soluble U(VI) concentration according to the two methods in section 4.3.5.1

4.4.4.1 *In situ* bioreduction

Once U(VI) reducing conditions corresponding to those observed from section 3.4.4 were established, the bioreactor was gradually spiked with uranyl acetate as described in section 4.3.4. U(VI) was increased stepwise (Figure 4.5), allowed to reach maximal reduction/removal. Then the diversity was assessed and new spiking occurred.

The bioreactor was start up with 250 mg/l citric acid (10X theoretical donor demand) and approximately 30 µg/l U(VI). Considering the findings in the previous chapter that sulphate reducing conditions permit U(VI) reduction. Once these conditions were established, the bioreactor was spiked with uranyl acetate to a final concentration of 300 µg/l U(VI). A spectrophotometric U(VI) assay was performed in conjunction with ICP-MS in order to follow the reducing levels of the bioreactor.

Subsequent to 60% U(VI) reduction at day 14, the bioreactor was then spiked with 500 µg/l U(VI) and this resulted in an increase in the ORP since gradually over time the reduction and community allowed the bioreactor to adapt to reducing conditions.

As soon as the bioreactor went back to sulphate reducing conditions, the bioreactor was spiked 1 mg/l U(VI) at day 21 and allowed to run for the next 20 days of operation. At day 28 the donor fed to the column was decreased to 200 mg/l, since the bioreactor was stable for the removal of 1 mg/l. As a result of this donor decrease, the ORP increased and as this has been shown the U(VI) reducing capabilities decreased (to approximately 80%). However, the adaptability of the bioreactor allowed reduction of 100%.

This reduction level allowed an increase of U(VI) to 2 mg/l and a decrease of donor fed to 150 mg/l. The bioreactor was able to maintain 99% reduction even though the U(VI) was increased to 5 mg/l. With the ORP of the bioreactor deep in sulphate reducing conditions (300 mV), the donor was lowered to 100 mg/l citric acid while U(VI) in the influent water was increased to 10 mg/l. At this stage the bioreactor was still able to reduce 95% of the 10 mg/l U(VI) fed.

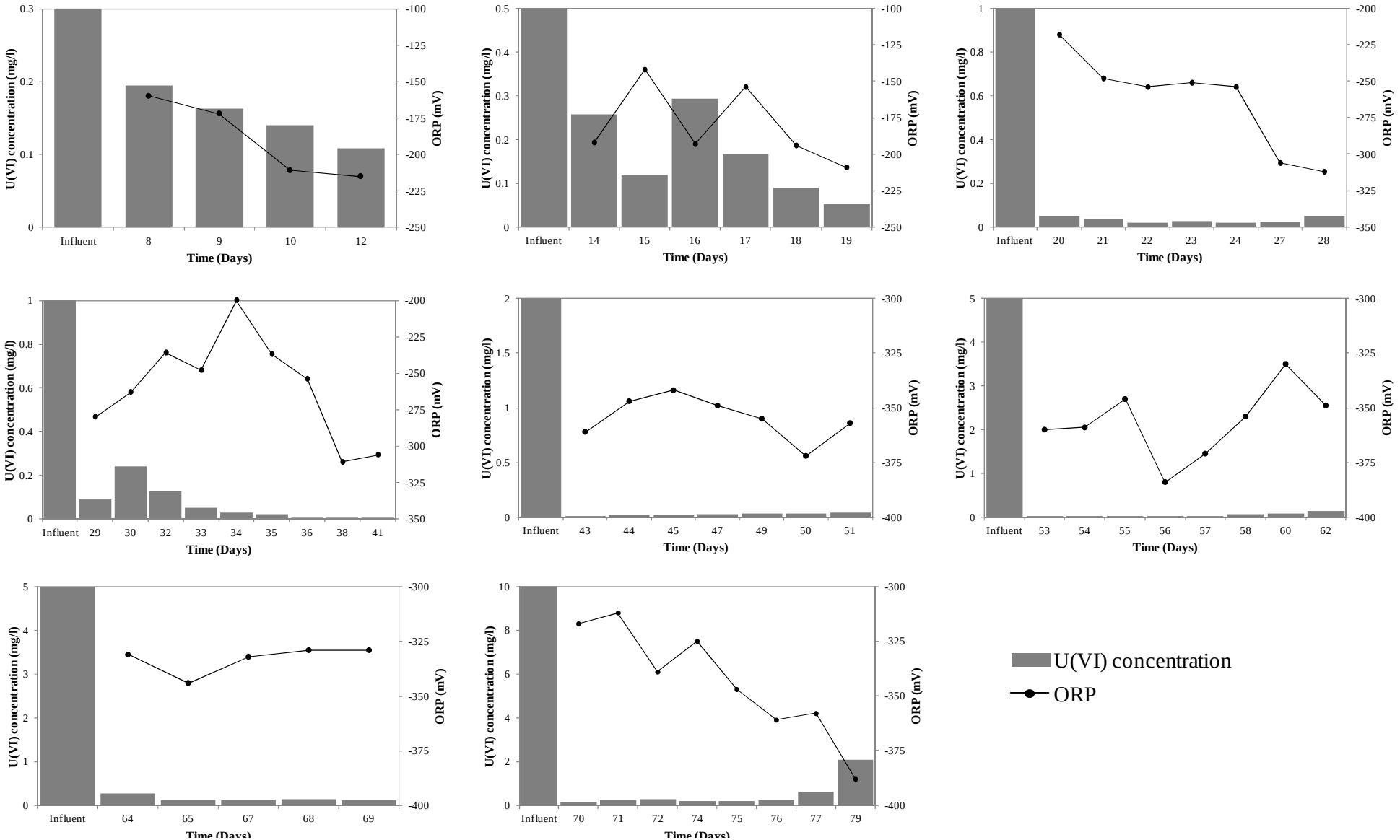

Figure 4.5: New influent donor premix preparation and U(VI) removal levels.

From Figure 4.6 it can be seen that there is a relationship between ORP and the uranium removed. Once again, it can be seen that when the ORP is not low enough, uranium reducing capability of the bioreactor is poor, this can be seen at day 10 where only 60% reduction was observed, and between day 30 and 32 where less than 80% was observed.

Successful U(VI) reduction was observed, this was confirmed by spectrophotometer U(VI) assay and ICP-MS of the effluent samples compared to the influent samples fed. This column studies have shown that U(VI) can be reduced under appropriate conditions by biostimulating the indigenous bacteria using citric acid as an electron donor.

One possible reason for this high U(VI) tolerance and reduction might be due to the fact that indigenous bacteria are well adapted to the U(VI), thereby are capable of using U(VI) as a terminal electron acceptor, since the bioreactor is under oxygen limiting conditions (Payne *et al*., 2002).

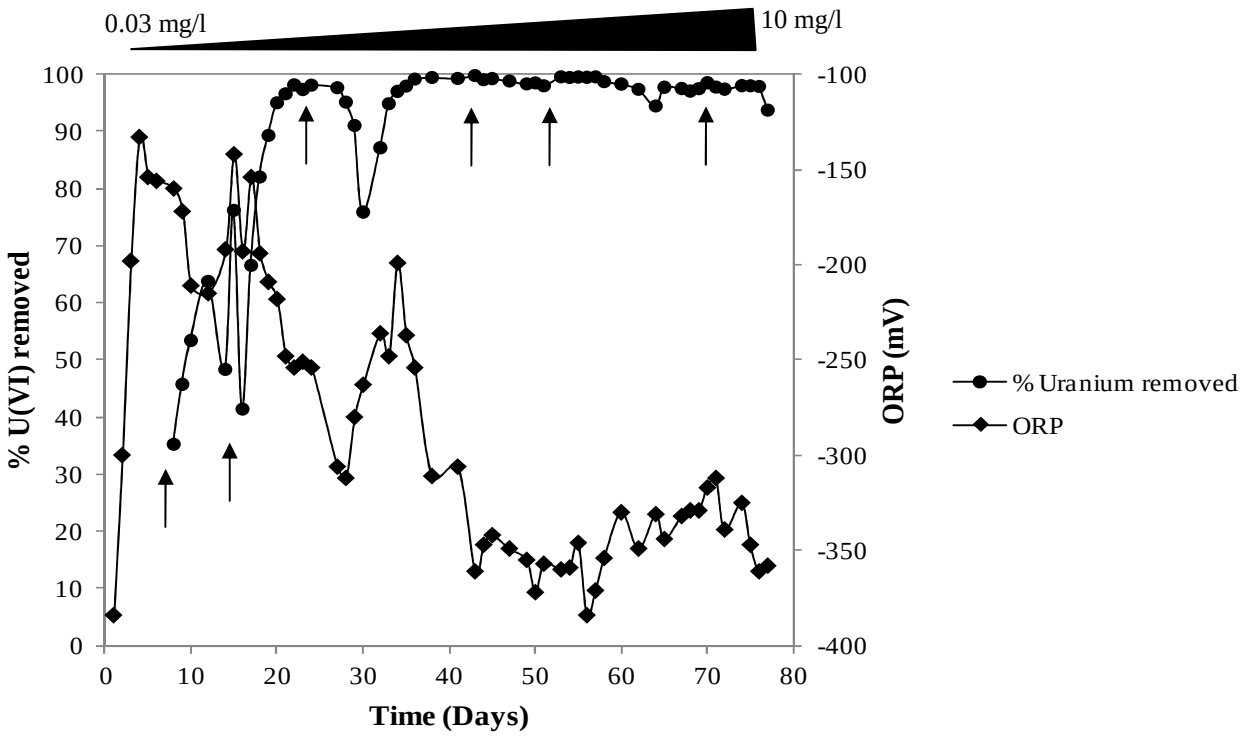

Figure 4.6: *In situ* U(VI) reduction in an upflow bioreactor with citric acid as electron donor. Arrows indicate the time at which the bioreactor was spiked with uranyl acetate.

4.4.5 Genomic DNA extraction and 16S rDNA amplification

Genomic DNA (gDNA) was successfully extracted from the water fractions as described in section 3.3.6.2. The resulting gDNA was then used in a 16S rDNA PCR thermal cycling reaction (Figure 4.7).

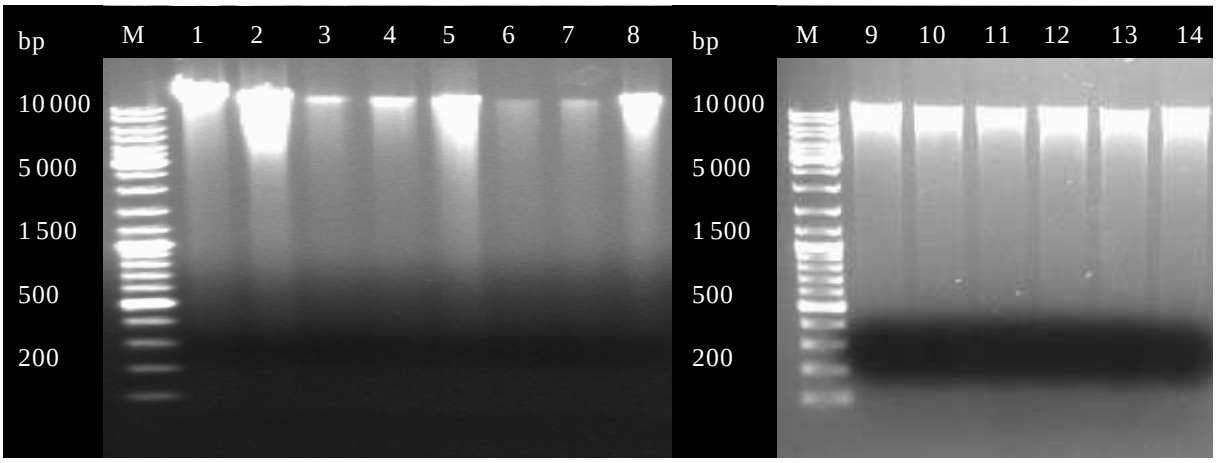

Figure 4.7: Genomic DNA extraction from selected daily samples [U(VI) bioreactor]. Lane M: GeneRulerTM DNA ladder, Lane 1: Day 2, Lane 2: Day 9, Lane 3: Day 15, Lane 4: Day 21, Lane 5: Day 28, Lane 6: Day 30, Lane 7: Day 34, Lane 8: Day 45, Lane 9: Day 50, Lane 10: Day 56, Lane 11: Day 60, Lane 12: Day 69, Lane 13: Day 75 and Lane 14: Day 79.

Partial 16S rDNA was amplified as described in section 3.3.6.2, using primers sets 907 RM and 341F with a GC clamp attached to the 5'end of the primer. Band amplicons of approximately 700 bp (Figure 4.8) were obtained which confirmed amplification. The PCR amplicons were then subsequently loaded onto the DGGE gel. Lane 11, 12 and 13 were re-amplified and positive amplicons were obtained (Data not shown).

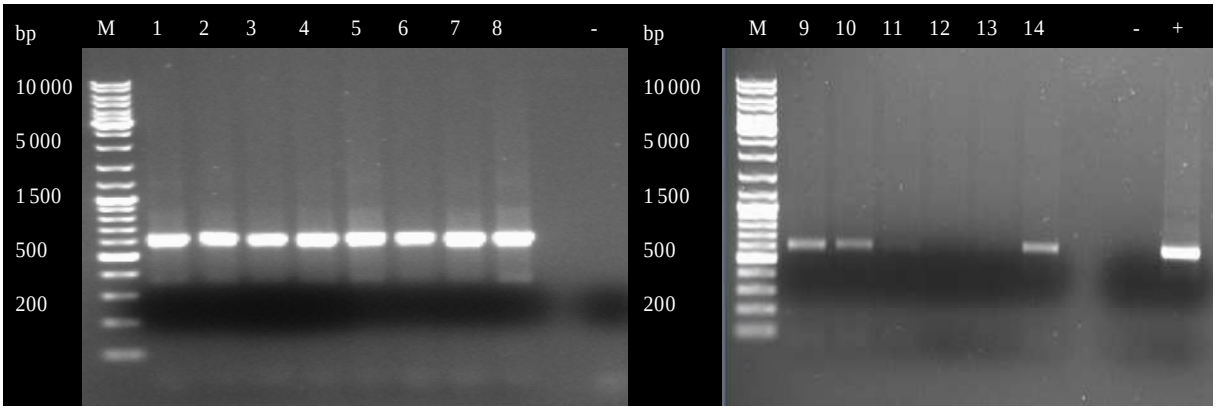

Figure 4.8: 16S rDNA amplification products from selected daily samples [U(VI) bioreactor]. Lane M: GeneRulerTM DNA ladder, Lane 1: Day 2, Lane 2: Day 9, Lane 3: Day 15, Lane 4: Day 21, Lane 5: Day 28, Lane 6: Day 30, Lane 7: Day 34, Lane 8: Day 45, Lane 9: Day 50, Lane 10: Day 56, Lane 11: Day 60, Lane 12: Day 69, Lane 13: Day 75, Lane 14: Day 79, Lane -: Negative control and Lane +: Positive control.

4.4.6 Denaturing gradient gel electrophoresis

DGGE gel that was run with PCR products amplified using 16S rDNA primer set 341F-GC and 907RM. The DGGE gel was operated at 100V for 16 hours at 60^{o}C. Bacterial phylogenetic identification was determined by sequencing predominant bands from the resulting DGGE profile.

The DGGE profile indicates that during the early phase (Day 2 - 9), a few bands could be observed, however at day 15 there is a shift in microbial population within the bioreactor, which can be seen by appearing bands Figure 4.9 (Lane 3 marked with red arrow). It is interesting to note that the bands are in correspondence to those in the influent water, which suggests the biostimulation of indigenous bacteria by citric acid. Additionally, the DGGE profile also shows (with exception of a few days) a uniform diversity is established in the bioreactor which ensures U(VI) reduction.

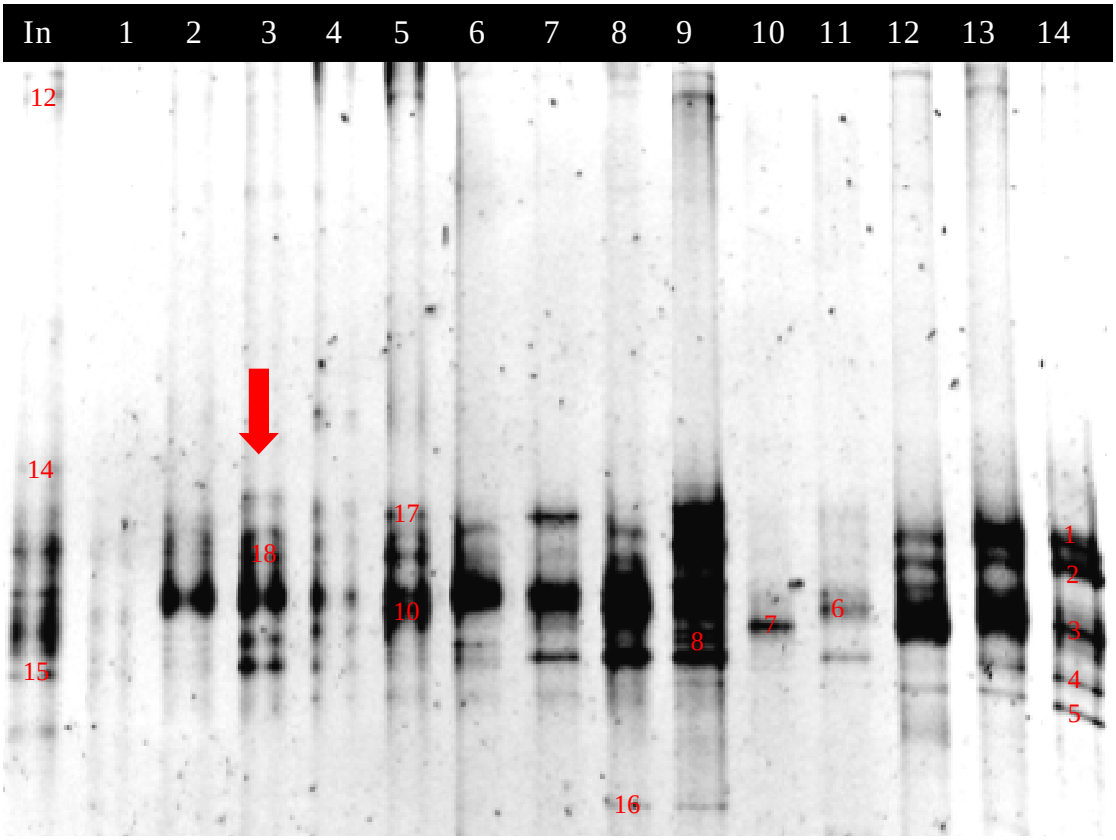

Figure 4.9: Lane In: Influent source water, Lane 1: Day 2, Lane 2: Day 9, Lane 3: Day 15, Lane 4: Day 21, Lane 5: Day 28, Lane 6: Day 30, Lane 7: Day 34, Lane 8: Day 45, Lane 9: Day 50, Lane 10: Day 56, Lane 11: Day 60, Lane 12: Day 69, Lane 13: Day 75 and Lane 14: Day 79

The sequence results (Table 4.4) show a number of uncultured bacterial clones which indicates the novelty in the biodiversity present in the effluent water from the bioreactor. However, most of the sequences retrieved from NCBI BLAST database (http://blast.ncbi.nlm.nih.gov/Blast.cgi) also shows bacterial sequences reported for the reduction of the following metals: chromium, uranium, sulphate, and iron or nitrate reduction. Thus it can be assumed that the is some level of U(VI) reduction within the bioreactor.

Bacterial species observed include *Geobacter* sp. and *Rhodobacter* sp., this species have been reported to reduce a number of metals such as U(VI), Cr(VI) and Fe(III) with the oxidation of external electron donors (Lovley, 1993). *Thiomonas* sp. was originally isolated from uranium impacted sites, and are known to oxidize both Fe(II) and sulphur (Chen *et al*., 2004; Vensteinsdottir *et al*., 2011). Enzymatic U(VI) reduction has been reported for *Desulfovibrio* sp. (Lovley and Phillips, 1992; Lovley *et al*., 1993a, b; Lovley and Phillips, 1994; Payne *et al*., 2002). Although this specie can reduce U(VI), it cannot yield energy for growth.

The bacterial sequences findings support that an interaction between uranium and the microbial community is taking place, and this may be a reduction process, since some of the bacteria have been reported for using U(VI) as the terminal electron acceptor. *Sulfuricurvum* sp. and *Thiomonas* sp. may also play a role in U(VI) precipitation since they are known metal oxidizing bacteria. The two groups of bacteria might be involved in the indirect immobilization of U(VI) (section 1.2.4) thereby a high U(VI) reduction capability.

Table 4.4: Sequencing results retrieved from BLASTN algorithm for the bioreactor.

Band	Accession number	Closest sequences with BLASTN	E-value	Maximum Identity (%)
1	FM204948.1	Uncultured epilsilon proteobacterium partial 16S rRNA gene	7e-134	85%
2	EU498374.1	Sulfuricurvum sp. enrichment culture clone 16S ribosomal RNA gene	0.0	99%
3	KC213941.1	*Agrobacterium tumefaciens* strain 16S ribosomal RNA gene, partial sequence	8e-84	78%
4	AM421802.1	*Geobacter* sp. 16S ribosomal RNA gene, complete	3e-133	83%
5	FJ536894.1	Uncultured *Thiomonas* sp. clone DMS24 16S ribosomal RNA gene, partial sequence	0.0	99%
6	AY780563.1	Uncultured *Geobacter* sp. clone KB-1 1 16S ribosomal RNA gene, partial sequence	3e-63	75%
7	JX949604.1	*Rhodobacter* sp. MDT1-69-1 16S ribosomal RNA gene, partial sequence	0.0	99%
8	KC836712.1	*Enterococcus italicus* strain RU36-3 16S ribosomal RNA gene, partial sequence	1e-116	86%
10	JQ764998.1	*Agrobacterium* sp. 16S ribosomal RNA gene, partial sequence	0.0	100%
12	HF548381.1	Flavobacterium sp. BA-97-09 partial 16S rRNA gene	0.0	93%
14	JN371404.1	Uncultured Bacteroidetes bacterium clone 16S ribosomal RNA gene, partial sequence	0.0	96%
15	JF151159.1	Uncultured Rhodobacteraceae bacterium clone, partial sequence	0.0	93%
16	JQ512033.1	*Desulfovibrio* sp. enrichment culture clone 16S ribosomal RNA gene, partial sequence	3e-119	99%
17	EU214542.1	Uncultured Anaerophaga sp. clone 16S ribosomal RNA gene, partial sequence	0.0	98%
18	GQ923765.1	*Legionella* sp. 16S ribosomal RNA gene	5e-49	70%

4.4.7 Bioreactor termination

4.4.7.1 Cell counts

DAPI staining was done according to section 3.3.6.1. The four bioreactor fractions were subjected to DAPI staining according to the section above. The DAPI staining preliminary confirm that the collected water fractions contained cells, with a gradient of cells obtained from fraction 1 to 4.

Using DAPI staining it was possible to count the number of cells for each fraction according to equation 3.4. It can be seen that the first fraction has counts of 3.9×10^4cells/ml, however the other fractions show 10^3cell/ml counted (Table 4.5). Since this was an upflow bioreactor with nutrients arrival at the bottom and consequently the maximal concentration of nutrients for resident would be at an inlet location near the bottom of the bioreactor (Figure 4.10), more cells will be at the bottom of the reactor as opposed to the upper portion of the bioreactor, thereby resulting in the most activity.

Table 4.5: DAPI cell counts for the terminated bioreactor.

Sample	Cells/ml
Fraction 1	3.9×10^4
Fraction 2	7.8×10^3
Fraction 3	4.2×10^3
Fraction 4	3.4×10^3

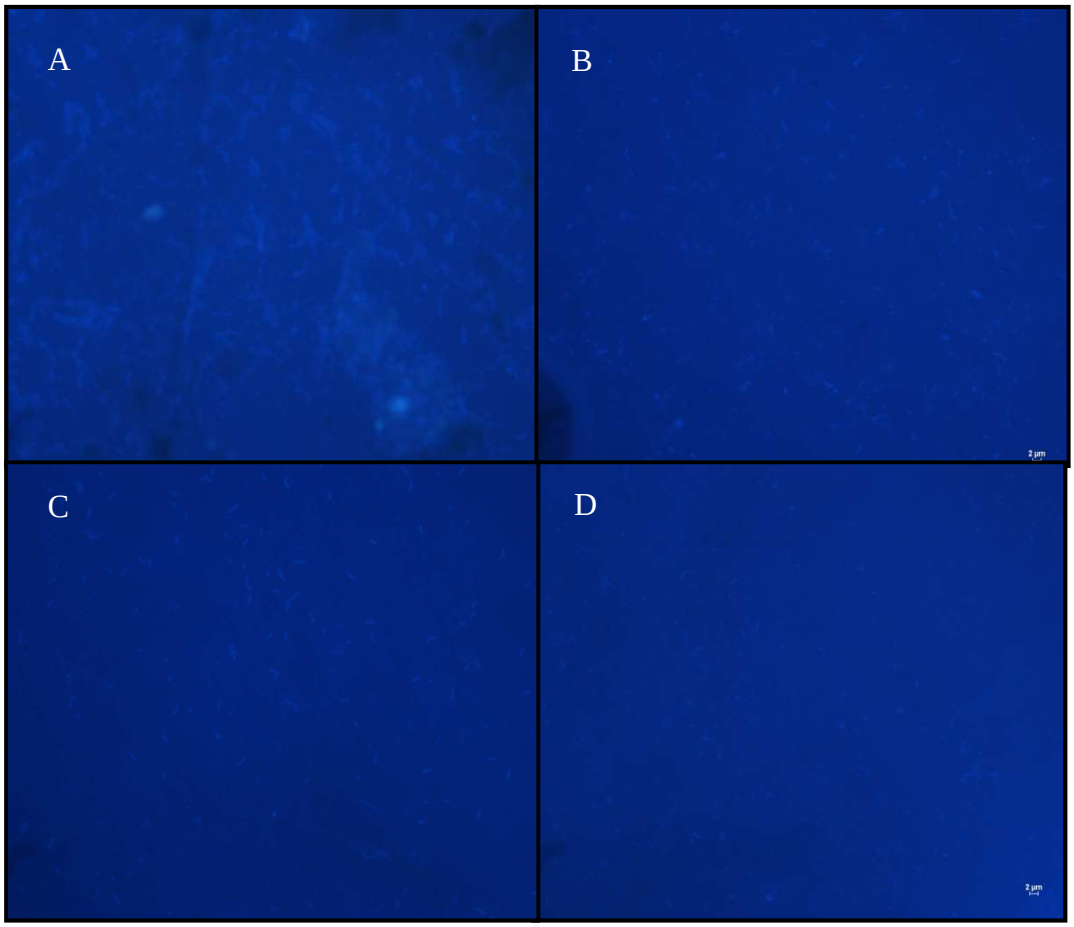

Figure 4.10: DAPI staining of the water fractions collected from the terminated bioreactor. (A) Fraction 1, (B) Fraction 2, (C) Fraction 3 and (D) Fraction 4.

4.4.7.2 Molecular analysis of fractions

The partial 16S rDNA sequencing results (Table 4.6) show a number of uncultured bacteria which indicates the novelty in the biodiversity present in the water fractions from the bioreactor. It can be seen that the resulting partial 16S rDNA bacteria sequences also resemble those that were obtained from the collected effluent samples. The obtained sequencing results have been reported for the reduction of uranium, chromium and sulphate. The *Enterobacteriaceae* family includes species such as *Pantoea* and *Pseudomonas* which have been reported for U(VI) (Chabalala and Chirwa, 2010b). Other species observed for the reduction of U(VI) are *Rhodobacter* and *Geobacter* sp.

Table 4.6: Sequencing results retrieved from BLASTN algorithm for the U(VI) bioreactor water fractions.

Band	Accession number	Closest sequences with BLASTN	E-value	Maximum Identity (%)
1	HM159969.1	Uncultured *Enterobacteriaceae* bacterium clone OTU14 16S ribosomal RNA gene, partial sequence	0.0	99%
2	JQ764998.1	*Agrobacterium* sp. BE516 16S ribosomal RNA gene, partial sequence	0.0	99%
4	HM584326.1	Uncultured bacterium clone BF3-14 16S ribosomal RNA gene, partial sequence	0.0	99%
5	FJ536894.1	Uncultured *Thiomonas* sp. clone DMS24 16S ribosomal RNA gene, partial sequence	0.0	99%
6	JX949604.1	*Rhodobacter* sp. MDT1-69-1 16S ribosomal RNA gene, partial sequence	0.0	99%
7	JF430007.1	*Propionibacterium acnes* strain 1452-10 16S ribosomal RNA gene, partial sequence	0.0	98%
8	FM877976.1	*Geobacter* sp. IST-3 partial 16S rRNA gene, isolate ALISIMBF42R42	0.0	92%

4.4.7.3 Scanning electron microscope and energy dispersive x-ray spectrometry

The SEM micrograph does not show visiable biofilm formation on the matrix. However, other biological life in the form of diatoms can be seen from the micrograph (Figure 4.11). This is not a surprise since diatoms are water quality indicators and are found at almost all levels of pollution (Michels, 1998).

Although biofilm formation by SRBs has been reported by Marsili and co-workers (2007), one should keep in mind that sulphate reduction is a low energy yielding reaction and as such this result in low biomass. An example is the *Desulfovibrio* sp, this specie is able to reduce U(VI) however it cannot yield energy for growth in this reduction process. In spite of

the fact that bacteria could not sturdily adhere to the matrix, the rate of U(VI) reduction was still above 90% even with 10 mg/l uranyl acetate spiked. These results are in accordance with Vrionis and co-workers (2005) who reported a high correlation between U(VI) reduction rates and abundance of planktonic cells. The high U(VI) reduction might be because since planktonic cells are free flowing, they are able to come in contact with U(VI) repeatedly, as such any residual U(VI) can be reduced by the established planktonic microbial community.

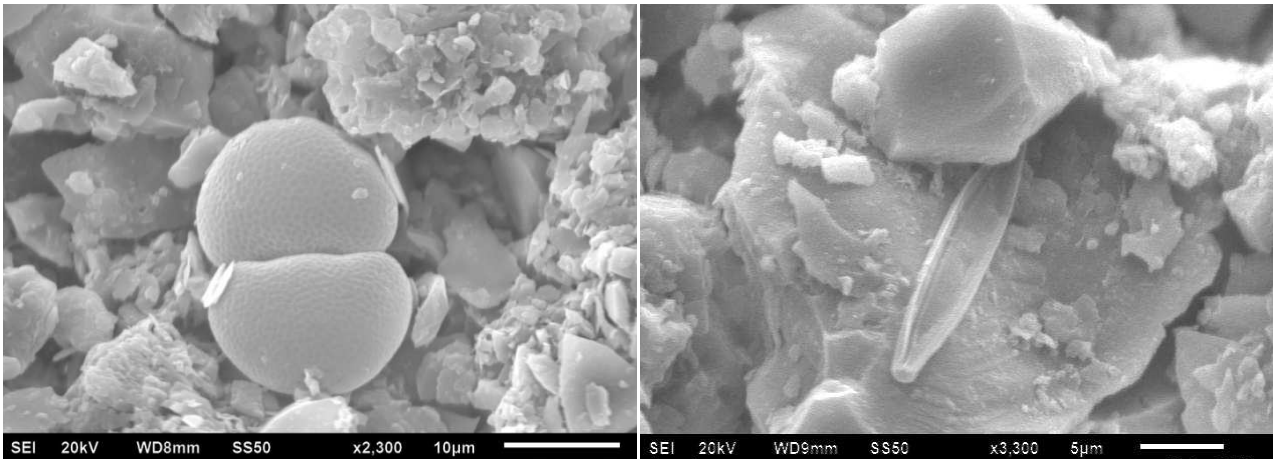

Figure 4.11: Scanning electron microscopy micrograph showing the presence of diatoms on the matrix.

4.4.7.4 X-ray fluorescence measurements

Matrix samples were sent to the Department of Geology, UFS for analysis. The whole-rock geochemistry of the matrix was analysed and confirmed to be quartzite rock (Table 4.7). A number of trace elements were measured: U, Cr, Co, Ni, Cu, Zn, V, Pb, etc. However for the purpose of this study, only uranium will be taken into consideration. The results obtained revealed that traces of uranium could be detected to a concentration of approximately 10 mg/l when compared to the control sample.

Table 4.7: Whole-rock geochemistry of matrix and trace element analysis by XRF.

Major elements of matrix (wt%)	**Control**	**Fraction**
SiO_2	97.715	97.421
Al_2O_3	0.692	1.155
Fe_2O_3	0.784	0.805
MnO	0.059	0.059
CaO	0	0.01
MgO	0.423	0.099
Na_2O	0	0
K_2O	0.148	0.356
TiO_2	0.097	0.155
P_2O_5	0.023	0.025
Total	**99.937**	**100.085**
Trace elements (mg/l)	**Control**	**Fraction**
V	5	4
Cr	7	8
Co	4	4
Ni	3	6
Cu	16	16
Zn	4	6
Pb	3	6
Th	35	36
U	0	10

4.4.7.5 Scanning electron microscopy

The TEM micrograph was used to determine the interaction of the bacterial community with uranium. Figure 4.12 shows an extra- and intracellular cluster of what appears to be uranium crystals (indicated by the arrows). These results provide an indication where uranium is immobilized. It can be seen that uranium is accumulated by the cells and also sorbed on the cell surface indicating multiple interactions.

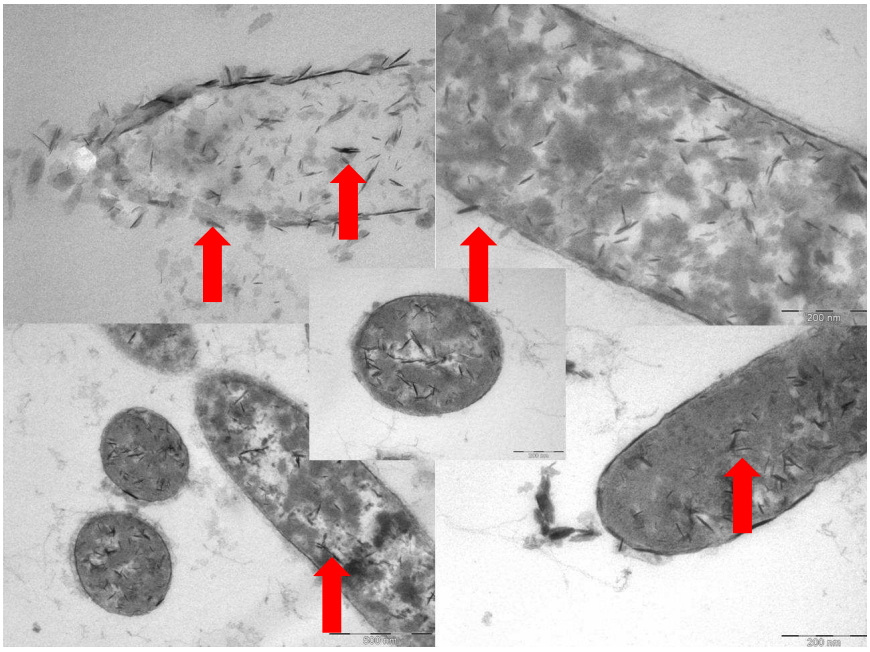

Figure 4.12: Transmission electron microscopy of thin sections of microbial cells obtained from the effluent water.

4.4.7.6 Uranium qualitative analysis

There were no detectable peaks indicating uranium for any of the samples except the precipitate obtained from the filtered effluent water sample (Table 4.8). The precipitate results show that of the 0.0333 g, only 27.9% of the mass was determined to be uranium. These findings suggest that uranium is being washed out of the bioreactor, probably through interaction with microbial cells as shown in section 4.4.7.5.

Table 4.8: ICP-OES analysis results for total uranium determination.

Sample	Sample Mass (g)	Mass % Uranium
Blank	4.8457	<LLOD*
Fraction 1	5.8204	<LLOD*
Fraction 2	5.7201	<LLOD*
Filtered Effluent	0.0333	27.9

*LLOD = Lower Limit of Detection.

4.5 Conclusions

The citric acid fed to the influent water promoted and stimulated the removal of U(VI) by the indigenous microbial community, as a result a suitable microbial community/population was established. High levels of U(VI) spiked to the source water did not hinder the U(VI) removal capabilities of the established microbial population in the bioreactor. Sequences retrieved from BLASTN reveal the presence of microorganisms that have been reported for metal reduction, particularly U(VI), therefore there is an interaction between U(VI) and the established microbial population because one can assume that the U(VI) levels decreased from the bioreactor since U(VI) could not be detected from the effluent samples. These findings suggest that the microbial population involved in U(VI) removal might have precipitated uranium rendering it immobile and insoluble.

The uranium detected by XRF verify that U(VI) is immobilized in the bioreactor. The TEM micrograph reveal the interaction of U(VI) and the community involved. The results provide a clear insight of where the uranium is immobilized, on the cell wall, accumulated by the cells, and also sorbed on the cell surfaces. Uranium might be washed out with the microbial cells in contact with uranium. From this, since U(VI) could not be detected from the effluent samples, the U(VI) might be converted to another form, U(IV).

4.6 References

- **Brandl, H. and Faramarzi, M.A.** (2006) Microbe-metal-interactions for the biotechnological treatment of metal-containing solid waste. *China Particuology*. **4**(2):93-97.

- **Brookman, S.K.E.** (1997) Estimation of biochemical oxygen demand on slurry and effluents using ultra-violent spectrophotometry. *Wat. Res*. **31**(2):372-374.

- **Camacho, L.M., Deng, S. and Parra, R.R.** (2010) Uranium removal from groundwater by natural clinoptilolite zeolite: Effects of pH and initial feed concentration. *Journal of Hazardous Material*. **175**:393-398.

- **Chabalala, S. and Chirwa, E.M.N.** (2010a) Removal of uranium(VI) under aerobic and anaerobic conditions using indigenous mine consortium. *Minerals Engineering*. **23**:256-231.

- **Chabalala, S. and Chirwa, E.M.N.** (2010b) Uranium(VI) reduction by high performing purified anaerobic cultures from mine soil. *Chemospere*. **78**(1):52-55.

- **Chen, X.-G., Geng, A.-L., Yan, R., Gould, W.D., Ng, Y.-L. and Liang, D.T.** (2004) Isolation and characterization of sulphur-oxidizing *Thiomonas* sp. and its potential application in biological deodorization. *Letters in Applied Microbiology*. **39**:495-503.

- **Department of Water Affairs (DWA)** (2011) South African national standard – Drinking water. Part 1: Microbiological, physical, aesthetic and chemical determinants.

- **Finneran, K.T., Housewright, M.E. and Lovley, D.R.** (2002) Multiple influences of nitrate on uranium solubility during bioremediation of uranium-contaminated subsurface sediments. *Environmental Microbiology*. **4**(9):510-516.

- **Fowle, D.A., Fein, J.B. and Martin, A.M.** (2000) Experimental study of uranyl adsorption onto *Bacillus subtilis*. *Environ. Sci. Technol*. **34**:3737-3741.

- **Goulhen, F., Gloter, A., Guyot, F. and Bruschi, M. (2006)** Cr(VI) detoxification by *Desulfovibrio vulgaris strain Hilden*borough: microbe-metal interactions studies. *Appl Microbiol Biotechnol.* **71**:892-897.

- **Islam, E., Dhal, P.K., Kazy, S.K. and Sar, P.** (2011) Molecular analysis of bacterial communities in uranium ores and surrounding soils from Banduhurang open cast uranium mine, India: A comparative study. *Journal of Environmental Science and Health*. **46**(3):271-280.

- **Kumar, A., Bisht, B. and Joshi, V.D.** (2010) Biosorption of heavy metals by four acclimated microbial species, *Bacillus* spp., *Pseudomonas* spp., *Staphylococcus* spp. and *Aspergillus niger*. *J. Biol. Environ. Sci*. **4**(12):97-108.

- **Kumlanghan, A., Kanatharana, P., Asawatreratanakul, P., Mattiasson, B. and Thavarungkul, P.** (2008) Microbial BOD sensor monitoring treatment of wastewater from a rubber latex industry. *Enzyme and Microbial Technology*. **42**:483-491.

- **Lovley, D.R.** (1993) Dissimilatory metal reduction. *Ann. Rev. Microbiol*. **47**:263-290.

- **Lovley, D.R., Phillips, E.J.P., Gorby, Y.A. and Landa, E.R.** (1991) Microbial reduction of uranium. *Nature*. **350**:413-416.

- **Lovley, D.R. and Phillips, E.J.P.** (1992) Bioremediation of uranium contamination with enzymatic uranium reduction. *Environ. Sci. Technol*. **26**:2226-2234.

- **Lovley, D.R. and Phillips, E.J.P.** (1994) Reduction of chromate by *Desulfovibrio vulgaris* and its c_3 cytochrome. *Applied and Environmental Microbiology*. **60**(2):726-728.

- **Lovley, D.R., Roden, E.E., Phillips, E.J.P. and Woodward, J.C.** (1993a) Enzymatic iron and uranium reduction by sulfate-reducing bacteria. *Marine Geology*. **113**:41-53.

- **Lovley, D.R., Widman, P.K., Woodward, J.C. and Phillips, E.J.P.** (1993b) Reduction of uranium by cytochrome c_3 of *Desulfovibrio vulgaris*. *Applied and Environmental Microbiology*. **59**(11):3572-35276.

- **Macaskie, L.E., Bonthrone, K.M., Yong, P. and Goddard, D.T.** (2000) Enzymatically mediated bioprecipitation of uranium by a *Citrobacter* sp.: a concerted role for exocellular lipopolysaccharide and associated phosphatase in biomineral formation. *Microbiology*. **148**:1855-1867.

- **Marsili, E., Beyenal, H., Di Palma, L., Merli, C., Dohnalkova, A., Amomette, J.E. and Lewandowski, Z.** (2007) Uranium immobilization by sulfate-reducing biofilms grown on hematite, dolomite, and calcite. *Environ. Sci. Technol*. **41**:8349-8354.

- **Michels, A.** (1998) Use of diatoms (Bacillariophyceae) for water quality assessment in two tropical streams in Costa Rica. *Rev. Biol. Trop*. **46**(6):143-152.

- **Payne, R.B., Gentry, D.M., Rapp-Giles, B.J., Casalot, L. and Wall, J.D.** (2002) Uranium reduction by *Desulfovibrio desulfuricans* strain G20 and a cytochrome c_3 mutant. *Applied and Environmental Microbiology*. **68**(6):3129-3132.

- **Shnug, E., Steckel, H. and Haneklaus, S.** (2005) Contribution of uranium in drinking waters to the daily uranium intake of humans – a case study from Northern Germany. *Landbauforschung Volkenrode*. **55**(4):227-236.

- **Suzuki, Y., Kelly, S.D., Kemner, K.M. and Banfield, J.F.** (2005) Direct microbial reduction and subsequent preservation of uranium in natural near-surface sediment. *Applied and Environmental Microbiology*. **71**(4):1790-1797.

- **Tripathi, R.M., Sahoo, S.K., Jha, V.N., Khan, A.H. and Puranik, V.D.** (2008) Assessment of environmental radioactivity at uranium mining, processing and tailings management facility at Jaduguda, India. *Applied Radiation and Isotopes.* **66**:1666-1670.

- **Vesteinsdottir, H., Reynisdottir, D.B. and Orlygsson, J.** (2011) *Thiomonas islandica* sp. nov., a moderately thermophilic, hydrogen- and sulphur-oxidizing betaproteobacterium isolated from a hot spring. *International Journal of Systematic and Evolutionary Microbiology*. **61**:132-137.

- **Volesky, B. and May-Phillips, H.A.** (1995) Biosorption of heavy metals by *Saccharomyces cerevisiae*. *App Microbiol Biotechnol*. **42**:797-806.

- **Vrionis, H.A., Anderson, R.T., Ortiz-Bernad, I., O'Neill, K.R., Resch, C.T., Peacock, A.D., Dayvault, R., White, D.C., Long, P.E. and Lovley, D.R.** (2005) Microbiological and geochemical heterogeneity in an *in situ* uranium bioremediation field site. *Applied and Environmental Microbiology*. **71**(10):6308-6318.

- **Winde, F.** (2010) Uranium pollution of the Wonderfonteinspruit, 1997-2008. Part 2: Uranium in water – concentrations, loads and associated risks. *Water SA*. **36**(3):257-278.

Summary

Uranium (U) and chromium (Cr) in groundwater are a serious public health concern due to their chemical toxicity. Even so, microorganisms have developed mechanisms which permit them to thrive under previously perceived uninhabitable conditions. A number of bacteria have been isolated from areas impacted with the soluble heavy metals, and can be exploited as bioremediation agents since they are well adapted to these metals. To date, the use of microbial mechanisms for bioremediation processes is a growing industry since it provides green and sustainable technologies.

In this study, the upflow bioreactors were used as a low cost, low maintenance effective bioremediation strategy in comparison to the available methods of remediation. Two metals known to be toxic in their soluble state were treated. The first was Cr(VI) from an impacted site in Limpopo and the second was U(VI) from the Wonderfonteinspruit catchment, North West Province. The system was efficient for the removal of soluble Cr(VI) and U(VI) from the impacted water through biostimulation of indigenous bacterial communities. This system can be up scaled and employed for the remediation of impacted sites, and it will be useful especially at low levels of U(VI). Indigenous bacterial community from impacted sites have the capability to reduce Cr(VI) and U(VI) effectively over a sustainable period. The shortage of electron donor and continuous oxygen exposure in the case of U(VI) act as a limiting factor. However, in this study successful Cr(VI) and U(VI) reduction rates were increased by the addition of an electron donor to stimulate the indigenous bacterial community.

Furthermore, a third upflow bioreactor showed that it is even possible with gradual increases of U(VI) concentration that U(VI) bioreduction is possible at very high levels. The influent water was spiked step wise with uranyl acetate, allowed to reach maximal U(VI) reduction/removal and then the diversity was assessed. Despite the 10 mg/l U(VI) fed to the bioreactor, the established microbial community was able to tolerate, adapt and thereby remove the U(VI) from the spiked water. Even though biofilm could not sturdily adhere to the matrix from the bioreactor, high levels of U(VI) removal could be achieved and the planktonic community maintained. No biofilm could be observed from SEM analysis from the TEM it was observed that the planktonic microbial community have an interaction with uranium. Since no U(VI) could be detected from the effluent samples, it is thus postulated the uranium in contact with the microbial cells is in another form, probably U(IV) as previously shown in this laboratory. This study allows for the understanding of the metal microbe

interactions in impacted environments, the use of this biome to remediate the water in an effective, low cost and maintenance bioreactor.

Keywords

Biostimulation, DGGE, Indigenous bacteria, Upflow bioreactor, Uranium reduction.

Opsomming

Uraan (U) en chroom (Cr) wat in grondwater voorkom veroorsaak ernstige publieke gesondheids probleme as gevolg van hulle toksisiteit. Mikroorganismes het meganismes ontwikkel wat hulle in staat stel om in toestande te oorleef wat voorheen gesien is as onbewoonbaar. ‘n Aantal bakterië is al geïsoleer uit areas wat gekontamineer is met oplosbare swaar metale, en kan dus gebruik word vir bioremediasie aangesien hulle reeds aangepas is tot die teenwoordigheid van hierdie swaar metale. Die gebruik van mikrobiese meganismes vir bioremediasie prosesse is ‘n groeiende industrie omdat dit ‘n meer groen en volhoubare tegnologie is.

In hierdie studie is opvloei bioreaktors gebruik as ‘n lae koste, lae onderhoud effektiewe bioremediasie strategie in vergelyking met ander beskikbare metodes van remediasie. Twee metale wat toksies is in hulle oplosbare vorm was behandel. Die eerste was Cr(VI) vanaf ‘n gekontamineerde area in Limpopo en die tweede was U(VI) vanaf die Wonderfonteinspruit opvangs gebied, Noord Wes Provinsie. Die sisteem was effektief vir die verwydering van beide oplosbare Cr(VI) en U(VI) vanuit die gekontamineerde water deur biostimulasie van inheemse bakteriële gemeenskap. Hierdie sisteem kan opgeskaal en gebruik word vir die remediasie van gekontamineerde areas, en sal veral nuttig wees waar lae vlakke van U(VI) voorkom. Die inheemse bakteriële gemeenskap van gekontamineerde areas het die vermoë om Cr(VI) en U(VI) effektief te reduseer oor ‘n volhoubare periode. Die tekort aan elektron donor en die deurlopende blootstelling aan suurstof in die geval van U(VI) is die beperkende faktore. Alhoewel, gedurende hierdie studie is die Cr(VI) en U(VI) reduksie tempo’s verhoog deur die byvoeging van ‘n gepaste elektron donor om die inheemse bakteriële gemeenskap te stimuleer.

Verder, deur ‘n derde opvloei bioreaktor waartydens die U(VI) konsentrasie gelydelik verhoog is, is gewys dat bioremediasie ook moontlik is teen hoë vlakke van U(VI). Die U(VI) konsentrasie in die water was stapsgewys verhoog deur die byvoeging van uranyl asetaat, gevolg deur die reduksie van die U(VI) en die bepaling van die bakteriële diversiteit. Ten speite van die 10 mg/l U(VI) wat in die reaktor ingevoer is, was die gevestigde mikrobiese gemeenskap in staat om aan te pas en sodoende die U(VI) te verwyder vanuit die water. Alhoewel die biofilm nie op die matriks van die bioreaktor kon heg nie, kon hoë vlakke van U(VI) steeds verwyder word deur die handhawing van die planktoniese gemeenskap Geen biofilm was waargeneem deur SEM analise nie. Daar was waarneembare interaksie tussen die

planktoniese mikrobiese gemeenskap en uraan volgens die resultate verkry uit die TEM analise. Omdat geen U(VI) in die behandelde water opgespoor kon word nie, is dit gepostuleer dat die uraan wat geassosieer word met die mikrobiese selle in ‘n ander form voorkom, waarskynlik U(IV) soos voorheen gesien in die laboratorium. Hiedie studie maak dit moontlik om die metaal-mikrobe interaksies te verstaan in gekontamineerde omgewings, asook om hierdie biome te gebruik om gekontamineerde water te remidieer in ‘n effektiewe, lae koste en onderhoud bioreaktor.

Sleutelwoorde

Biostimulasie, DGGE, Inheemse bakterië, Opvloei bioreaktor, Uraan reduksie.